ATLE WILLIAM HESKESTAD

REACTION TO FIRE CLASSIFICATION OF BUILDING PRODUCTS: ASSESSMENT OF THE SMOKE PRODUCTION

HAZARD ASSESSMENT, ISO FIRE TEST METHODS AND DEVELOPMENT OF EMPIRICAL SMOKE PREDICTION MODELS

NTH
UNIVERSITETET I TRONDHEIM
NORGES TEKNISKE HØGSKOLE

DOKTOR INGENIØRAVHANDLING 1994:130
INSTITUTT FOR BYGG- OG ANLEGGSTEKNIKK
TRONDHEIM

UNIVERSITY OF TRONDHEIM
THE NORWEGIAN INSTITUTE OF TECHNOLOGY
FACULTY OF CIVIL ENGINEERING
DEPARTMENT OF BUILDING AND CONSTRUCTION ENGINEERING

REACTION TO FIRE CLASSIFICATION OF BUILDING PRODUCTS: ASSESSMENT OF THE SMOKE PRODUCTION

Hazard Assessment, ISO Fire Test Methods and Development of Empirical Smoke Prediction Models

by
ATLE WILLIAM HESKESTAD

THESIS FOR THE DEGREE OF DOCTOR OF ENGINEERING
DECEMBER 1994

NTH-TRYKK

ABSTRACT

The thesis presents a comprehensive study on assessment of smoke production properties of building products. Primarily the hazard related to the loss of visibility is considered. The starting point has been to investigate whether smoke prediction models can be developed to predict smoke test data from the full scale ISO Room Corner Test by the use of test data from the bench scale ISO Cone Calorimeter. The thesis outlines a theoretical base for fire parameters, then a set of fire parameters is developed. All fire parameters are then used in empirical approaches to develop smoke prediction models. The approaches are based on test data from 34 building products, and only models with a scientifically sound basis are accepted. By use of a found model, full scale smoke data from pre-flashover fires are sufficently well predicted. The predictions are principally based on bench scale CO data. It is argued that bench scale smoke data might not have general suitability for such predictions. The study shows that the success of prediction depends on the elimination of the temperature dependency of the smoke production.

Then the *generality* of the full scale test data is considered. This means verifying whether the smoke data are predominantly governed by the building products and less the fire scenario. The verification is done by comparison of the *smoke production (generation)* from the ISO Room Corner Test with corresponding data from three other enclosure tests. The verification validates smoke data from pre-flashover fires. This verification also implicitly validates the ISO Room Corner Test to be *consistent* with the fire scenarios the test is meant to cover. This leads to the conclusion that the ISO Room Corner Test can be used to assess smoke production from building products in growing fires.

The relationship between bench scale and full scale data seems to disappear as a fire grows. This has been pointed out to be caused by complex full scale combustion conditions which need further investigation. There are some indications that post-flashover smoke and CO data might possibly be predicted by reduced scale enclosure tests.

Finally, the hazard related to the loss of visibility is considered. The assessment relates to the occurrence of flashover. In pre-flashover fires the smoke hazard is identified to occur both outside and inside the plume. The lethal hazard outside the plume is identified to be a combination of high irradiance level and loss of visibility, while lethal hazard inside the plume (fire effluents) is identified to be a combination of loss of visibility and the irritant effects of the fire effluents. The ISO Room Corner Test is validated as applicable to evaluate the pre-flashover smoke hazard. It is argued that a benchmark of smoke hazard occurs when the combustible changes from a moderately smoky product like wood to a highly smoky plastic based product. A proposal for how this could be implemented in a functionally based classification system is also given. The hazard assessment of post-flashover fires shows that the loss of visibility can be a significant hazard even when the fire atmosphere has a relatively low toxicity. It is argued that the hazard related to loss of visibility in post-flashover fires should provisionally be left out of classification.

ACKNOWLEDGEMENTS

The study has been made possible by financial support from The Norwegian Institute of Technology. I have also received financial support from the Total Norge AS and the Research Council of Norway (through the research programme Fire, Explosion and Major Accidents).

Above all, I want to thank my supervisor Professor Per Jostein Hovde. He has continuosly encouraged, supported and helped me, and made this work worthwhile. I would also thank my colleagues at Department of Building and Construction Engineering and at SINTEF NBL Norwegian Fire Research Laboratory. Kristen Opstad should be especially acknowledged. I am especially grateful to SINTEF NBL for letting me use all their facilities in an unlimited way.

I am also grateful to Claude Moye and the others at Centre Scientifique et Technique du Bâtiment, Marne la Vallée, France, for making my one year stay there enjoyable. Bernard Hognon should be especially acknowledged.

Then, I want to express sincere thanks to my Scandinavian colleagues:

- Lazaros Tsantaridis and Birgit Östman at the Swedish Institute for Wood Technology Research. They have supported me with test data from the Cone Calorimeter, reports and help with the data.
- The staff at the Swedish National Testing and Research Institute, particularly Ulf Göranson, Ulf Wickström, Per Thureson and Björn Sundström. They have supported me with data from the ISO Room Corner Test and other tests, reports and interesting discussions.
- Esko Mikkola and Matti Kokkola at the Technical Research Centre of Finland. They have supported me with requested data.

This work would not have been possible without the support from the mentioned people and organizations.

I also want to express sincere thanks to Gunnar Heskestad for interesting discussions and editoral corrections.

Vytenis Babrauskas should also be acknowledged for interesting discussions.

General thanks should also be given to Björn Karlsson (Lund University, Sweden), Silvio Messa and Franco Carradory (Laboratorio di Studi e ricerche Fuoco, Italy), Mr. Werther (BASF AG, Germany) and Christian Molnier (Laboratoire National d'Essais, France).

Finally, I want to thank my wife and my parents and my family who always have supported me.

Contents

Nomenclature

Latin letters

c_λ	smoke particulate extinction coefficient
C_S	Smoke concentration
f	carbon conversion factor
f_v	smoke particulate fraction
G_j	mass generation of specie j
HR	heat release
I_λ	intensity of transmitted light
$I_{0\lambda}$	intensity of incident light
k	light extinction coefficient
K	visibility constant
k_λ	light extinction coefficient (monochromatic light)
$k_{m\lambda}$	specific extinction coefficient
l	path length
M_0	the initial mass of the specimen
ML	mass loss
M_W	molecular mass
Q	heat release
$r_{C/H}$	the ratio between carbon and hydrogen in the fuel
RHR	rate of heat release
$RMCO_2$	rate of mass CO_2 production
RMCO	rate of mass CO production
RML	Rate of mass loss
RPP	rate of particulate production
rS/Q	smoke to flame ratio
$r_{S/Q}(10)$	full scale $r_{S/Q}$ averaged over 10 minutes
RSP(04)	identical to RSP(400)
RSP(1000)	the full scale smoke production at 1000 kW heat release
RSP(400)	full scale smoke production at 400 kW rate of heat release rate
RSP	rate of smoke production
RVCO	rate of volumetric CO production
$RVCO_2$	rate of volumetric CO_2 production
SEA	smoke extinction area
SP	smoke production
t_{eof}	time to cease of flaming
t_{FO}	time to flashover
T_g	gas temperature
THR	total heat release

t_i	time to incapacitation
t_{ign}	time to ignition
t_{max}	time to maximum heat release rate
TMCO	total mass of CO production
$TMCO_2$	total mass of CO_2 production
TML	total mass loss
TSP	total smoke production
TSP(10)	full scale total smoke production after 10 minutes
$t_{w,j}$	the «width» of the production of specie j
t_{width}	the «width» of the heat release
V	volume
V_d	volume flow in duct
Vis	visibility
Y_j	Yield of specie j

Greek letters

ρ_S	smoke density
λ	wavelength
$\Delta h_{c,eff}$	effective heat of combustion
ϕ	global equivalence ratio
ϕ_S	smoke equivalence ratio factor
ϕ_{CO}	CO equivalence ratio factor
η_j	generation efficiency factor of specie j
ν_j	maximum stoichiometric coefficient
ψ_j	maximum conversion of the fuel into specie j
ν_{res}	residue fraction

Subscripts and superscripts

μ	mass fraction
a	absorbed
a	scattered
ad	adiabatic
ccs	completely combusted species
CO	carbonmonoxyde
conv	convective
fe	fire effluents
kpcs	known partly combusted species
L	achromatic light source

S	smoke
upcs	unknown partly combusted species
vol	volumetric

Abbreviations

A	air
F	fuel
FO	flashover
FR	fire retarded
GER	global equivalence ratio
gpp	gypsum paper plaster board
n.c.	non combustible
PE	polyethylene
PS	polystyrene
PU	polyurethane
PVC	polyvinylchloride
T	transformed

1 INTRODUCTION

1.1 Background and Objective of the Thesis

The reaction to fire classification of combustible building products in the national building codes should have a sound and verified relationship to the real fire hazard. This should be an obvious requirement for any classification system. In fact a classification system is not proved to be suitable for its purpose if such documentation does not exist.

The Nordic research programme EUREFIC (European Reaction to Fire Classification) [1] [2] was finished in 1991. The programme identified the philosophy for a sound and scientifically based classification system for linings and surface products. The system was based on ISO fire test methods, and primarily considered the heat release properties of building products. This thesis is an extension of the Nordic programme, and concerns primarily assessment of the smoke production of building products.

The principal objective of the thesis is to procure a scientific basis to assess and evaluate the hazard to human life posed by smoke produced from building products in fires. The smoke released in building fires may result in a loss of visibility for the occupants and consequently reduce the speed of escape. The risk to be overcome by heat and toxic fire effluents then increases.

Efforts have been made to regulate the life hazard associated with loss of visibility and many national building codes have requirements regarding the smoke production of combustible building products. These regulations are normally based on laboratory test results. However, the essential relationships between the laboratory fire test methods and the real life hazard occurring in fires have been questioned and doubted.

The issue is whether the fire test methods can be used to assess the products in a way that is relevant. This is organised into *three* topics. The *first* topic is to find out whether relationships exist between test data obtained in the bench scale ISO Cone Calorimeter test and the full scale ISO Room Corner Test. If relationships are found between the methods, then the full scale test results might be predicted by use of test results from the bench scale.

The *second* topic concerns the link between the smoke production in the ISO Room Corner Test and the smoke production occurring in the real fires. The topic is to verify whether the smoke production and ranking found by the ISO Room Corner Test are conserved in the real fire scenarios the test is meant to simulate. This depends on what governs the smoke production in full scale. It can be predominantly governed by the burning product and/or the combustion conditions. The topic is essential, because if the smoke production in real fires is predominantly governed by the burning conditions (and not the product burning), then it is of limited interest to assess the smoke production by a classification system based on the ISO Room Corner Test. Because such assessment is then only valid in those cases where the real burning conditions are sufficiently close to the conditions in the ISO Room Corner Test. In other words, if the burning conditions are slightly changed, then the smoke performance of the building products becomes significantly changed.

The *third* topic concerns the identification of the increase in hazard associated with loss of visibility in real fires. The applicability of the ISO Room Corner Test to predict the smoke hazard occurring in building fires has to be verified. The reason for this is that the toxic hazard has been associated with post-flashover fires and it is therefore questionable whether the smoke represents a hazard in the growth stage (i.e. pre-flashover) of the fire and/or in the post-flashover stage. Fire statistics show that toxic hazard is the predominant reason for fire deaths, thus it has to be investigated when the loss of visibility poses a hazard. If it is found that post-flashover fires are the cases where the loss of visibility has the predominant effects on hazard, then post-flashover fire tests might be more appropriate than pre-flashover tests to evaluate the smoke production properties of building products. As a consequence it has to be verified that the choice of the full scale ISO Room Corner Test also is appropriate to predict the smoke hazard occurring in building fires.

1.2 Structure of the Thesis

The thesis consists of two main parts: a collection of four publications and a monograph. The monograph is based on the previous publications, thus they should be read first, or preferably in combination with the next section.

The total work has included five steps, the publications present the results of the first four steps, and the monograph represents the fifth and final step.

The four publications (which are collected after the monograph) are

1. The paper entitled «Smoke Production from Building Products. Comparison of Test Methods and Correlation of Test Results» presented at the Sixth International

Fire Conference INTERFLAM'93, University of Oxford, 30 March - 1 April 1993 [3].
2. The NORDTEST Technical Report entitled «Evaluation of Smoke Test Methods for Classification of Building Products» [4].
3. The paper entitled «Assessment of Smoke Production from Building Products» presented at the Fourth International Symposium on Fire Safety Science, Ottawa, 13 - 17 June 1994 [5].
4. The Work-in-Progress poster entitled «Smoke and CO Production in Bench Scale, Medium Scale and Large Scale Fires. Effect of Scale and the Combustion Conditions» presented at the 25th International Symposium on Combustion, University of California, Irvine, California, 31 July - 5 August 1994 (the abstract is presented in [6]).

In the monograph these publications are referred to as the INTERFLAM'93-publication, the NORDTEST-publication, the IAFSS'94-publication and the ISC'94-publication respectively.

Chapter 2 in the monograph is a general description of smoke in a way that is relevant for this research. Chapter 3 presents the materials, methods and experimental data which the thesis is based on.

Chapter 4 concerns development of the parameters that are used in the thesis. The *reactant-product equation model* is presented here, and most of the deducted fire parameters are based on this model . Totally 46 parameters are developed.

Chapter 5 presents the statistics used in the thesis. This also includes a study of the variation in some of the bench scale and full scale parameters.

Chapter 6 describes the development of smoke prediction models. The approaches concern prediction of specified data from the ISO Room Corner Test by use of data from the ISO Cone Calorimeter. The Chapter ends in a discussion of the results.

Chapter 7 presents an assessment of the three ISO fire test methods considered within the thesis; the ISO Cone Calorimeter, the ISO Dual Chamber Box and the ISO Room Corner Test. The main emphasis is being placed on the latter method. This is referred to as the validation of the *generality and consistency* of the ISO Room Corner Test. It is done by comparison of test data from the ISO Room Corner test with test data from three other tests; the Medium Scale Room Corner Test, the full scale French CSTB Room Fire Test and the Enlarged Scale Room Corner test.

Chapter 8 discusses the hazard occurring in real fires and whether it can be assessed by a system that is based on the ISO Room Corner Test as the main core. The topic is

discussed in relation to the occurrence of flashover. The topic is of current interest since a major proportion of the fire deaths has been related to post-flashover conditions and inhalation of toxic smoke. A simple method for evaluation of the hazard posed by loss of visibility in relation to the toxicity of the smoke is also outlined.

Chapter 9 gives the overall discussion, the conclusions and the recommendations to further work.

1.3 Brief Presentation of Publications

Unfortunately some of the bench scale smoke test data used in the four publications had a systematic error. The error was that the smoke production was calculated by use of the volume duct flow at 294 K, instead of the volume duct flow at the actual temperature. Thus the values used were too low, but mainly within a range of 20%. However, in most cases the error did not cause misleading results.

1.3.1 The INTERFLAM'93 and the NORDTEST Publication

The paper entitled «Smoke Production from Building Products. Comparison of Test Methods and Correlation of Test Results» was presented at the Sixth International Fire Conference INTERFLAM'93 and concerned preliminary results found within the NORDTEST project. It concerned comparison of two bench scale test methods (the ISO Cone Calorimeter and the ISO Dual Chamber Box) and evaluation against full scale (the ISO Room Corner Test). Note that the smoke test data of the ISO Cone Calorimeter in Figure 2 to Figure 7 are somewhat higher than what is shown in the figures (caused by the calculation error).

The Nordtest project was entitled «Evaluation of Smoke Test Methods for Classification of Building Products» and the starting point was smoke test data for 22 building products tested in the two bench scale test methods mentioned and the full scale test. Smoke test data from the bench scale test methods were compared to each other and evaluated by correlation studies against full scale test data. Correlations were found only if the products were divided into groups according to their performance in full scale [1]:

- **Product group 1**: The products which caused flashover before 10 minutes in the ISO Room Corner Test.

[1] The division of the building products into product groups 1 and 2 according to the performance in the ISO Room Corner Test is used throughout the monograph.

- **Product group 2**: The rest of the products, and divided into
  - **Product group 2A**: The products which caused flashover when the burner output was increased from 100 kW to 300 kW (i.e. after 10 minutes).
  - **Product group 2B**: The products which did not at all cause flashover within the test time (i.e. 20 minutes).

Correlations were only obtained for product group 2. The study revealed that the success of the correlation probably was governed by the full scale combustion conditions, and that product group 2 had a simpler fire scenario than product group 1. Product group 2B has a pyrolysed area which is governed by the flame spread properties and the heat release of the combustible and the burner. Since flashover did not occur the flame spread was to some degree limited. Thus the total smoke production originated from an area which was more or less fully pyrolysed, and that might be the reason for the correlations obtained.

For the products which caused flashover within 10 minutes, the smoke production originated from an area of unknown size and where there might be a varying degree of pyrolysis. Such full scale smoke test data did not correlate for smoke test data obtained in bench scale where the specimen had a constant exposed area which was fully pyrolysed.

The study further revealed that smoke parameters with the same units in bench scale and full scale could have different fire physical interpretations and they did not necessarily correspond.

The ISO Dual Chamber Box test was left out for further research. It was revealed that further research needed more advanced approaches that involved fire parameters and test data that are not possible to obtain with the ISO Dual Chamber Test.

The NORDTEST project identified lack of interpretation of full scale burning conditions, thus this was identified as an objective for further research.

1.3.2 The IAFSS'94-publication

The third publication within the thesis was entitled «Assessment of Smoke Production from Building Products» and was presented at the Fourth International Symposium on Fire Safety Science.

The starting point for the publication was fire test data for 38 building products. All products were tested in the ISO Cone Calorimeter and 31 were tested in the ISO

Room Corner Test. The 7 other products were full scale tested in the French CSTB Room Fire Test (these 7 products are defined as **product group 3**).
A new smoke parameter was introduced to analyse the relationship between bench scale and full scale: the ratio between the smoke production and the heat release (the parameter was denoted the smoke normalized to heat, or simply the normalized smoke. It has later been denoted *the smoke to flame ratio*). The advantage of that parameter is that it avoids the problems associated with the pyrolysed area. But still no correlations were found between the Cone Calorimeter data and the ISO Room Corner Test data.

Good correlations were found between the data from the Cone Calorimeter and the French CSTB Room Fire Test, but the study also gave further insight into the full scale combustion conditions and which questioned these correlations. The good correlation shown in the left panel of Figure 4 is probably fortuitous. However, the figure shows that the smoke generation is less in full scale than in bench scale.

The study revealed that further research on the full scale combustion conditions still was necessary. The study initiated also some thoughts whether the ISO Room Corner Test was appropriate to represent the real fire hazard associated with smoke obscuration and loss of visibility. (The topic is elucidated in Chapter 8)

1.3.3 The ISC'94 Publication

The fourth publication was the work-in-progress poster entitled «Smoke and CO Production in Bench Scale, Medium Scale and Large Scale Fires. Effect of Scale and the Combustion Conditions» presented at the 25th International Symposium on Combustion. The purpose of it was to obtain better understanding of the full scale combustion conditions.

The starting point of the study was bench scale and full scale test data for the products in product groups 1 and 3. A new parameter was introduced in the study: the fraction of the pyrolysed carbon in the combustion gases converted into carbonaceous smoke (it was denoted the smoke conversion factor). A similar parameter was also made for the CO production.

The study revealed that the combustion conditions in full scale changed as a function of the fire growth. This is crudely shown in Figure 1 and Figure 2 in the paper. Figure 1 shows the smoke generation factor as a function of heat release rate, and Figure 2 shows the CO generation factor as a function of heat release rate. The figures show that the smoke and CO generation factors increase during the initial stages of the growth stage to the fire (i.e. from approximately 200 kW to 500-600

kW). This is probably caused of heat losses to the «cold» adjacent boundaries and limited ventilation. The smoke and CO generation factors have peaks when the fires are in the range of 500-800 kW. For higher heat release rates the normalized smoke production is either constant or decreasing. Reasons for this were pointed out to be hotter boundaries (thus less heat losses) and a larger combustion volume.

The room fire combustion conditions are a complex topic. Still no complete interpretation and explanation of these phenomena have been given, but the topic is under investigation [7] [8] [9]. The effect of temperature is important, and it seems that the smoke production is more sensitive to temperature than the CO production (e.g. compare Figure 1 and Figure 3). (The incineration of CO is reported to stop below around 800 K [9].)

It was shown that a direct and simple correlation hardly exists between bench scale and full scale smoke parameters.

It is worth noticing that the changes in combustion conditions influence the smoke generation. Thus if a full scale smoke parameter is averaged over the whole scenario, it will contain information which originates from different types of combustion. Since the onset of different combustion conditions vary from material to material, averaged smoke parameters will contain different information, and this will probably complicate the empirical correlation study. Thus instant values are probably the best choice, because these originate from one overall type of burning.

The choice of the criteria for selecting the full scale instant smoke parameters are important. Since the gas temperature is assumed to be important for the production of smoke (and CO), the rate of heat release could be used as a criterion for choosing full scale smoke parameters. This is because the ventilation of the room fire is governed by the heat release. At a specific level of the rate of heat release rate approximately the same ventilation rate and gas temperature within the room should be expected. However, the heat losses to the boundaries will also influence the temperature conditions.

2 SMOKE

2.1 Definition and Characterisation of Smoke

Here smoke is defined as the airborne liquid and solid particulates carried in the fire gases evolved when a combustible burns. In addition to the smoke particulates and entrained air, the fire gases can consist of CO_2 and H_2O (ie. saturated gases), partly burnt combustion gases as CO, H_2, partly burnt hydrocarbons and unburnt fuel.

Generally the liquid smoke particulates are tar like droplets or mists composed of liquid products of pyrolysis or their partially oxidized derivatives and water, while the solid smoke particulates contain carbon flakes, soot beads, ash, sublimed pyrolysis products and oxides of inorganic compounds [10].

The character of the smoke is governed by the burning conditions:

- Mode of decomposition; flaming, pyrolysis or smoldering combustion. Flaming burning where the temperature is high and there is absence of oxygen gives carbonaceous solid particulates (ie. soot) while non-flaming combustion (i.e. pyrolysis and smoldering) gives «white» smoke which consists of pyrolysis volatiles that condense to spheric droplets (fogs) when the smoke is cooled.
- The temperature and oxygen concentration where the smoke is produced.
- The ventilation of the fire [11] and the configuration of the combustible.
- The cooling of the fire gases and the time between the smoke formation and the smoke measurements. Due to coagulation, condensation, evaporation and settling the smoke becomes changed with time [18]. Thus aged cold smoke can be different from young hot smoke [12].

Generally little is known about the processes during combustion which lead to formation of smoke, and the list above could have been longer. Also there are interactions between the processes.

Depending on the burning conditions the smoke particulates consist of conglomerates of liquid and spherical aggregates with diameters from 2 nm to 0.5 μm [10]:

- Low temperature pyrolysis yields larger aggregates with diameters from 50 nm to 0.5 μm (and an average of 0.1 μm).
- Combustion during higher temperature conditions (in a flaming fire) yields minute particles (with diameters of 10-100 nm) on the fuel rich side of the flame (these

cause the yellow luminosity to the flames) [13]. The minute particles can oxidize within the flame, but if the temperature and oxygen concentration are not high enough they agglomerate to particles with diameters ranging approximately between 0.6 and 1.1 μm , and they escape the flames as smoke.

One of the parts of smoke is soot. The soot from flaming fires is formed from the intermediate pyrolysis products which mostly are aliphatic and aromatic components. Soot is formed during high temperature combustion but with lack of oxygen.

2.2 Production of Smoke

The production of smoke is governed by the burning conditions and the chemical nature of the combustible.

Smoke originates from incomplete combustion of the pyrolysis products. The pyrolysis products consist mainly of aliphatic and aromatic components. Depending on the nature of the combustible, one of them predominates [10].

The significance of the chemical composition and structure of the fuel on smoke production is complex and not well known, however some general conclusions can be based on laboratory tests of combustible solids [10]:

- Hydrocarbon combustibles form more smoke particulates than oxygenated combustibles. Thus under free-burning conditions oxygenated fuels such as wood, polyacrylates and polyacetals produce less smoke than hydrocarbon fuels such as polyethylene and polystyrene.
- The aromatic content of the pyrolysis gases increases the smoke production (thus polystyrene produces more smoke than polyethylene).
- Thermosets give less smoke production than thermoplastics. This is due to the cross linked structure of thermosets which renders them liable to char and liberate fewer decomposition products to the gas phase. However if the thermosettings contain aromatic structures they form a lot of smoke.
- The tendency to char limits the smoke production, thus nitrogen-containing thermosets such as urea and melamine resins produce little smoke.
- Some pure fuels do not produce smoke (CO, formaldehyde, metaldehyde, formic acid and methyl alcohol) [13].

2.3 Measurement and Quantification of Smoke

Within fire testing the gravimetrical and the optical methods are frequently used as smoke measurement methods. Gravimetically measurement is done by filtering and weighting the smoke. Optical smoke measurement is done by measuring the obscuration of a light or laser beam through a smoke filled volume. This can be done either on a volume where the smoke is collected or by measurement of a smoke flow. (These two types of measurement are often referred to as static and dynamic respectively.)

Optical smoke measurement is done according to Bouger's Law (which is also called the Lambert-Beer Law [14]) and presumes uniform particles:

$$I_\lambda / I_{0\lambda} = e^{-k_\lambda l}$$

Eq. 2.1

where $I_{\lambda 0}$ is the intensity of the incident monochromatic light (with wavelength λ), I_λ is the intensity of the light transmitted through a path length l (m) in the smoke and k_λ is the light extinction coefficient (also called the smoke turbidy).

k_λ can be expressed as the product of the specific extinction coefficient $k_{m\lambda}$ and the mass concentration of the smoke particulates C_S (g/m³)

$$k_\lambda = k_{m\lambda} \cdot C_S$$

Eq. 2.2

$k_{m\lambda}$ can be divided into two parts according to whether the light is absorbed or scattered.

$$k_{m\lambda} = k_{m\lambda}^{\ a} + k_{m\lambda}^{\ s}$$

Eq. 2.3

where superscripts a and s denote absorbed and scattered. C_S can also be expressed as

$$C_S = \frac{Y_S \cdot RML}{V_d} = \rho_S \cdot f_v$$

Eq. 2.4

where Y_S is the yield of smoke (g/g), RML is the rate of mass loss, V_d is the volume duct flow (m³/s), ρ_S is the smoke particulate density (kg/m³) and f_v is the volume fraction of smoke particulates (m³/m³). The smoke extinction area (SEA; m²/kg) is

defined as:

$$SEA = k_{m\lambda} \cdot Y_S = \frac{k_\lambda \cdot V_d}{RML} = \frac{RSP}{RML}$$

Eq. 2.5

where the rate of smoke production (RSP; m^2/s) is defined as $k_\lambda \cdot V_d$.

In [15] Newman and Steciak studied smoke particulates from well-ventilated diffusion flames where the particle sizes ranged between 40 and 80 nm. They found that the smoke particulate volume fraction f_v could be determined by

$$f_v = \frac{k_\lambda \cdot \lambda}{c_\lambda}$$

Eq. 2.6

where c_λ is the smoke particulate extinction coefficient. By experiments they found an average value of the smoke particulate extinction coefficient of 7.0 and an average value of ρ_S of 1100 kg/m^3.

Thus for a monochromatic light source with wavelength 634 nm

$$k_{m\lambda} = \frac{c_\lambda}{\rho_S \cdot \lambda} = \frac{7.0}{1.1 \cdot 10^3 \cdot 634 \cdot 10^{-9}} = 10.0\ m^2/g$$

Eq. 2.7

It should be emphasized that corresponding research done with the Cone Calorimeter has not shown exactly the same results [16]. However as an approximation the results to Newman and Steciak will be used.

The rate of smoke particulate production (RPP) can be defined as

$$RPP = m_S = C_S \cdot V_f = \frac{\rho_S \cdot \lambda}{c_\lambda} \cdot k_\lambda \cdot V_f = \frac{1}{k_{m\lambda}} \cdot RSP \approx 0.1\ g/m^2 \cdot RSP$$

Eq. 2.8

If it is assumed that the smoke particulates follow the ideal gas law, then RPP can also be found with units moles per second:

$$RPP_{vol} = \frac{RPP}{M_W} \quad (\text{units: moles/s})$$

Eq. 2.9

where M_W is the particulate molar mass.

Thus for the same light source

$$RPP_{vol} = 8.289 \cdot 10^{-3} \cdot RSP \text{ (units: mol/s).}$$

$k_{\lambda m}$ is in the range of 10 000 - 12 000 m²/kg for soots consisting of nearly pure graphic carbon. For white smoke the literature suggests 2000 - 5000 m²/kg [16].

For bench scale flaming and non-flaming combustion average values of $k_{\lambda m}$ of 7600 m²/kg and 4400 m²/kg respectively are found (based on measurements on both wood and plastic combustibles) [16].

2.3.1 The Impact of the Optical Smoke Measuring System

Two commonly used smoke measurement systems are the helium-neon laser (e.g. the ISO Cone Calorimeter) and systems which simulate a human eye (e.g. the ISO Room Corner Test). Testing in the Cone Calorimeter have shown that the difference between two such systems is small [35].

Figure 2-1 and Figure 2-2 show the comparison between smoke test data obtained in the Cone Calorimeter with two different smoke systems. On the X-axis the results are obtained with the helium neon laser, and on the Y-axis the results are obtained with an eye simulating system. Figure 2-1 shows the comparison of the peak smoke production, and Figure 2-2 shows the total smoke production. The numbers are related to building product identification (cf. Chapter 3). As the figures show, differences between the two measurement systems are in most cases small. (The figures are based on the same data as in [35].) To some degree the same has also been shown for static smoke measurements [17].

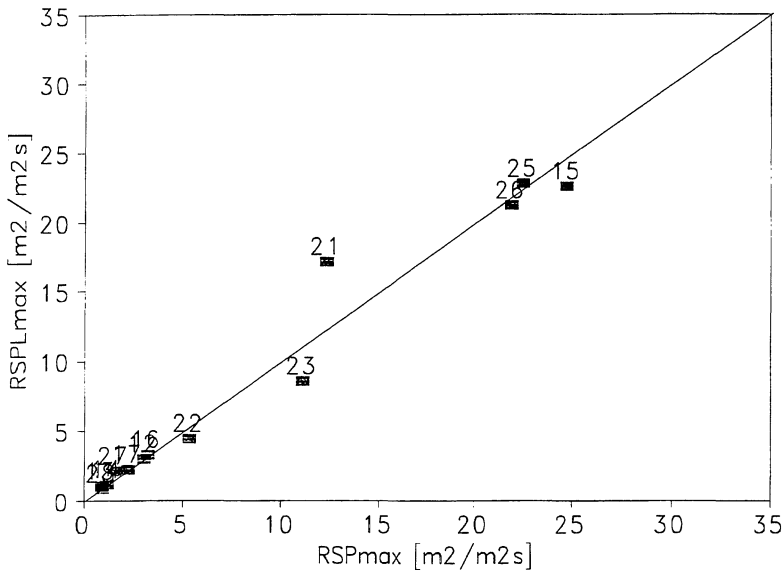

Figure 2-1 *Comparison of the maximum rate of smoke production measured with a Helium-Neon laser (X-axis: RSP_{max}) and an eye simulating system (Y-axis; $RSP_{L,max}$).*

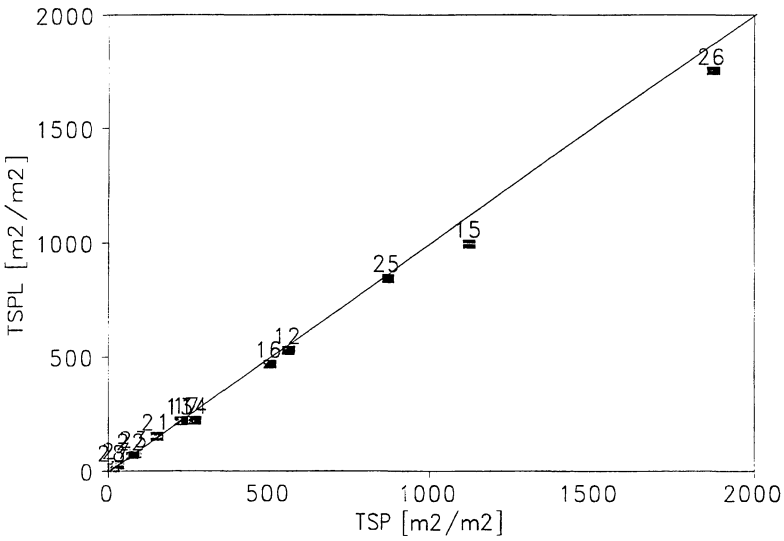

Figure 2-2 *Comparison of the total smoke production measured with a Helium-Neon laser (X-axis: TSP) and an eye simulating system (Y-axis; TSP_L).*

2.4 Visibility through Smoke

The visibility through smoke depends on three main factors:
- The smoke concentration and the characteristics of the smoke.
- Visual acuity and exposure of the evacuee.
- The object.

The smoke concentration depends on the amount of smoke and the size of the volume it is dispersed in. The characteristics depend on the combustion conditions (pyrolysing, smoldering or flaming fire) and the effect of ageing. Non-flaming produced smoke can also be light scattering, and this also reduces the visibility. Generally the size of the smoke particulates which are visible for the human eye have diameters ranging between 0.05 and 10 μm [18], and those with diameter around 1 μm impair visibility most [10].

The visibility also depends on the visual acuity of the observer and whether the smoke irritates the eyes [19]. The object is also important; whether it is illuminated or not, the background illumination and the contrast between the objects (or the object and the background).

Jin has proposed the following relationship between visibility (Vis; m) and the light extinction coefficient k (Jin is referred to in [19]):

$$Vis = K / k$$

Eq. 2.10

where K is equal to 6 for illuminated signs and 2 for reflecting signs and building component in reflected light.

Another relationship has been found by Heskestad (who is referenced in [19]):

$$Vis = K / k^{0.69}$$

Eq. 2.11

where K is equal to 6.6 for focused lamps and illuminated signs.

There can be quite large differences between the visibility determined by Eq. 2.10 and Eq. 2.11 and this indicates uncertainty of visibility predictions.

The equations do not reflect the influence of physiological and eye irritating effects on visibility. The irritating effects on the eyes and the respiratory tract depend on the type of smoke. In general it is predicted that smoke from a mixed fuel source with an

extinction coefficient of 1.2 m^{-1} would be strongly irritant [77], and this value can be used as a tenability limit.

2.5 Impact on the Visibility of Ageing of Smoke

The ageing of smoke both increases and decreases the optical density of the smoke. The ageing of smoke produced under flaming conditions has been reported to increase the optical smoke density [20] [21]. Testing in static small scale tests shows a slight decrease in the smoke obscuration as a function of time. Thus it seems that effects of ageing initially increase the smoke optical density, then after some time it has some decreasing effects. The reason for this might be the change in the size distribution to the smoke particulates. As the smoke ages the particulates conglomerate and they becomes larger. Thus after some time the smoke might become more obscurate. However as the anglomoration continues some parts of the particulates can become quite large (e.g. cf. [22]) and thus invisible (smoke particulates with diameters exceeding 2-4 μm are invisible).

3 MATERIALS, METHODS AND EXPERIMENTAL RESULTS

3.1 Introduction

Experimental fire test data have been collected from nine fire test organizations and two material suppliers within Europe. In addition fire test data have also been procured by the University of Trondheim, The Norwegian Institute of Technology (NTH), Norway (by the author). The laboratories and material suppliers are:

1. SINTEF NBL Norwegian Fire Research Laboratory (NBL), Norway.
2. Swedish National Testing and Research Institute (SP), Sweden.
3. Technical Research Centre of Finland (VTT), Finland.
4. Danish Fire Research Institute, Denmark.
5. Rockwool Systems (RW), Denmark.
6. Centre Scientifique et Technique du Bâtiment (CSTB), France
7. University of Lund, Sweden
8. Swedish Institute for Wood Technology Research (Trätek), Sweden.
9. BASF AG, Germany.
10. Laboratorio di Studi e ricerche sul fuoco (LSF), Italy.
11. Laboratoire National d'Essais (LNE), France.

The material data originate from six enlarged scale, full scale, medium scale and bench scale fire test methods:

Enlarged scale:
- The Enlarged Room Corner Test

Full scale:
- The ISO Room Corner Test (which is equivalent to NT FIRE 025 [23])
- The French CSTB Room Fire Test

Medium scale:
- The Medium Scale Room Corner Test

Bench scale:
- The ISO Cone Calorimeter
- The ISO Dual Chamber Box

3.2 Materials

According to their origin the construction products are divided into 6 sets:

1. The EUREFIC products (nos. 1 - 11).
2. The Nordic Round Robin products (nos. 12 - 15).
3. The Scandinavian products (nos. 16 - 28).
4. The IMO products (nos. 29 - 32).
5. Other products (nos. 33 - 34).
6. The French products (nos. 60 - 77).

The material data are given in Table 3-1 to Table 3-6. The following abbreviations are used throughout the tables:

gpp	gypsum paper plaster board
FR	fire retarded
nc	non-combustible
PU	polyurethane
*	thickness of surface layer(s)
**	total

Table 3-1 The EUREFIC products

No.	Product	Thickness [mm]	Density [kg/m^3]
1	Painted gpp	12	800
2	Ordinary birch plywood	12	600
3	Textile wallcovering on gpp	12+1*	800
4	Melamine faced high density nc board	12+1.5*	1055**
5	Plastic faced steel sheet on mineral wool	13+0.15+0.7*	640**
6	FR particle board, type B1	16	630
7	Combustible faced mineral wool	30+1*	87**
8	FR particle board	12	750
9	Plastic faced steel sheet on PU foam	80+0.1+1*	160**
10	PVC wallcovering on gpp	12+0.9*	800
11	FR polystyrene foam	25	37

Table 3-2 The Nordic Round Robin Products.

No.	Product	Thickness [mm]	Density [kg/m^3]
12	Birch plywood	12	600
13	FR plywood	9	620
14	Melamine faced particle board	12+0.1*	680
15	FR polystyrene foam	25	30

Table 3-3 The Scandinavian products.

No.	Product	Thickness [mm]	Density [kg/m^3]
16	Particle board	10	670
17	Insulating wood fibre board	13	250
18	Medium density wood fibre board	12	655
19	Wood panel, spruce	11	450
20	Melamine faced particle board	12+1	870
21	PVC wallcovering on gpp	13+0.7	725
22	Textile wallcovering on gpp	13+0.5*	725
23	Textile wallcovering on mineral wool	42+0.5*	150
24	Paper wallcovering on particle board	10+0.5*	670
25	Polyurethane foam	30	32
26	Polystyrene foam	49	18
27	Paper wallcovering on gpp	13+0.5*	725
28	gpp	13	700

Table 3-4 The IMO products.

No.	Product	Thickness [mm]	Density [kg/m^3]
29	PVC faced steel sheet on mineral wool	50+0.7+0.15*	-
30	0.8 mm formaldehyde on nc board	19+0.8*	-
31	1.4 mm formaldehyde on nc board	19+1.4*	-
32	Painted steel plate	0.7+0.15*	-

Table 3-5 Other products.

No.	Product	Thickness [mm]	Density [kg/m^3]
33	Polyethylene foam with nc coating	50	24
34	Steel sheet on polyurethane foam	50	38

Table 3-6 The French products.

No.	Product	Thickness [mm]	Density [kg/m^3]
60	Plywood	10	470
61	Particle board	8	850
63	Polyisocyanurate foam with surface coating	30	47
67	Polyurethane foam with surface coating	40	40
69	Polystyrene foam	79	14
70	Plastic wallcovering on gpp	12+1-7*	-
71	PVC wallcovering on gpp	12+1.1*	-

The 11 EUREFIC products (nos. 1 - 11) were tested in full scale (i.e. the ISO Room Corner Test) in the EUREFIC programme [24]. The 4 Nordic Round Robin products (nos. 12 - 15) were full scale tested between May 1989 and June 1990 in a Room Corner test round robin project. Five laboratories participated: FRS[2], NBL, RW, SP and VTT [25] [26]. The 13 Scandinavian products (nos. 16 - 28) were full scale tested by SP in the early eighties [27]. The 4 IMO products (nos. 29 - 32) were full scale tested in a project at SINTEF NBL Norwegian Fire Research Laboratory [28]. The 2 «other» products (nos. 33 - 34) were full scale tested in 1994 (references are not given due to the agreement with the principals).

The French products (nos. 60 - 76) were full scale tested in the French CSTB Room Fire Test during the early nineties [29]. Five products are left out (nos. 72 - 76) [30] due to questionable full scale smoke test data.

(The testing in bench scale, medium scale and enlarged scale are referred to in the experiment results sections.)

3.3 Methods; The ISO 9705 Room Corner Test

3.3.1 General Description

The ISO 9705 Room Corner Test [31] is a full scale fire test method for evaluation of building products. The method evaluates the contribution to fire growth provided by building products. Examples of building products are surface products (e.g. wallcoverings), wood based products (e.g. wood, plywood and particle board), insulation products (e.g. plastic foams) and laminated and sandwich products.

2 Fire Research Station, United Kingdom.

The arrangement of the test is shown in the some of the previous publications (i.e. the Nordtest and the ISC'94 publication). The room has a floor area of 8.64 m^2 (2.4 m x 3.6 m) and a height of 2.4 m. The doorway has dimensions of 0.8 m x 2.0 m. The building product is mounted on three walls (not on the doorway wall) and in the ceiling. The fire source is a propane burner mounted in floor height in one of the inner corners. The burner heat release is 100 kW for the first 10 minutes, then it is raised to 300 kW for the last 10 minutes. The test is stopped when flashover conditions occur, else the test duration is 20 minutes.

Flashover occurs per definition when the gross heat release rate exceeds 1000 kW. Another common flashover criterion is when flames emerge out of the opening.

Outside the door is the exhaust duct system where the fire gases are collected. The following measurements are normally done on the fire gases in the exhaust system:

- the volume duct flow rate V_d
- the temperature to the fire gases T_d
- the oxygen concentration
- the concentration of the species CO and CO_2
- the smoke density

Gas and surface temperatures are also measured within the room.

The rate of heat release (RHR) is calculated according to the oxygen consumption principle. The smoke density is measured with a multichromatic white light system which simulates a human eye.

3.3.2 System Performance and Time Delays

The time from the combustion reactions actually occur to the measurements are logged by the computer is called the time delay. The time delay can be divided into four parts:

1. The time from when the combustions occur to when the fire gases are transported outside the room.
2. Time for the fire gases to be transported from outside the room to the sampling line in the exhaust duct.
3. Time for the fire gases to be transported from the sampling line to the analysers.
4. The response time of the analysers.

The first and second parts are the same for all duct measurements. The third and fourth parts are small for the measurements of the volume duct flow, the duct temperature and the smoke density, because these are measured directly in the duct, and their response times are within seconds. Table 3-7 gives an indication of response times for the other measurements [25].

Table 3-7 Response time for duct measurements.

Type of measurement	Response time [s]	Resolution [‰]	Total delay [s]
$[O_2]$	4-15	0.2-1	13-70
[CO]	6-15	0.005-0.1	12-48
$[CO_2]$	6-15	0.1-0.5	12-48

According to the ISO standard [31] neither the paramagnetic oxygen analyser nor the infrared CO and CO_2 analysers should have a time constant (i.e. response time) exceeding 3 seconds, and the transport system delay should not exceed 1 second.

Based on assessments of around 34 data files from the test, the experience is that the corrections of the time delays need special attention, because the corrections are difficult to do properly. Poor corrections cause minor problems when the time to flashover is evaluated, but when it comes to smoke (and CO) data, poor corrections can cause problems. Then poor corrections increase the variation to the data.

Another problem was that the logging intervals were too large. Since the flashover fires tend to grow exponentially, the fires might grow to flashover within seconds. In these cases a logging interval of 5 seconds gives few measurements and the smoke production can only be crudely estimated (this was especially the case for product no. 25).

3.3.3 The Fire Source

The stochiometric reaction for propane is

$$C_3H_8 + 5O_2 \rightarrow 3CO_2 + 4H_2O$$

Complete combustion yields production rates of CO_2 of 6.5 g/s and 19.4 g/s with burner heat release rate of 100 kW and 300 kW respectively. The observed values for nearly non-combustible products are approximately 9 g/s and 22 g/s (respectively), thus the combustion is quite complete.

Figure 3-3 shows the rate of heat release and CO_2 as a function of time for product Nos. 27 and 28. The right panel indicates that it takes approximately 100 seconds to reach a heat output of 100 kW.

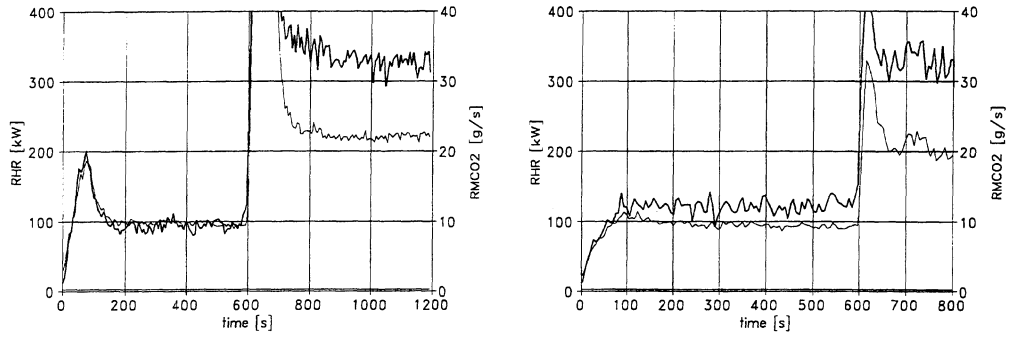

Figure 3-3 *The rate of heat release (Y1-axis and heavy solid line) and rate of CO_2 production (Y2-axis) as a function of time. Left panel: No. 27 Paper wallcovering on gypsum paper plaster board. Right panel: No. 28 Gypsum paper plaster board.*

Thus if the heat release from the burner should be subtracted to obtain an estimate of the net heat release from the combustible product, an estimate of the net burner output for the first 10 minutes can be 55 MJ.

The «background» rate of smoke production for the burner has been estimated to be about 0.1 m^2/s and 0.23 m^2/s for burner output of 100 kW and 300 kW respectively [24]. Figure 3-4 shows the rate of smoke production for nos. 27 and 28.

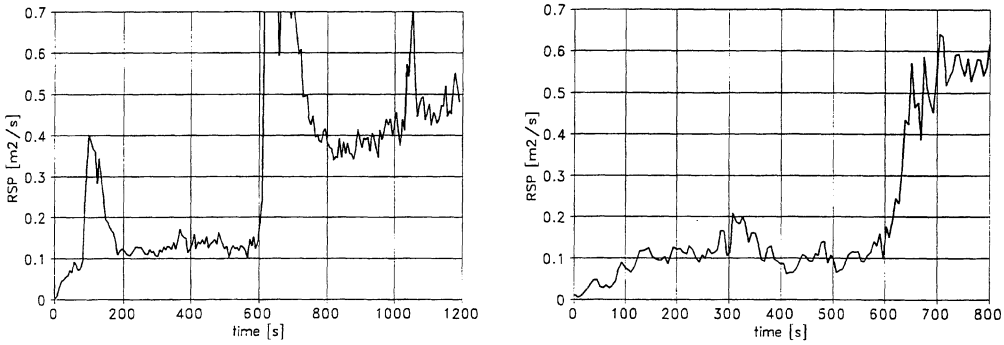

Figure 3-4 *Rate of smoke production as a function of time. Left panel: No. 27 Paper wallcovering on gypsum paper plasterboard Right pane: No. 28 Gypsum paper plasterboard.*

3.4 Methods; The French CSTB Room Fire Test

The French CSTB Room Fire Test is designed by Centre Scientifique et Technique du Bâtiment and used in their research (among other things on toxicity [29]). A draft of the test is shown in the ISC'94 publication.

The room has a floor area of 10.4 m^2 (2.8 m x 3.7 m), height 2.5 m and a door opening of 0.9 m x 2.0 m. The exhaust system is outside the room. The exhaust duct system consists of a natural convection chimney. The exhaust duct measurements are the same as in the ISO Room Corner Test. The specimens are mounted on the walls behind the fire source, and the covered area is varied. The duration of a test is 25 minutes (without regard to the occurrence of eventual flashover). The fire source is a wood crib of 12-13 kg and with a maximum heat release rate of 380 kW after about 6 minutes. After 20 minutes the total heat release from the fire source is around 240 MJ (which is approximately the same as for the ISO Room Corner Test after 20 minutes).

3.5 Methods: The ISO 5660 Cone Calorimeter

A draft of the ISO 5660 Cone Calorimeter [32] is given in some of the previous bublications (i.e. the Nordtest and the ISC'94 publication). The specimen (denoted sample in the figure) is wrapped in aluminium and mounted in a frame where the opening is 9.4 cm x 9.4 cm. Thus the exposed area is 0.0088 m^2. The specimen is either horizontally or vertically heat exposed by a cone heater with adjustable irradiance level (0 - 100 kW/m^2). The data considered here are found by horizontal testing at an irradiance level of 50 kW/m^2. There is also a spark igniter presented to ignite eventual gases during non-flaming burning. The mass loss is measured by a load cell, and in the exhaust duct system the same measurements are normally done as in the ISO Room Corner.

The smoke measurement system consists of a monochromatic laser light system with a wavelength of 634 nm. The heat release is calculated according to the oxygen consumption principle. Based on the measurements the fire test parameters presented in Table 3-8 can be obtained.

Table 3-8 Experimental test parameters obtained by the Cone Calorimeter test.

Test parameter	Brief description	Units
M_0	the initial mass of the specimen	[g]
t_{ign}	time to ignition	[s]
t_{max}	time to maximum heat release rate	[s]
t_{eof}	time to cease of flaming	[s]
RML_{max}	maximum rate of mass loss	[g/s·m^2]
RHR_{max}	maximum rate of heat release rate	[kW/s·m^2]
RSP_{max}	maximum rate of smoke production	[m^2/s·m^2]
$RMCO_{max}$	maximum rate of CO production	[g/s·m^2]
$RMCO_{2,max}$	maximum rate of CO_2 production	[g/s·m^2]
TML	total mass loss	[g/m^2]
THR	total heat release	[MJ/m^2]
TSP	total smoke production	[m^2/m^2]
TMCO	total CO production	[g/m^2]
$TMCO_2$	total CO_2 production	[g/m^2]

In addition parameters are also calculated that are combinations of those in Table 3-8. Examples are the effective heat of combustion ($\Delta h_{c,eff}$; units [MJ/kg]) and the smoke extinction area (SEA; units [m^2/kg]):

$$\Delta h_{c,eff} = \frac{HR}{ML} \quad \text{and} \quad SEA = \frac{SP}{ML}$$

where HR is the heat release, SP is the smoke production and ML is the mass loss.

Also other types of such parameters can be developed, and Chapter 4 is a study of the development of such parameters.

3.6 Methods; The Enlarged Room Corner Test

The Enlarged Room Corner Test has much in common with the ISO Room Corner Test - except that it is based on a larger space. Figure 3-5 shows the test. The area of the floor is 60.8 m^2 (6.75 m x 9.00 m) and the room height is 4.90 m. The door opening is 4 m^2 (2 m x 2 m). The opening factor ($AH^{1/2}/A_T$) is 0.020 m$^{1/2}$, i.e. approximately 40% lower than in the ISO Room Corner Test. The fire source consists of three burners identical to those in the Room Corner Test. The duration of a test is 30 minutes, if flashover has not occured (then the test is stopped). In the first 10 minute period the burner output is 100 kW, then it is raised to 300 kW for the next 10 minutes period, and finally it is raised to 900 kW for the last 10 minute period of the test. Several measurements were done in the room, in the opening and in the duct.

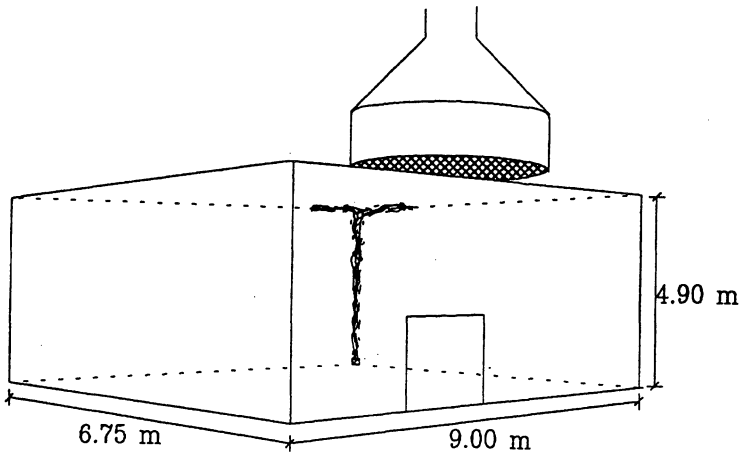

Figure 3-5 The Enlarged Scale Room Corner test

Five of the EUREFIC products are tested in the Enlarged Room Corner Test.

3.7 Methods; The Medium Scale Room Corner Test

The Medium Scale Room Corner Test is a 1/3 scale model of the ISO Room Corner Test. Specimens are mounted on three walls and in the ceiling. The room has a floor area of 0.96 m^2 (0.8 m x 1.2 m) and a ceiling height of 0.8 m. The door opening has a width of 0.56 m and a height of 0.67 m. The burner is mounted in the rear corner and has an output of 11 kW the first 10 minutes. Then it is raised to 33 kW for the last 10 minutes. The test is stopped if flashover conditions occur (here defined as when flames emerge out of the opening). A draft of the apparatus is shown in the ISC'94 publication.

3.8 Experimental Test Results; the ISO 9705 Room Corner Test

Table 3-9 gives the data for the 17 products which caused flashover within 10 minutes (i.e. product group 1). Table 3-10 gives the data for the 17 products in product group 2.

Note that the names of the products in the tables are abbreviated. If convinience these abbreviations are used later.

Table 3-9 Experimental test results for product groups 1 and 2A.

No.	Product	RSP(400) [m^2/s]	t_{FO} [min:sec]	RSP(1000) [m^2/s]
2	Plywood	1.1	2:30	10.3
7	Comb.faced min. wool	0.8	1:20	1.4
9	Steel on PU foam	1.4	3:15	7.4
11	FR PS foam	5.3	1:20	7.5
12	Plywood	0.9	2:17	10.6
14	Mel.faced particle board	2.2	3:02	17.2
16	Particle board	1.6	2:37	15.4
17	Wood fibre board	0.5	0:59	8.3
18	Wood fibre board	1.3	2:11	13.0
19	Wood	1.2	2:11	12.6
20	Mel.faced particle board	9.5	7:45	25.3
23	Textile on min.wool	0.3	0:43	14.3
24	Paper on particle board	1.5	2:23	7.1
25	PU foam	10.5	0:06	30.4
26	PS foam	4.0	1:55	17.2
33	PE foam	4.6	4:00	38.3
34	Steel on FR PU foam	10.9	5:15	12.5

gpp *gypsum paper plaster board*
RSP(400) *RSP at RHR 400 kW*
t_{FO} *time to reach 1000 kW (criterion for flashover)*
RSP(1000) *RSP at 1000 kW*

(In the testing of no. 2 and no. 7 in the ISO Room Corner Test, flames emerged out of the opening after 142 seconds and 205 seconds respectively [24]. For no. 2 the corresponding RHR and RSP then was 952 kW and 10 m^2/s. No. 7 was in the decay period, so these values are not used. The values used instead are selected at maximum heat release used: RHR = 1433 kW and RSP = 2.8 m^2/s. These values are necessary in the evaluation in Chapter. 8.)

Most of the test data presented are found on the original logging files. The full scale test data of the EUREFIC, the IMO and the «Other» products are found by the use of magnetically logged experimental test files and the Data Converting System developed at SINTEF NBL [33]. (The DCS is compatible with the Fire Data Management System [34].) The full scale test data of the Scandinavian products are found by the use of test data on magnetic files received from SP. (The full scale test data from the Nordic Round Robin products are found by communication with the respective test organizations.)

In some cases the time delay corrections were questionable, and these cases required a careful choice of the smoke data.

Table 3-10 Experimental test results for product group 2.

No.	Product	THR(10) [MJ]	TSP(10) [m^2]	THR(20) [MJ]	TSP(20) [m^2]
3	Textile on gpp	99	259	-	-
6	FR particle board, B1	79	558	-	-
10	PVC on gpp	79	965	-	-
21	PVC on gpp	55	275	-	-
22	Textile on gpp	76	53	-	-
32	Painted steel	67	254	-	-
1	Painted gpp	65	80	272	486
4	Melamine on n.c. board	57	191	270	2332
5	Steel on mineral wool	50	432	202	1722
8	FR particle board	68	189	281	3819
13	FR plywood	60	215	457	1210
15	FR PS foam	74	610	367	1810
27	Paper on gpp	60	84	305	46
28	Gpp	69	60	235	200
29	PVC on steel	60	573	248	2063
30	Formaldehyde on n.c. board	66	46	303	481
31	Formaldehyde on n.c. board	69	44	363	1417

nc non combustible

3.9 Experimental Test Results; The French CSTB Room Fire Test

The data are found on the logging sheets from the tests. The study of the data was limited because the data were not accessible on magnetic media and time delay corrections had not been done. The data are presented in Table 3-11. The output of the wood crib is not subtracted.

Table 3-11 Test data from the full scale experiments in the French CSTB Room Fire Test.

No.	Product	Ref.	A_b [m^2]	RHR_{max} [kW]	$[O_2]_{min}$ [vol%]	RSP_{max} [m^2/s]	$RVCO_{max}$ [m^3/s]	$RVCO_{2.max}$ [m^3/s]
60	Plywood	111	7	1 146	7	0	3	71
		112	15	2 254	1	9	19	129
		113	18	2 350	1	13	37	118
61	Particle board	121	8.3	1 820	-	6	7	104
		122	12.4	2 322	1	15	22	135
		123	16.5	2 427	-	15	40	141
63	Polyisocyanurate	312	3	781	12	13	6	41
	foam	313	3.75	912	12	12	6	47
67	Polyurethane	322	6	1700	4	23	10	87
	foam	323	12	2197	-	23	22	105
69	Polystyrene	331	3	1750	4	17	7	87
	foam	332	6	n.m.	1	n.m.	n.m.	n.m.
		333	6	2111	2	23	15	99
70	Plastic on gpp	211	7	1552	2	8	6	76
		212	7	1245	4	5	4	62
71	PVC on gpp	221	5	556	-	16	7	31
		222	7	830	11	11	9	35

$[O_2]$ Oxygen concentration in the duct
gpp gypsum paper plaster board
Ref experimental test references according to [29].
A_b burned area
n.m. not measured

3.10 Experimental Test Results; the ISO 5660 Cone Calorimeter

The test data originate either from testing done by Trätek or The Norwegian Institute of Technology (NTH). The tests done by Trätek have previously been reported in [35] (The Scandinavian products), [36] (the Round Robin Products) and [37] (the Scandinavian products). The bench scale testing of the IMO products is reported in [28] and [38]. The bench scale testing of the French and «Other» products is done by the author at SINTEF NBL Norwegian Fire Research Laboratory. The test data are presented in Table 3-12 to Table 3-17.

Table 3-12 *The maximum values (under flaming conditions) for product group 1 tested horizontally in the Cone Calorimeter at 50 kW/m^2.*

No.	t_{ign} [s]	RMLmax [g/sm^2]	RHR_{max} [kW/m^2]	RSP_{max} [m^2/sm^2]	$RMCO_{max}$ [mg/sm^2]	$RMCO_{2,max}$ [g/sm^2]
2	30	36	386	4	111	33
7	5	6	171	3	18	4
9	19	15	142	16	436	9
11	31	21	490	32	1098	33
12	28	25	287	3	102	27
14	34	18	176	1	23	17
16	34	18	272	3	9	11
17	12	15	199	2	67	18
18	31	17	167	3	59	13
19	20	15	161	2	2	12
20	44	15	146	2	57	10
23	11	38	512	11	412	52
24	35	18	179	2	2	14
25	2	19	258	22	1514	15
26	39	13	321	22	678	20
33	5	55	411	5	477	27
34	6	42	260	23	1460	19

Table 3-13 *The accumulated values for product group 1 tested horizontally in the Cone Calorimeter at 50 kW/m^2.*

No.	TML [g/m^2]	THR [MJ/m^2]	TSP [^{m2}/m^2]	TMCO [g/m^2]	$TMCO_2$ [g/m^2]
2	7421	83	659	7	6561
7	34	1	20	0	33
9	1511	15	1350	42	1020
11	983	22	1588	53	1457
12	7500	86	560	18	7479
14	6921	87	270	2	6408
16	6534	94	504	3	3591
17	2972	41	246	4	3499
18	7284	80	875	13	6119
19	5363	59	378	1	4320
20	9318	94	856	59	5465
23	392	6	82	3	461
24	7006	75	454	2	5512
25	733	10	868	57	635
26	1119	31	1875	58	1931
33	1403	49	409	76	3342
34	1608	28	1588	154	1931

Table 3-14 The maximum values (under flaming conditions) for product group 2 tested horizontally in the Cone Calorimeter at 50 kW/m².

No.	t_{ign} [s]	RMLmax [g/sm²]	RHR_{max} [kW/m²]	RSP_{max} [m²/sm²]	$RMCO_{max}$ [mg/sm²]	$RMCO_{2,max}$ [g/sm²]
3	25	21	255	5	60	22
6	21	16	124	3	17	11
10	15	16	102	10	341	7
21	10	16	208	12	688	15
22	20	30	431	5	258	33
32	12	6	111	7	174	8
1	47	16	219	1	152	16
4	25	9	61	2	241	3
5	53	5	80	7	135	2
8	700	9	68	1	272	3
13	469	7	63	1	95	4
15	25	17	387	25	854	28
27	21	16	234	2	173	19
28	34	11	158	1	35	13
29	19	12	39	19	413	6
30	110	33	81	10	814	7
31	98	13	68	4	568	7

Table 3-15 The accumulated values for product group 2 tested horizontally in the Cone Calorimeter at 50 kW/m².

No.	TML [g/m²]	THR [MJ/m²]	TSP [m²/m²]	TMCO [g/m²]	$TMCO_2$ [g/m²]
3	1637	12	97	15	726
6	3693	23	241	171	985
10	1460	11	337	28	554
21	722	7	150	23	427
22	796	9	75	13	689
32	136	4	?	9	448
1	648	4	17	10	230
4	1517	8	249	38	385
5	165	1	153	3	44
8	5693	31	886	228	1380
13	3767	8	224	104	987
15	727	18	1124	35	1340
27	500	5	30	11	383
28	347	3	16	7	212
29	302	2	?	30	153
30	2136	6	?	105	859
31	2174	13	?	79	1369

Table 3-16 *The maximum values (under flaming conditions) for product group 3 tested horizontally in the Cone Calorimeter at 50 kW/m^2.*

No.	t_{ign} [s]	RMLmax [g/sm^2]	RHR_{max} [kW/m^2]	RSP_{max} [m^2/sm^2]	$RMCO_{max}$ [mg/sm^2]	$RMCO_{2,max}$ [g/sm^2]
60	28	32	175	2	360	19
61	37	101	278	3	432	30
63	10	53	254	12	1019	22
67	5	82	173	12	682	14
69	23	34	364	18	886	27
70	11	34	367	7	341	25
71	13	43	230	24	2716	14

Table 3-17 *The accumulated values for product group 3 tested horizontally in the Cone Calorimeter at 50 kW/m^2.*

No.	TML [g/m^2]	THR [MJ/m^2]	TSP [m^2/m^2]	TMCO [g/m^2]	$TMCO_2$ [g/m^2]
60	4348	54	367	91	5754
61	6786	82	421	144	8741
63	1169	20	278	205	1590
67	1433	25	580	82	1690
69	523	27	922	51	1951
70	1239	15	153	32	1201
71	1909	14	697	100	935

RSP_{max}, $RMCO_{max}$ and $RMCO_{2,max}$ are the maximum values under flaming conditions. THR, TSP, TMCO and $TMCO_2$ are integrated from the start of the test and until a mass loss criterion occurs (the mass loss rate falls below 0.02 g/s).

Nos. 33 and 34 were tested without surface protection.

The experimental test data for the products tested at Trätek [3] (i.e. nos. 1 - 28) have been found by repeated calculations of the original experimental data files. The experimental data of the products tested at Trätek are averages of two test runs, while the products in product group 3 are averaged over three test runs.

[3] The differences between smoke data in the monograph and in the four publications are caused of the systematic calculation error: The rate of smoke production was determined by use of the volume duct flow at 25°C instead of at actual temperature.

3.11 Experimental Test Results; The Enlarged Room Corner Test

Five EUREFIC products were tested in the Enlarged Room Corner Test. The results were reported in [39] and [40]. Only two of the products went to flashover in the sense that flames emerged out of the opening; no. 2 and 7. The data are presented in Table 3-18. They are found on magnetic files containing the experimental data (procured by SP).

Table 3-18 Test data from the tests done in the Enlarged Room Corner Test.

No.	t_{FO} [min: sec]	RHR_{FO} [kW]	RSP_{FO} [m^2/s]	THR [MJ] 10/20/30	TSP [m^2] 10/20/30
2	19:30	10 600	530	102/fo/(fo)	480/fo/(fo)
3	n.f	-	-	18/264/684	12/58/976
6	n.f	-	-	37/179/689	153/1919/21993
7	21:40	4 776	60	20/133/fo	36/1068/fo
10	n.f.	-	-	19/163/684	192/1672/14886

FO flashover; flashover criteria: Flames emerge out of the opening.
10/20/30 values integrated over the periods 0-10 min, 0-20 min and 0-30 min respectively

3.12 Experimental Test Results; The Medium Scale Room Corner Test

The testing of the Scandinavian products in the Medium Scale Room Corner test were reported in [41]. The data are presented Table 3-19.

Table 3-19 Experimental data at flashover conditions for the Scandinavian products tested in the Medium Scale Room Corner Test.

No.	t_{FEO} (min:s)	RHR_{FEO} [kW]	RSP_{FEO} [m^2/s]
16	3:50	48	1.0
17	1:15	55	0.4
18	3:30	66	0.8
19	4:40	48	0.2
20	13:25	48	1.7
21	10:20	58	1.2
22	10:35	49	0.4
23	0:55	55	1.1
24	3:40	50	0.7
25	0:12	70	n.m
26	10:40	74	0.7
27+28	n.f.	-	-

4 DEVELOPMENT OF FIRE PARAMETERS

4.1 Introduction

The experimental test results from fire test methods can either be directly used to assess fire properties of the tested product, or the assessment can be based on *deduced* parameters. Deduced parameters are combinations of the original test data. For example the average effective heat of combustion $\Delta h_{c,eff,avg}$ or the average smoke extinction area SEA_{avg} are deduced parameters based on the original test data (i.e. THR, TSP and THR):

$$\Delta h_{c,eff,avg} = \frac{THR}{TML} \quad \text{and} \quad SEA_{avg} = \frac{TSP}{TML}$$

Often the deduced parameters are ratios and thus can be identified as intensive parameters, while original test data are of the extensive type. The advantage with the deduced parameters is that they can be more informative than original test data and easier to interpret and understand. They can also be used to assess fire test results and they can have advantages when building smoke prediction models. This chapter concerns the development of a collection of deduced fire parameters and they are used in the model building study (Chapter 6).

4.2 The Reactant-Product Equation Model

The deduced parameters here have their origin in the reactant-product equation model. In the reactant-product equation model it is assumed that a combustible consists of C-, H- and O-atoms. The following distinguishes between whether the hydrocarbon consists of just C- and H-atoms or C-, H- and O-atoms.

4.2.1 Non-Containing Oxygen Hydrocarbon Combustible

A combustible which consists of C- and H -atoms is generally described as C_nH_m. When it burns completely with the oxygen in the air the reaction products are CO_2 and H_2O. Then C-, H- and O-balance give the following stoichiometric reaction equation:

$$xC_nH_m + (xn + \frac{xm}{4})(O2 + 3.76N_2) \rightarrow xnCO_2 + \frac{xm}{2}H_2O + 3.76(xn + \frac{xm}{4})N_2$$

Eq. 4.1

where x is the number of moles of combustible which react completely with the oxygen in the air.

If there is excess of air the excess moles of air are simply added to the stoichiometric reaction equation:

$$xC_nH_m + (xn + \frac{xm}{4})\alpha + e\alpha \rightarrow xnCO_2 + \frac{xm}{2}H_2O + 3.76(xn + \frac{xm}{4})N_2 + e\alpha$$

Eq. 4.2

where e is the number of moles of excess of air and $\alpha = O_2 + 3.76N_2$.

If the combustion occurs with deficiency of oxygen, then partly burnt species will be formed. The according reaction equation is then:

$$xC_nH_m + (xn + \frac{xm}{4} - \frac{1}{2}f - g - \frac{19}{2}h - \frac{1}{2}i)\alpha \rightarrow$$

$$(xn - f - g - 6h)CO_2 + (\frac{xm}{2} - 7h - i)H_2O + fCO + gC + hC_6H_{14} + iH_2 + 3.76(xn+..)N_2$$

Eq. 4.3

In the equation it is assumed that soot (ie. C), CO, unburnt hydrocarbons and H_2 are the only partly burnt species (the unburnt hydrocarbons are converted to equal amounts of n-hexane).

Other works have identified that several other species are also produced [1]. Thus the term $(pC+qH+rO)_{upcs}$ (where subscript upcs denotes *unknown partly combusted species*) has to be added. This term (which includes also unburnt fuel) includes the species which are not recorded as the terms in Eq. 4.3.

$$xC_nH_m + (xn + \frac{xm}{4} - \frac{1}{2}f - g - \frac{19}{2}h - \frac{1}{2}i - p - \frac{1}{4}q + \frac{1}{2}r)\alpha \rightarrow$$

$$(xn - f - g - 6h - p)CO_2 + (\frac{xm}{2} - 7h - i - \frac{1}{2}q)H_2O + fCO + gC + hC_6H_{14} + iH_2$$

$$+(pC + qH + rO)_{upcs} + 3.76(xn+..)N_2$$

Eq. 4.4

Notation for simplicity:

$$a = xn + \frac{xm}{4}$$

Eq. 4.5

$$j = xn + \frac{xm}{4} - \frac{1}{2}f - g - \frac{19}{2}h - \frac{1}{2}i - p - \frac{1}{4}q + \frac{1}{2}r$$

Eq. 4.6

$$k = xn - f - g - 6h - p$$

Eq. 4.7

$$l = \frac{xm}{2} - 7h - i - \frac{1}{2}q$$

Eq. 4.8

j can also be rearranged to consist of three terms:

$$j = (xn - \frac{1}{2}f - g - \frac{19}{2}h - p) + (\frac{xm}{4} - \frac{1}{2}i - \frac{1}{4}q) + \frac{1}{2}r = (k + \frac{1}{2}f) + \frac{1}{2}l + \frac{1}{2}r$$

Eq. 4.9

Eq. 4.9 makes the interpretation of j more obvious: The first term is the oxygen consumed to more or less pyrolyze the carbon in the combustible, the second term is the same for the hydrogen in the combustible and the third term is the amount of the consumed oxygen which has been used to form other species.

Hence:

$$xC_nH_m + j\alpha \rightarrow$$
$$kCO_2 + lH_2O + fCO + gC + hC_6H_{14} + iH_2 + (pC + qH + rO)_{upcs} + 3.76jN_2$$

Eq. 4.10

The equations above were for either excess of oxygen or lack of oxygen. In real combustion both excess of oxygen and also partly combusted species as CO, smoke and unburnt hydrocarbons can be observed. This is due to a too low temperature for complete combustion.

Thus the most realistic reaction equation is:

$$xC_nH_m + j\alpha + e\alpha \rightarrow$$
$$kCO_2 + lH_2O + fCO + gC + hC_6H_{14} + iH_2 + (pC + qH + rO)_{upcs} + e\alpha + 3.76(j+e)N_2$$

Eq. 4.11

4.2.2 Oxygen Containing Hydrocarbon Combustible

C-, H- and O-balance for an oxygen containing hydrocarbon combustible $C_nH_mO_s$ gives the following reaction equation:

$$xC_nH_mO_s + (xn + \frac{xm}{4} - \frac{xs}{2})(O_2 + 3.76N_2) \rightarrow$$
$$xnCO_2 + \frac{xm}{2}H_2O + 3.76(xn + \frac{xm}{4} - \frac{xs}{2})N_2$$

Eq. 4.12

Accordingly for e moles excess of air:

$$xC_nH_mO_s + (xn + \frac{xm}{4} - \frac{xs}{2})\alpha + e\alpha \rightarrow$$
$$xnCO_2 + \frac{xm}{2}H_2O + 3.76(xn + \frac{xm}{4} - \frac{xs}{2})N_2 + e\alpha$$

Eq. 4.13

For deficiency of oxygen:

$$xC_nH_mO_s + (xn + \frac{xm}{4} - \frac{1}{2}f - g - \frac{19}{2}h - \frac{1}{2}i - \frac{1}{2}xs - p - \frac{1}{4}q + \frac{1}{2}r)\alpha \rightarrow$$
$$(xn - f - g - 6h - p)CO_2 + (\frac{xm}{2} - 7h - i - \frac{1}{2}q)H_2O + fCO + g \cdot C + hC_6H + iH_2$$
$$+(pC + qH + rO)_{upcs} + 3.76(xn+..)N_2$$

Eq. 4.14

Notation for simplicity:

$$j' = xn + \frac{xm}{4} - \frac{1}{2}f - g - \frac{19}{2}h - \frac{1}{2}i - \frac{1}{2}xs - p - \frac{1}{4}q + \frac{1}{2}r$$

Eq. 4.15

Hence:

$$xC_nH_mO_s + j'\alpha \rightarrow kCO_2 + lH_2O + fCO + gC + hC_6H_{14} + iH_2 + (pC + qH + rO)_{upcs} + 3.76jN_2$$

Eq. 4.16

Thus the most realistic reaction for the oxygen containing combustible is:

$$xC_nH_mO_s + j'\alpha + e\alpha \rightarrow kCO_2 + lH_2O + fCO + gC + hC_6H_{14} + iH_2 + e\alpha + (pC + qH + rO)_{upcs} + 3.76(j + e)N_2$$

Eq. 4.17

Further on only the reactant-product equation for the non oxygen containing combustible (ie. C_nH_m) will be used, because in the fire tests considered the chemical composition of the material is normally unknown.

4.2.3 The modified reactant-product equation

In the fire tests considered here, normally the only measured species are the concentration of O_2, CO_2 and CO (and smoke). And the chemical composition of the combustibles is generally unknown. Thus the starting point for the development of the deduced parameters is the equation for the non-containing oxygen combustible C_nH_m modified to

$$xC_nH_m + (xn + \frac{xm}{4} - \frac{1}{2}f - g)\alpha \rightarrow (xn - f - g)CO_2 + \frac{xm}{2}H_2O + fCO + gC$$

Eq. 4.18

It should be emphasized that the preceeding equations are very simplifyed. Only carbon, hydrogen and oxygen atoms in the chemical composition is considered. Soot does not appear as pure carbon particles, but contain about 1% hydrogen [43]. However, to obtain a systematic starting point these equations are convenient.

4.3 The Global Equivalence Ratio

The global equivalence ratio GER is defined as [44]:

$$GER = \phi = \frac{(F/A)}{(F/A)_{st}}$$

Eq. 4.19

where F/A is the ratio between fuel and air and subscript st denotes stoichiometric value. Normally the GER is calculated by measurements of the mass burning rate, the air inflow and the knowledge of the stoichiometric fuel to air ratio of the fuel. The GER can also be determined by use of the measurements done in the combustion gases: Eq. 4.1 gives for the C_nH_m combustible:

$$(F/A)_{st} = \frac{xC_nH_m}{(xn + \frac{xm}{4})\alpha}$$

Eq. 4.20

For complete reaction with excess of oxygen (ie. Eq. 4) the fuel to air ratio becomes:

$$(F/A) = \frac{xC_nH_m}{(a+e)\alpha}$$

Eq. 4.21

Eq. 4.20 and Eq. 4.21 into Eq. 4.19 gives

$$\phi = \frac{a}{a+e}$$

Eq. 4.22

The fuel to air ratio for the oxygen deficiency reaction equation is:

$$F/A = \frac{xC_nH_m}{(xn + \frac{xm}{4} - \frac{1}{2}f - g - \frac{19}{2}h - \frac{1}{2}i - p - \frac{1}{4}q + \frac{1}{2}r)\alpha}$$

Eq. 4.23

Thus:

$$\phi = \frac{a}{j} = \frac{xn + \frac{xm}{4}}{xn + \frac{xm}{4} - \frac{1}{2}f - \frac{19}{2}h - \frac{1}{2}i - p - \frac{1}{4}q + \frac{1}{2}r}$$

Eq. 4.24

Eq. 4.24 can be shown to be:

$$\phi = 1 + \frac{1}{2}\frac{f}{j} + \frac{g}{j} + \frac{19}{2}\frac{h}{j} + \frac{1}{2}\frac{i}{j} + \frac{p}{j} + \frac{1}{4}\frac{q}{j} - \frac{1}{2}\frac{r}{j}$$

Eq. 4.25

If the most real reaction equation is used, then it can be shown that the equation for ϕ for the C_nH_m combustible is:

$$\phi = 1 + \frac{1}{2}\frac{f}{j+e} + \frac{g}{j+e} + \frac{19}{2}\frac{h}{j+e} + \frac{1}{2}\frac{i}{j+e} + \frac{p}{j+e} + \frac{1}{4}\frac{q}{j+e} - \frac{1}{2}\frac{r}{j+e}$$

Eq. 4.26

This means that if all fire effluents in the combustion gases were determined, then ϕ based on Eq. 4.25 would have given the same result as the ratio of pyrolysed mass and ventilation (i.e. Eq. 4.19).

4.4 Deduced Fire Parameters

4.4.1 The Global Equivalence Ratio Factors

The global equivalence ratio equation developed here consists of several terms according to the partly combusted species. According to Eq. 4.25 the following parameters are defined:

$$\phi = 1 + \frac{1}{2}\frac{f}{j} + \frac{g}{j} + \frac{19}{2}\frac{h}{j} + \frac{1}{2}\frac{i}{j} + \left(\frac{p}{j} + \frac{1}{4}\frac{q}{j} - \frac{1}{2}\frac{r}{j}\right)_{upcs}$$

$$= 1 + \frac{1}{2}\phi_{CO} + \phi_S + \frac{19}{12}\phi_{C_nH_m} + \frac{1}{2}\phi_{H_2} + \phi_{upcs} = 1 + \phi_{kpcs} + \phi_{upcs}$$

Eq. 4.27

where subscript kpcs denotes *known partly combusted species*. ϕ_S and ϕ_{CO} can be interpreted as smoke and CO production per oxygen (i.e. O_2) consumed. They are referred to as the smoke and CO equivalence ratio factor respectively.

Another parameter that is used is the smoke production (SP) per heat release (HR). The heat release so far has been calculated based on the oxygen consumption method and it has been assumed that all used oxygen has produced complete combustion products (i.e. CO_2 and H_2O), thus

$$\frac{SP}{HR} = \phi_S \cdot \frac{120.4\,m^2 / mol\,C}{0.419\,MJ / mol\,O_2} = r_{S/Q} = 287 \cdot \phi_S$$

Eq. 4.28

This parameter has already been used in the IAFSS'94-publication and by others [45]. The parameter is denoted $r_{S/Q}$ and referred to as the *smoke to flame ratio*. ϕ_S also has a relation to the smoke extinction area SEA (i.e. smoke production per mass loss):

$$\phi_S = \frac{SP}{HR} \cdot \frac{0.419\,MJ / molO_2}{120.4\,m^2 / molC} = \frac{SEA}{\Delta h_{c,eff}} \cdot \frac{0.419\,MJ / molO_2}{120.6\,m^2 / molC}$$

$$= \frac{SP}{HR} \cdot 0.003\,MJ / m^2 = 0.003 \cdot r_{S/Q}$$

Eq. 4.29

4.4.2 Carbon Conversion Factors

Based on the reactant-product equations the conversion of pyrolysed carbon from the fuel into smoke and CO can also be calculated. The conversion of pyrolysed carbon in the fuel into smoke (f_S) and CO (f_{CO}) is respectively:

$$f_S = \frac{g}{xn}$$

Eq. 4.30

and:

$$f_{CO} = \frac{f}{xn}$$

Eq. 4.31

which is identical to

$$f_S = \frac{g}{k + f + g + 6h + p}$$

Eq. 4.32

and

$$f_{CO} = \frac{f}{k + f + g + 6h + p}$$

Eq. 4.33

f_S and f_{CO} are identical in mass and molar basis, but note that in other literature sometimes f_{CO} is calculated in mass basis with the molar mass of CO (and not C). In the test data considered here the coefficients h and p are not known, thus f_S and f_{CO} are estimated with the term (k+f+g) as the denominator.

It can be shown that the f_j parameters (where j can be S and CO) here are identical to the generation efficiency parameter η_j used by Tewarson et al. [46] . They define η_j as

$$\eta_j = \frac{G_j}{m_f \cdot \psi_j}$$

where G_j is the mass generation of specie j and m_f is the mass loss of fuel. ψ_j is the maximum conversion of the fuel into specie j:

$$\psi_j = \nu_j \cdot \frac{M_{W,j}}{M_{W,f}}$$

where ν_j is the maximum stoichiometric coefficient of specie j and $M_{W,j}$ and $M_{W,f}$ are the molecular mass of specie j and fuel, respectively.

A simplified version of the reactant-product equation is

$$xC_nH_m + j\alpha \rightarrow kCO_2 + lH_2O + fCO + gC + 3.76jN_2$$

If the specie j considered for example is CO, then ν_{CO} is n:

$$C_nH_m + j\alpha \rightarrow lH_2O + nCO + 3.76jN_2 .$$

Thus

$$\eta_{CO} = \frac{G_{CO}}{m_f \cdot \psi_{CO}} = \frac{f \cdot M_{W,CO}}{x \cdot M_{W,C_nH_m} \cdot n \cdot \frac{M_{W,CO}}{M_{W,C_nH_m}}} = \frac{f}{xn} \qquad \text{(q.e.d.)}$$

(And the same can be shown for other fire effluents.)

4.4.3 The C/H ratio

The C/H-ratio $r_{C/H}$ may be an important parameter for the overall smoke production (it is shown to influence the CO production). In the actual fire tests the C/H ratio of the fuel is not known, but an estimated value can be found from the measurements in the combustion gases:

$$r_{C/H} = C / H = \frac{xn}{xm} = \frac{k + f + g + 6h + p}{2l + 14h + 2i + q}$$

Eq. 4.34

Since neither H_2O (i.e. the l coefficient in the reactant-product equation model) nor other species which contain H-atoms are measured, the amount of H-atoms have to be estimated. If it is assumed that all O-atoms not used to produce CO_2 and CO are used to produce H_2O, then

$$l = 2(j - k - 0.5f)$$

Eq. 4.35

Thus if it is further assumed that all the pyrolysed C-atoms appear either in the CO_2, CO or the smoke, then Eq. 4.34 is modified to

$$r_{C/H} \approx \frac{k + f + g}{4(j - k - 0.5f)}$$

Eq. 4.36

4.4.4 Residue fraction (ν)

If the initial mass of the specimen (M_0) and the total mass loss (TML) are known, then the mass residue fraction ν (units: g/g) can be found:

$$\nu_{res} = \frac{M_0 - TML}{M_0}$$

Eq. 4.37

When the specimen consists of incombustible parts (such as steel sheets) this will also be included as residue fraction. In such cases the residue fraction is not identical to the char fraction.

4.4.5 Conversion of mass loss into mass fractions (μ)

The mass loss (ML) can be divided into fractions according to the combustion products.

The mass loss converted into complete combustion products (ie. CO_2 and H_2O) can be determined by

$$\mu_{ccs} = \frac{k \cdot M_{W,C} + 2l \cdot M_{W,H}}{ML} = \frac{k \cdot M_{W,C}}{ML} + \frac{2l \cdot M_{W,H}}{ML} = \mu_{CO_2} + \mu_{H_2O}$$

Eq. 4.38

where μ_{ccs} is the mass fraction of the mass loss converted into complete combustion species (i.e. CO_2 and H_2O) and $M_{W,C}$ and $M_{W,H}$ is the molar mass of carbon and hydrogen respectively. Note that the equation does not take into account that the combustible might consist of other atoms than C and H. For example if polyurethane is burning the N atoms might end up as HCN and NO_x.

The mass fraction converted into partly combusted species (μ_{pcs}) is

$$\mu_{pcs} = 1 - \mu_{ccs}$$

Eq. 4.39

μ_{pcs} can be further divided into two parts according to whether the partly combusted species is known (i.e. identified) or unknown:

$$\mu_{pcs} = \mu_{kpcs} + \mu_{upcs}$$

Eq. 4.40

where subscripts kpcs and upcs mean *known partly combusted species* and *unknown partly combusted species* respectively. *Known partly combusted species* can be the measured CO, carbonaceous smoke, H_2 and partly combusted hydrocarbons (in the reactant-product equation model identified as C_6H_{14}). Thus μ_{kpcs} can be determined by

$$\mu_{kpcs} = \frac{(f + g + 6h) \cdot M_{W,C} + i \cdot M_{W,H}}{ML}$$

Eq. 4.41

The *unknown partly combusted species* μ_{upcs} are all those not measured, i.e., the group $(pC+qH+rO)_{upcs}$, and their mass fraction is determined by

$$\mu_{upcs} = 1 - (\mu_{ccs} + \mu_{kpcs})$$

Eq. 4.42

The μ-factors are related to the yield Y of the chemical compounds. The yield of compound i Y_i (units: g/g) is defined as the ratio between the mass of specie i and the total mass loss. Thus for CO_2 it can be shown that

$$Y_{CO2} = \frac{k \cdot M_{W,CO2}}{ML} = \frac{k \cdot M_{W,CO2}}{x \cdot M_{W,CnHm}} = \mu_{CO2} \cdot \frac{M_{W,CO2}}{M_{W,C}}$$

Eq. 4.43

A similar equation can be shown for other compounds.

Since the test methods considered here only measure the specie concentrations of CO_2, CO and smoke in the combustion gases, only some estimate of μ_{ccs} can be found

$$\mu_{ccs} \approx \frac{k \cdot M_{W,C} + 2 \cdot 2(j - k - 0.5f) \cdot M_{W,H}}{ML}$$

Eq. 4.44

(where it is presumed that all used O-atoms are used to produce CO_2, CO and H_2O.)

And

$$\mu_{kpcs} = \frac{(f+g) \cdot M_{W,C}}{ML}$$

Eq. 4.45

4.4.6 Heat release related parameters

To model the heat release properties in bench scale two parameters have been developed; *the growth rate* and the t_{width}.

The growth rate is defined as

$$\frac{\partial RHR}{\partial t} = \ddot{Q} = \frac{RHR_{max}}{t_{max} - t_{ign}}$$

Eq. 4.46

And the t_{width} is defined as

$$t_{width} = \frac{THR}{RHR_{max}}$$

Eq. 4.47

A physical interpretation of t_{width} is the burn out time of a fuel element.

The left panel of Figure 4-1 shows an example for FR polystyrene foam [4]. These parameters can also be used to describe a combustible with several peak heat releases, and an example is given in the right panel of Figure 4-1 for ordinary birch plywood. Here the RHR_{max} is the arithmetic average of the two maxims, and denoted $RHR_{max,avg}$.

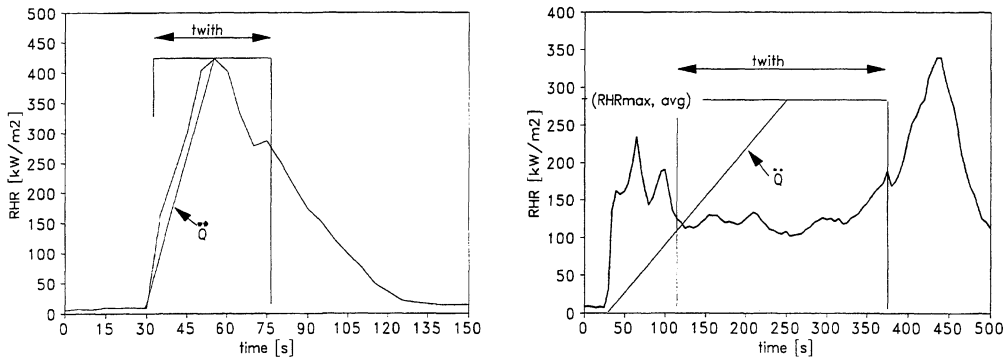

Figure 4-1 Left panel: The first (of two) test run of FR polystyrene foam (no. 11) in the ISO Cone Calorimeter at irradiance level 50 kW/m². Right panel: The first (of two) test run of ordinary birch plywood (no. 2) in the ISO Cone Calorimeter at irradiance level 50 kW/m².

[4] Note that t_{width} is misspelled with t_{with} in the figures

4.4.7 Dummy variables

Two dummy variables will also be used in the model building study.

The first dummy variable is 0 if the combustible does not have oxygen atoms in the chemical composition, and 1 if there is. The dummy is denoted [..O_s?]

The second dummy varible is 0 if the combustible is mainly wood based, and 1 if it is mainly plastic based. The dummy is denoted [plst?]

4.5 Relationship between Bench Scale Parameters

There are relationships between some of the bench scale variables, i.e. some of them are correlated. Knowledge of the relationships between the bench scale parameters is important background information in the model building study. This is given special attention here. Such knowledge can also be used to assess the data and detect outliers.

4.5.1 The ϕ- and f-factors

The predominant factor in the denominator of the global equivalence factors and the carbon conversion factors is the amount of CO_2. Since the combustion is quite efficient much CO_2 is produced and therefore the ϕ- and f-factors tend to be identical. This can be shown with two correlation plots. Figure 4-2 shows the correlation plot between $\phi_{S,avg}$ and $f_{S,avg}$. Figure 4-3 shows the correlation plot between $\phi_{CO,avg}$ and $f_{CO,avg}$.

4.5.2 The t_w-factors

The t_w-factors are the t_{width}, $t_{w,CO2}$, $t_{w,S}$ and $t_{w,CO}$. t_{width} is plotted versus $t_{w,CO2}$, $t_{w,S}$ and $t_{w,CO}$ in Figure 4-4, Figure 4-5 and Figure 4-6 respectively. Good correlations exist between t_{width} and $t_{w,CO2}$. There is also some correlation in the other two plots. Note that no. 8 was an outlier in Figure 4-5, and that nos. 6, 13, 20 and 28 were outliers in Figure 4-6.

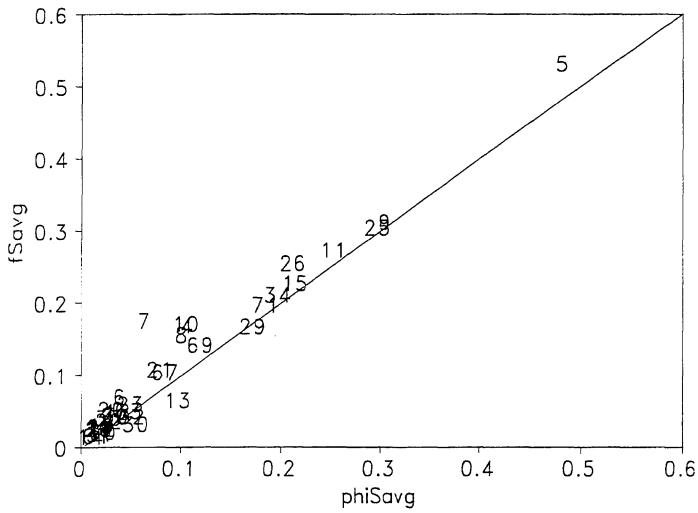

Figure 4-2 *The correlation plot between $\phi_{S,avg}$ and $f_{S,avg}$*

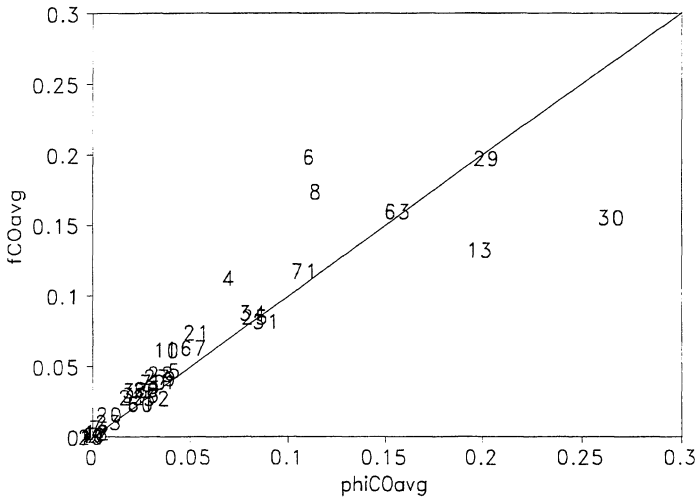

Figure 4-3 *The correlation plot between $\phi_{CO,avg}$ and $f_{CO,avg}$*

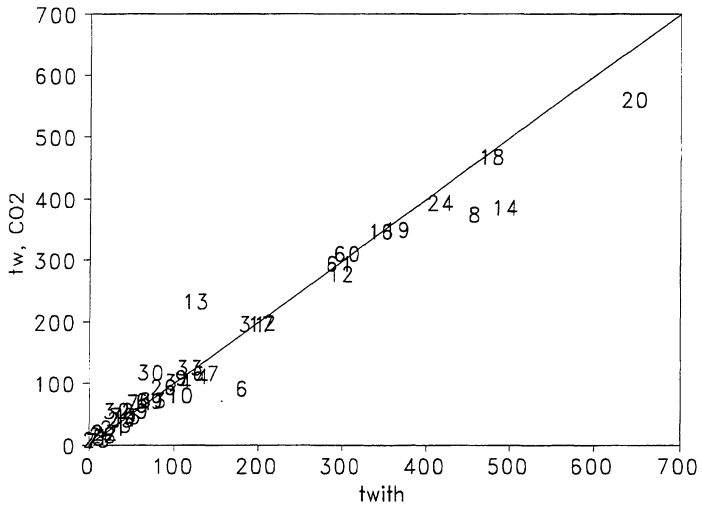

Figure 4-4 *The correlation plot between t_{width} and $t_{w,CO2}$.*

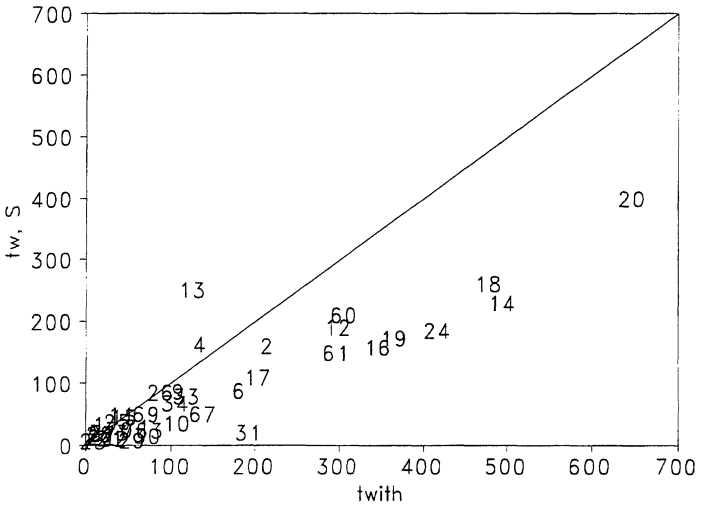

Figure 4-5 *The correlation plot between t_{width} and $t_{w,S}$.*

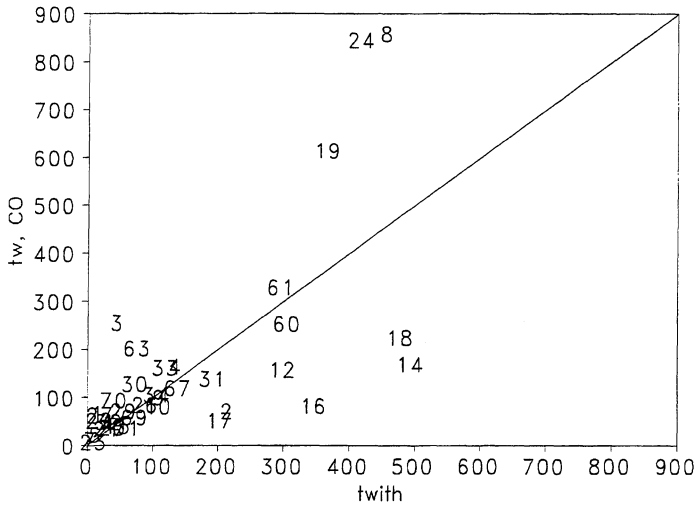

Figure 4-6 The correlation plot between t_{width} and $t_{w,CO}$.

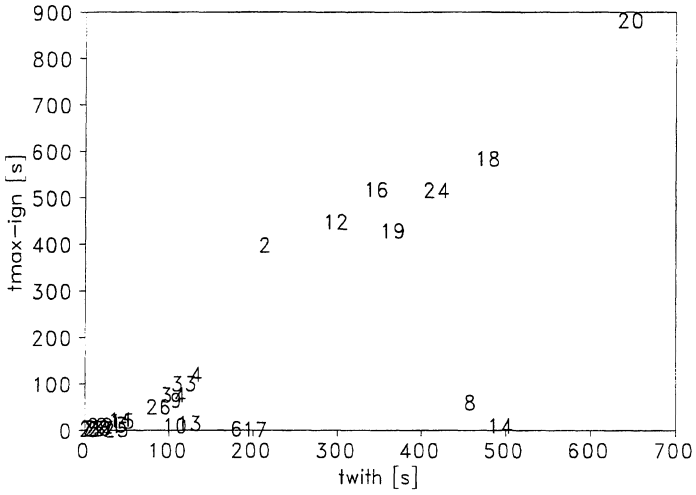

Figure 4-7 The correlation plot between t_{width} and $t_{max\text{-}ign}$.

5 STATISTICS

5.1 Introduction

The theory considered has mainly been found in [47] - [56] The model building study is conducted by use of the statistical package Minitab [56]. Some of the printouts from the package are included in the text in Chapter 6.

5.2 Basic Statistics

5.2.1 Type of Distribution

The choice of a distribution can be tested by a chi-square test which measures the goodness of the fit [53]. Such testing requires a sample consisting of several tests. The experiments considered here were repeated a maximum of three times. This is not sufficient to test the type of distribution, thus the type of distribution of the data considered here are not studied.

5.2.2 Sample Mean and Variance

The mean and variance of a population are denoted μ and σ^2 respectively. For a population they can be estimated by a sample consisting of n observations.

$$E(\mu) = \frac{\sum_{k=1}^{n} z_k}{n}$$

Eq. 5.1

$$Var(\mu) = \frac{1}{n-1} \sum_{k=1}^{n} (z_k - z_.)^2$$

Eq. 5.2

where subscript «.» (a dot) means average value.

5.2.3 Variation of the Deduced Fire Parameters

Many of the deduced fire parameters in Chapter 4 are combinations of several fire test parameters. Generally this was done by linear combinations of two or more fire test parameters and by the ratio between two parameters. The mean and variance of a deduced fire parameter which is based on linear combinations of k fire test parameters are

$$E(\mu) = a_1 \cdot \mu_1 + a_2 \cdot \mu_2 + ... + a_k \cdot \mu_k$$

Eq. 5.3

$$Var(\mu) = \sum_{i=1}^{k} a_i^2 \cdot \mu_i + 2 \sum_{i=1}^{k} \sum_{j=1}^{k} a_i a_j Cov(\mu_i, \mu_j)$$

Eq. 5.4

The variance of a deduced parameter which expresses the ratio between two fire test parameters have a more complex relationship. The important point is that if there is correlation between the fire test parameters that a deduced fire parameter is based on, then the correlation influences the variance of the deduced parameter.

5.2.4 Sample Covariance and Correlation

The sample covariance is a measure of how closely two variables tend to move together. If the two variables are denoted z and y, then the covariance s_{zy} between them is

$$s_{zy} = \frac{\sum_{i=1}^{n} z_i \cdot y_i}{n-1}$$

Eq. 5.5

where n is the number of observations of z and y. If s_{zy} is divided into the standard deviation of z and y, then the sample correlation coefficient r is obtained:

$$r = \frac{s_{zy}}{s_z \cdot s_y}$$

Eq. 5.6

where s_z and s_y are the sample standard deviations of z and y. r varies between ±1. +1 is obtained for a perfect positive relation between z and y.

5.2.5 Type of Variance

There are two types of variance: the homoscedasticity and the heteroscedasticity types. The former means that the variance is constant and independent of the size of the variable, while in the latter the variance depends on the size of the variable. A special case of heteroscedasticity is when the standard deviation increases proportionally with the variable z, i.e.

$$\frac{s}{z} = \text{constant}$$

Eq. 5.7

5.3 Regression Analysis

Regression analysis is the statistical methology for predicting values of one or more *response* variables from a collection of *predictor* [5] variable values [49]. This can be expressed as

$$y = g(z_1, z_2, .., z_k)$$

Eq. 5.8

where y is the response, z_1, z_2,..,z_k are the predictor variables and g is the estimated regression model. Only linear models are considered in the model building study. A linear model is of the form

$$y = \beta_0 + \beta_1 \cdot z_1 + \beta_2 \cdot z_2 + .. + \beta_k \cdot z_k + \varepsilon$$

Eq. 5.9

where the βs are the regression coefficients and ε is the error term. The error term ε has mean 0 and variance σ^2. σ^2 is the variance about the regression line. Estimates of the regression coefficients are found by the least square estimation method. That is minimizing of

$$S(b_0, b_1, b_2, .., b_k) = \sum_{i=1}^{n} \varepsilon_i^2 = \sum_{i=1}^{n} (y_i - \hat{y}_i)^2$$

Eq. 5.10

where y(hat) is the predicted or fitted value according to

---

5 Predictor variables are also named regressor variables.

$$\hat{y} = b_0 + b_1 \cdot z_1 + b_2 \cdot z_2 + .. + b_k \cdot z_k + \varepsilon$$

Eq. 5.11

An estimate of σ^2 can be found by

$$s^2 = \frac{\sum_{j=1}^{n} \varepsilon_j^2}{n-k-1} \left(= \frac{\text{SS Error}}{\text{d.f.}} = \text{MS Error}\right)$$

Eq. 5.12

where d.f. means degrees of freedom. SS Error and MS Error are the sum of squares and mean squares of error (or residuals) respectively. (They are defined below.) s^2 is also a measure of the lack of fit to the model y(hat).

The square of the correlation between y and y(hat) is called *the coefficient of determination* (R^2). It is defined as

$$R^2 = \frac{\text{SS Regression}}{\text{SS Total}} = 1 - \frac{\text{SS Error}}{\text{SS Total}}$$

Eq. 5.13

where

$$\text{SS Total} = \text{SS Regression} + \text{SS Error}$$

Eq. 5.14

where

$$\text{SS Total} = \sum_{i=1}^{n} (y_i - y.)^2$$

Eq. 5.15

$$\text{SS Regression} = \sum_{i=1}^{n} (\hat{y}_i - y.)^2$$

Eq. 5.16

$$\text{SS Error} = \sum_{i=1}^{n} (y_i - \hat{y}_i)^2$$

Eq. 5.17

SS Total is the total variation of y. SS Regression is the part of SS Total which is explained by the regression equation and SS Error is the unexplained part.

5.4 Evaluation of Regression Models

The prediction models can be roughly evaluated by the coefficient of determination (R^2) and the standard deviation about the regression line (s). In addition the regression model has to be verified for model deficiencies. This can be done by examining the residuals. The *i*th residual is defined as

$$\varepsilon_i = y_i - \hat{y}_i$$

Eq. 5.18

The residuals ε_i sum out to zero, but they have not the same variance. To overcome this deficiency a standardized (also called studentized) residual is defined [51]. The *i*th standardized residual ε_{si} is defined as

$$\varepsilon_{si} = \frac{\varepsilon_i}{\text{estimated standard error of } \varepsilon_i}$$

Eq. 5.19

The standardized residuals do not sum to zero, but they all have the same variance. Examination is then done by studying the residual plots. The residual plots are the plots of the (standardized) residuals versus the fitted values $y(hat)_i$ and versus the regressors. In general when the model is correct, the residuals tend to fall between ±2 and are randomly distributed.

5.5 Selection of Predictors

In Chapter 4 the number of identified bench scale predictors was as much as 46. Thus it is not possible to evaluate all possible multiple regressor models. No suitable procedure to build smoke prediction models was found in the literature. Thus a procedure was designed as part of this work. The procedure is presented in the Research Design in Section 7.2. Some parts of this procedure are explained. The procedure is referred to as *the six step procedure*. An important element in the six step procedure is the use of the *stepwise regression procedure*. The stepwise regression procedure provides a systematic technique for examining at most a few subsets [6] of each size. These techniques essentially choose a path through the possible models, looking first at a subset of one size, and then looking only at models obtained from preceding ones by adding or deleting regressor variables [52].

---

[6] A subset is a collection of regressors. The size of the subset is according to the number of regressors included.

(The method is further described in the literature.) In Minitab the procedure calculates an F-statistic for each regressor variable in the model. The square root of the F-statistic is a t-statistic. At each step, Minitab prints the coefficient and t-statistic for each variable in the model. If no variable can be removed, the procedure tries to add a variable [56]. Regression analyses are also included in the six step procedure. The printout from Minitab of the regression analyses include the standard deviation of the regressor coefficients. Also included in the printout is an analysis of variance and unusual observations.

5.6 Considerations about this Type of Model Building

In the model building study considered here both the regressor variables and the predictor variables have variance. The regression analysis presumes that there is only variance in the response [51], thus this has to be taken into consideration. The choice of predictor variables is influenced by this.

The unexplained variation (SS Error) can be divided into two parts; The lack of fit to the model and the pure error. The pure error is caused by the variation of the response y and eventual variation of the predictor(s) z_i.

The variance of the response and the predictor(s) induce unexplained error into the model (i.e. SS Error becomes increased). The result of this is that not even a «perfect» model can obtain a coefficient of determination equal to 1.0 or a standard deviation about the regression line of zero.

If the lack of fit to the model induces less unexplained variation than the pure error caused by the variation in the response and the regressors(s), then the lack of fit will be governed by the pure error (which is induced). Thus the pure error cannot be lower than the «white noise» (i.e. pure error) caused of the variation in the response and the regressor(s).

This can be of importance when two models obtain approximately the same variance about the regression equation and coefficient of determination. Then the model where the response and regressors induce largest variation should be chosen. as this model can have the highest scientific basis.

The subject was given some thought during the study and a tool to handle was considered. However this problem was overshadowed by the deficiency in the data set (e.g. measurements errors). Thus the problem was not dwelt on particularly.
However, these thoughts are mentioned here because they are relevant to this type of model building. Recommended literature on the subject is [57] and [58].

Note that if the variance in bench scale is reduced by testing several replicates, then the choice of predictors to be included in the model might be changed. Thus the number of replicates should be preferred to be the same for standardized and exploratory testing if prediction models are based on the exploratory testing. This is not the case in this study. The study is mainly based on only two replicates, while the standard for the ISO Cone Calorimeter requires three.

5.7 Variation of ISO Room Corner Test Data

Normally just one test is conducted in the ISO Room Corner Test (due to costs). However no. 12 Birch Plywood and no. 14 Melamine faced particle board were tested several times in the Nordic Round Robin project. The values for the smoke production at 400 kW and 1000 kW are given in Table 5-1. The table also includes the mean y and the standard deviation s to the smoke production.(The type of distribution of the full scale smoke test data is not known.)

Note that the smoke data of the first replicate for no. 14 deviates from the other two. Except from this the variation is little.

Table 5-1

	No.12 Birch plywood		No. 14 Melamine faced particle board	
	RSP(400) [m^2/s]	RSP(1000) [m^2/s]	RSP(400) [m^2/s]	RSP(1000) [m^2/s]
Replicate no. 1	0.9	10.3	1.3	11.3
Replicate no. 2	1.0	12.4	2.7	20.3
Replicate no. 3	0.7	9.1	2.6	19.5
Mean ($\bar{y}$)	0.87	10.6	2.2	17.2
St. deviation (s)	0.15	1.67	0.78	5.1

RSP(400) *Rate of smoke production at 400 kW heat release rate*
RSP(1000) *Rate of smoke production at 1000 kW heat release rate*

5.8 Variation of ISO Cone Calorimeter Data

The ISO Cone Calorimeter Standard requires two replicates. The test procedure in the standard limits the variation between the 180 s mean heat release for the three test runs to be less than 10% of the arithmetic average. (If not, three additional tests have to be conducted.)
If two of the three tests give equal values, then the maximum $s/\bar{x}$ is 14% (if the above mentioned 10% criterion is to be satisfied). If all three replicates had the same

deviation from the arithmetic average, then s/x̄ has to be lower than 8%. With only two replicates the corresponding s/x̄ have to be lower than 7% (compared to the above mentioned 10% criterion).

The variation in some of the bench scale parameters is shown here. Only some of the bench scale parameters which were selected to be included in the prediction models are shown. These are THR, TSP, TMCO, f_{COavg}, $\phi_{S,max}$, $\phi_{CO,max}$, t_{width}, $t_{w,S}$, $t_{w,CO}$, and $t_{max-ign}$.

Table 5-2 gives the references to the figures and identifies products which had particularly large variance. Large variance is defined to be the cases where the normalized standard deviation (i.e. s/z.) is larger than 0.25. In those cases where the normalized standard deviation exceeded 0.5, an «E» is noted after the product identification.

Table 5-2 Assessment of the variation to bench scale parameters.

Parameter	Figure reference	Detected outliers (product numbers are identified)
THR	Figure 5-1	6, 32, 67, 71
TSP	Figure 5-2	7, 14, 27, 30, 32, 60 (E), 61 (E)
TMCO	Figure 5-3	5, 6, 7, 10 (E), 12 (E), 17, 18 (E), 22, 27, 28, 32, 61
$f_{CO,avg}$	Figure 5-4	5, 7, 12 (E), 17, 18 (E), 21, 22, 27, 28, 61
$\phi_{S,max}$	Figure 5-5	1 (E), 2, 4, 8 (E), 29 (E), 30 (E), 31 (E), 32 (E), 60, 70
$\phi_{CO,max}$	Figure 5-6	2, 3, 4, 6 (E), 7 (E), 8, 12, 14 (E), 20(E), 22, 27, 28 (E)
t_{width}	Figure 5-7	6, 67, 71
$t_{w,S}$	Figure 5-8	1, 2, 7, 8 (E), 12, 14, 29 (E), 30 (E), 31, 32 (E) , 60, 61, 67, 70 (E)
$t_{W,CO}$	Figure 5-9	2, 6(E), 7(E), 9, 10, 12(E), 14(E), 17, 18(E), 20(E), 22, 24
$t_{max-ign}$	Figure 5-10	1(E), 3, 8(E), 13(E), 26

E Extreme outliers (i.e. the normalized standard deviation is larger than 50%)

The figures show that the normalized standard deviation often exceeds 8%. Unfortunately the high 25% limit was also often exceeded. (The table and the figures are referred to in the model building study.)

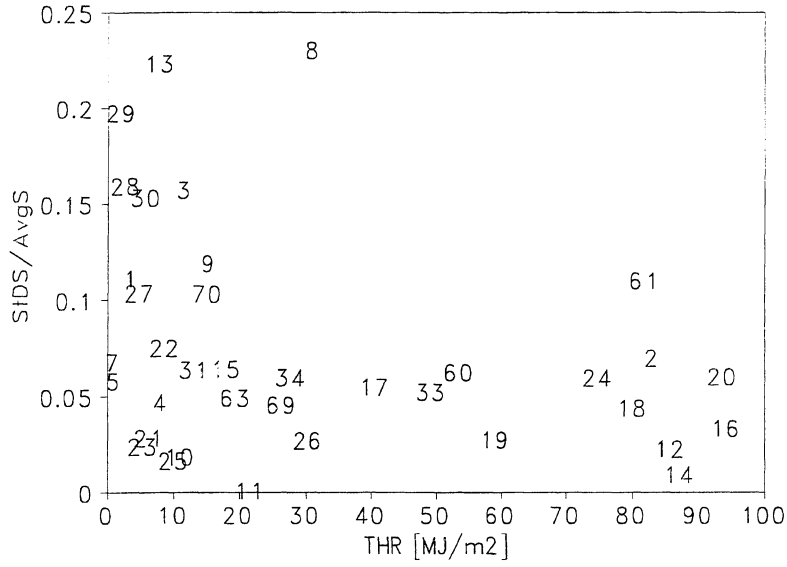

Figure 5-1 The normalized standard deviation of the bench scale total heat release.

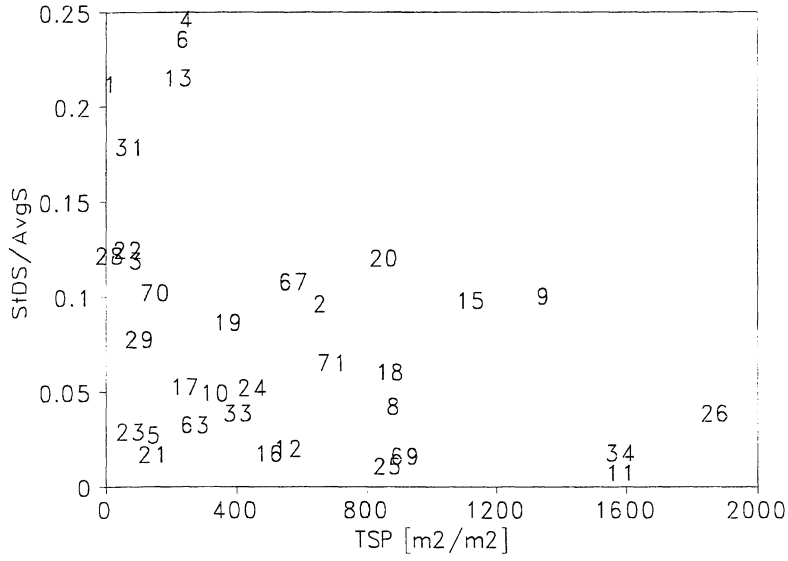

Figure 5-2 The normalized standard deviation of the bench scale total smoke production.

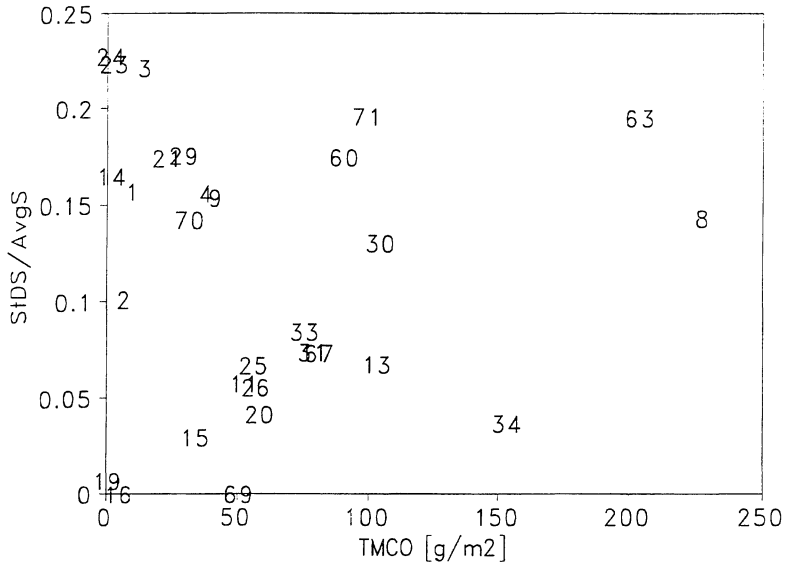

Figure 5-3 *The normalized standard deviation of the bench scale total mass of CO.*

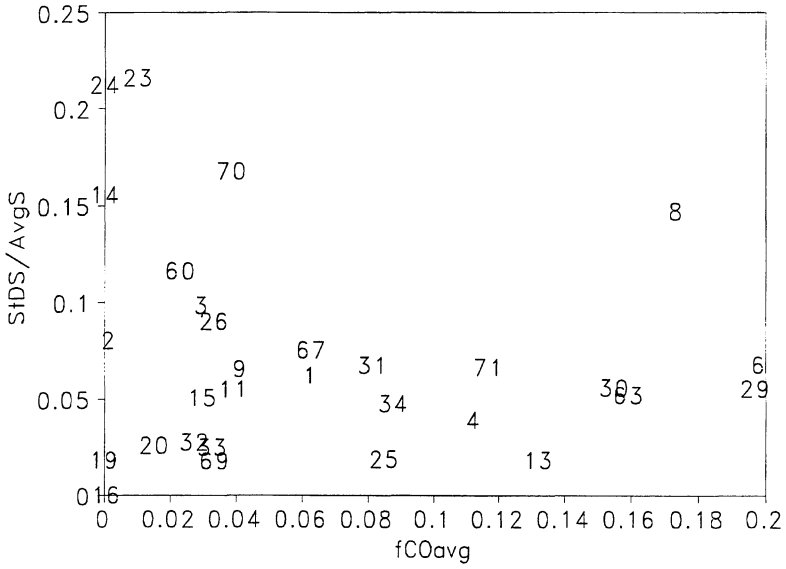

Figure 5-4 *The normalized standard deviation of the bench scale average parameter pyrolysed carbon conversed into CO.*

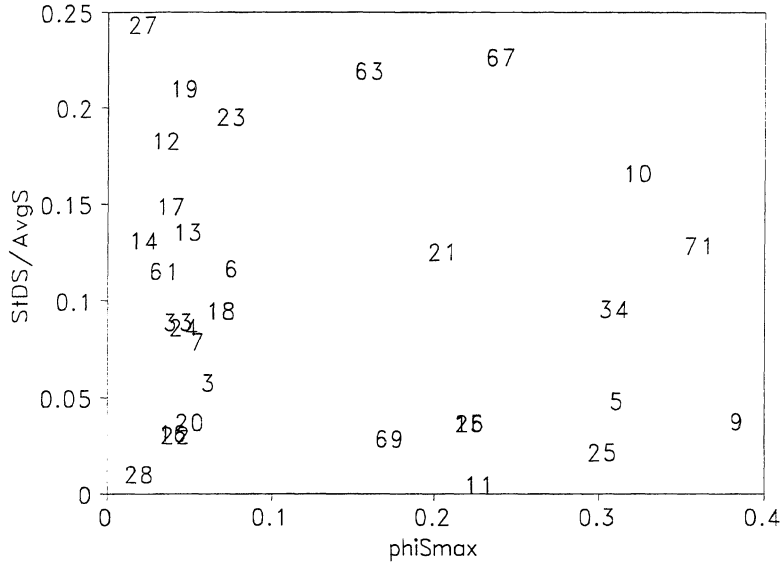

Figure 5-5 *The normalized standard deviation of the bench scale maximum global equivalence smoke ratio factor.*

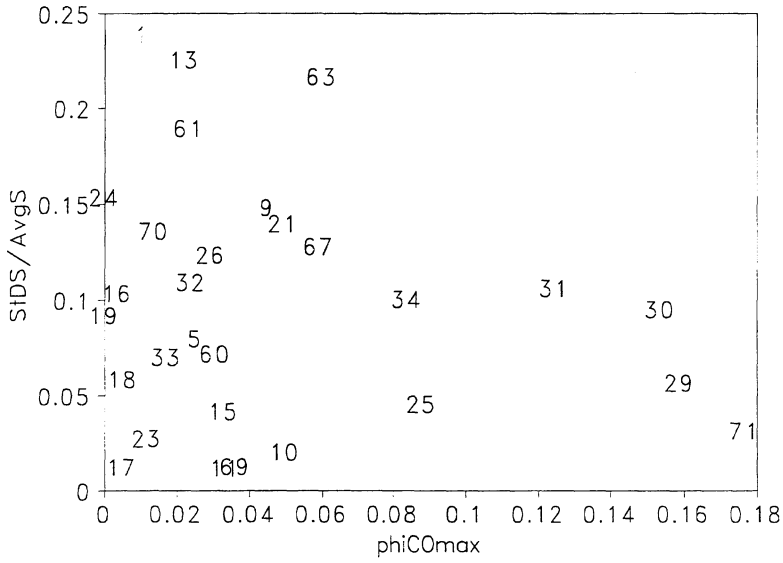

Figure 5-6 *The normalized standard deviation of the bench scale maximum global equivalence CO ratio factor.*

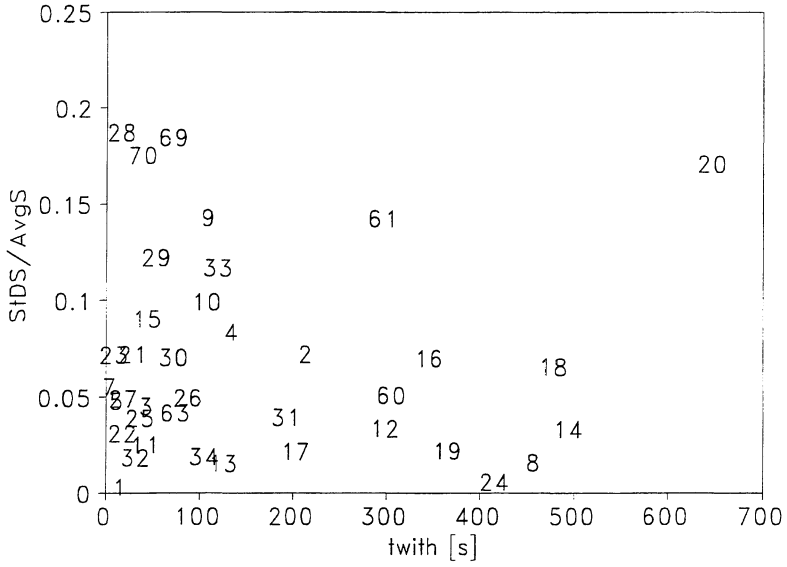

Figure 5-7 *The normalized standard deviation of the bench scale t_{width}.*

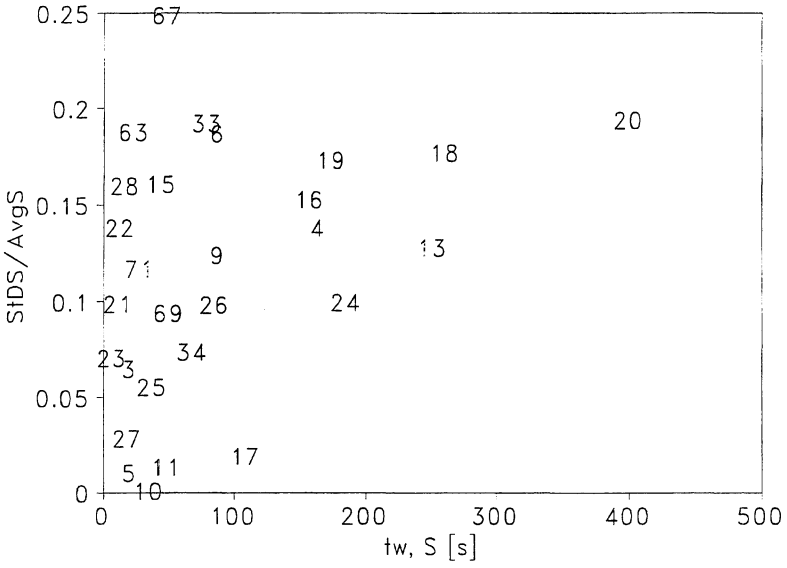

Figure 5-8 *The normalized standard deviation of the bench scale $t_{w,S}$.*

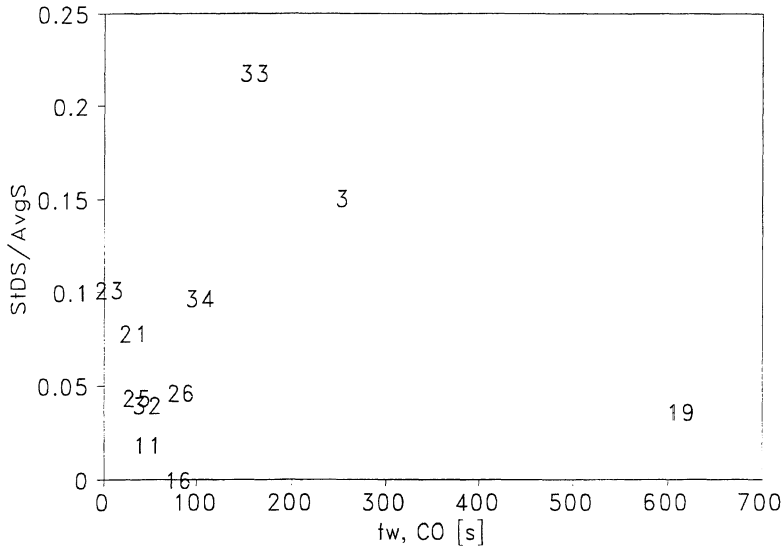

Figure 5-9 The normalized standard deviation of the bench scale $t_{w,CO}$.

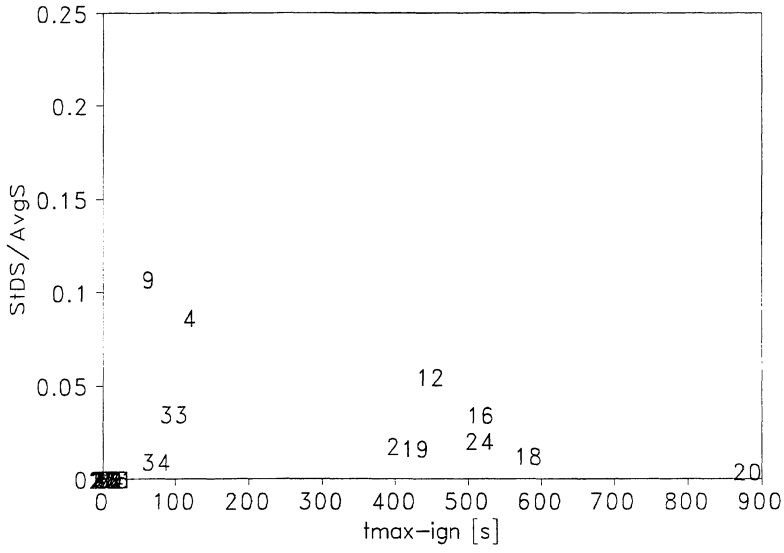

Figure 5-10 The normalized standard deviation of the bench scale $t_{max\text{-}ign}$.

6 DEVELOPMENT OF THE SMOKE PREDICTION MODELS

6.1 Introduction

Approaches on development of smoke prediction models are given in this chapter. The Research Design section gives an outline of these approaches.

The development of smoke prediction models is relevant to predict specified data. Empirical approaches are chosen because there is little relevant scientific information about correlations between bench scale and full scale smoke data. Empirical approaches can also reveal whether correlations between bench scale and full scale exist.

The models predict specified smoke data from the ISO Room Corner Test by use of test data from the ISO Cone Calorimeter.

6.2 Research Design

The research reported in the ISC'94 publication revealed that the full scale smoke generation [7] in the ISO Room Corner Test is sensitive to the burning conditions. Thus the building products are divided into groups according to their performance in the ISO Room Corner Test (cf. Section 1.3.1). Such divisions make the data within each group more homogeneous and thereby increase the possibility to reveal relationships between bench scale and full scale smoke test data. According to the division of the building products, approaches to develope three types of smoke prediction models are given. The models are according to three types of fire scenarios

1. **Growing fires** (pre-flashover fires) (Section 6.3)
2. **Fully developed fires** (flashover and post-flashover fires) (Section 6.4)
3. **Non-flashover fires** [8] (Section 6.5 and 6.6)

---

7 The term «generation» is used when referred to normalized smoke production (i.e. $r_{S/Q}$ or f_S).

8 This term is also used in [59].

Growing fires are represented by data from the building products which caused flashover within 10 minutes in the ISO Room Corner Test (i.e. product group 1). Smoke test data are selected at a heat release rate of 400 kW. This was a rough attempt to decrease the effect of temperature. As mentioned in Chapter 1 the fire gas temperature is determined by the heat release and the heat loss of the fire plume. Thus by choosing a criterion which is linked to the former factor, more uniform temperature conditions might be obtained. Setting the criterion at 400 kW is based on the recognition that the burning conditions become underventilated when the heat release rate exceeds 400-600 kW (results found in connection with the research reported in the ISC'94 publication). On the other hand, low levels are increasingly influenced by the burner. Thus a choice of 400 kW was assumed to be an appropriate criterion.

Fully developed fires are also represented by smoke test data from product group 1. The data are selected at 1 MW and when flames emerge out of the opening.

The third group of fires is the non-flashover fires. These are flaming fires where the heat release was not fast enough or/and sufficient enough to cause flashover. These fires are represented by test data from product group 2 (the products which did not cause flashover within 10 minutes). The non-flashover fires are sub-divided into two types; *small* and *large* non-flashover fires. The division is according to the burner heat release rate during the period the data were averaged over. The small non-flashover fires are represented by test data for the first 10 minutes of the ISO Room Corner Test, while the large non-flashover fires are represented by full scale test data for 20 minutes testing.

Two full scale smoke parameters are used as response variables:

- Total and rate of smoke production.
- Smoke to flame ratio $r_{S/Q}$ (units: [m^2/MJ].

The smoke to flame ratio might be easier to correlate since it is roughly independent of the pyrolysed mass for well ventilated flaming fires [9].

Each model building approach starts with a correlation analysis where all the 46 bench scale parameters are included. The correlation analysis gives hints about the most interesting bench scale parameters, and this information is valuable background information in the approaches to develop smoke prediction models .

---

9 This statement presumes that the degree of completeness of combustion is approximately the same in bench scale and full scale.

The large number of regressors in combination with the bench scale inter-collinearity resulted in that special procedures had to be developed and followed to identify the prediction models. This is probably not the best way to do this. A time-consuming but safe way is to assess many models. Due to practical reasons all possible multiple regressors models could not be assessed, thus a selection procedure had to be developed. Thus a *six step procedure* was developed:

1. Conduction of stepwise regression analyses to identify potential good combinations of bench scale variables (regressors).
2. Then the identified regressors were attempted to be replaced by other regressors. The choice of other regressors was based on the knowledge of the inter-collinearity between the regressors. Also included here was an assessment of the goodness of the regressors (i.e. which of them induced less variation and which of them had outliers and bad data in the data set).
3. The standard deviation about the regression line and the coefficient of determination to actual models were then assessed.
4. Steps 2 and 3 resulted in one or more regressors models being chosen and further assessed by regression analyses. This included assessments of the residual plots.
5. Assessment of the conservation of the ranking of the products.
6. Assessment of the «zero» point of the model (i.e. the constant b_0).

In addition, the bench scale regressors were scientifically assessed, i.e. relationships that were hard to understand were avoided.

Only «highlights» of the research, i.e. the successful results, are presented. Some intermediate steps are also presented to outline the procedure, doubts and choices that had to be made.

6.3 Prediction of Smoke Production in Pre-Flashover Fires

6.3.1 Preliminary Considerations

The full scale rate of smoke production at the rate of heat release of 400 kW is chosen as the data wanted predicted, i.e. RSP(400). Since RSP(400) is found at the specified level of rate of heat release of 400 kW, it is actually an intensive parameter:

$$\text{RSP(400)} / 0.4\ \text{MW} = \text{RSP} / \text{RHR} = r_{S/Q}(400)$$

Eq. 6.1

Figure 6-1 is the correlation plot between the bench scale average smoke to flame ratio and the full scale smoke to flame ratio at 400 kW. The full scale data are not corrected for the output from the burner. The line drawn in the figure represents equal values between bench scale and full scale. Figure 6-3 is the correlation plot between the bench scale maximum smoke to flame ratio and the full scale smoke to flame ratio at 400 kW. Unfortunately none of the plots indicate direct correlations between bench scale and full scale smoke test data.

Evaluation of the full scale test data.
In *full scale* the wood based products (i.e. nos. 2, 12, 16, 17, 18, 19 and 24) obtain instantaneous smoke to flame ratio values below 5 m^2/MJ, while the plastics (i.e. nos. 7, 9, 11, 25, 26, 33 and 34) have values between 10 and 30 m^2/MJ.

There are two melamine faced products in product group 1: nos. 14 and 20. Their full scale $r_{S/Q}$ values are about 5 and 25 m^2/MJ respectively, thus in full scale they vary considerably. The full scale value of no. 14 is based on the arithmetic average of three tests, thus this value is validated. No. 20 was tried verified, but no further verification was obtained.

Product group 1 contains three polyurethane foam products: nos. 9, 25 and 34. No. 25 is left out because there are too few measurements done to estimate the smoke production at 400 kW. Nos. 9 and 34 show large differences in both bench scale and full scale. Thus their values were verified against other full scale tests of polyurethane foams ([60] and [61]). Then the data of no. 9 were questioned (it seemed to have too low full scale smoke production). Thus no. 9 was also left out of the model building study.

The other full scale values seem to be in accordance with each other. The particle boards (nos. 16 and 24) have values close to each other. The same is also the case for the plywoods and wood (nos. 2 and 12 and no. 19). However the wood boards (nos. 17 and 18) seem to have some variance in full scale. The polystyrene foams (i.e. nos. 11 and 26) have roughly the same smoke production in full scale.

Evaluation of the bench scale test data.
In *bench scale* the wood based products obtain smoke to flame ratio values below 20 m^2/MJ, while the plastics seem to have values between 10 and 120 m^2/MJ.

The EUREFIC products were also *bench scale* tested within the EUREFIC programme [62]. Figure 6-5 shows a comparison between the average smoke to flame ratio obtained by Trätek and the EUREFIC programme (the EUREFIC tests were done either by SP or Danish Fire Research Institute). For nos. 2 and 7 there are some deviations. In Table 5-2 the variation in TSP_{CC} of no. 7 was identified as large,

thus this bench scale value is doubted. The differences might also more or less have been caused by different computational procedures. The EUREFIC data are computed for the period after ignition and upto 200 seconds after flaming has ceased or when the rate of mass loss is below 150 g/s·m^2. The Trätek data are computed from the start of the test and until the rate of mass loss is below 250 g/s·m^2.

It should be noted that some parts of the data have large variance (e.g. the TMCO data). Any observations of deviations and variations in the data are of importance for the model building study, because empirical models are not better than the data they are based on.

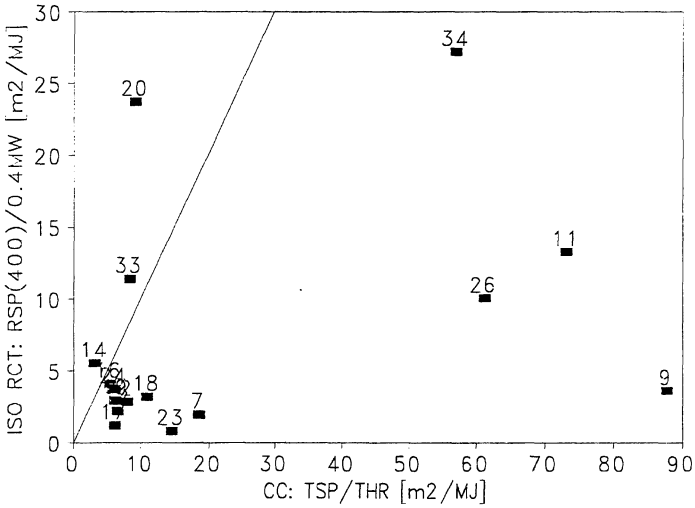

Figure 6-1 *The correlation plot between the bench scale average smoke to flame ratio and the full scale instant smoke to flame ratio at 400 kW.*

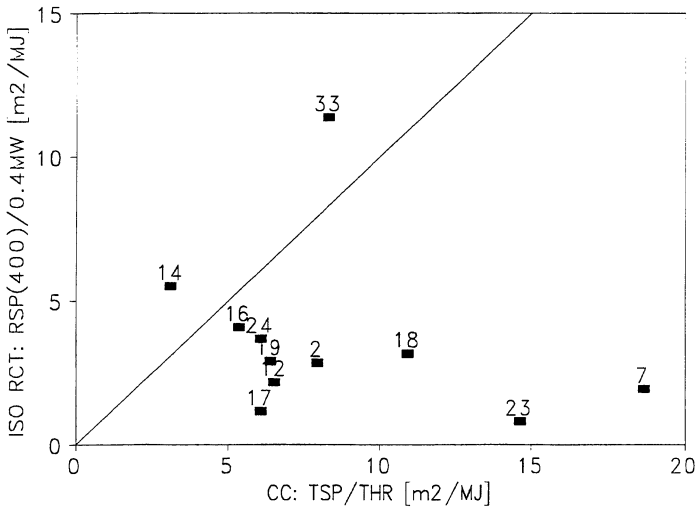

Figure 6-2 Enlargement of Figure 6-1.

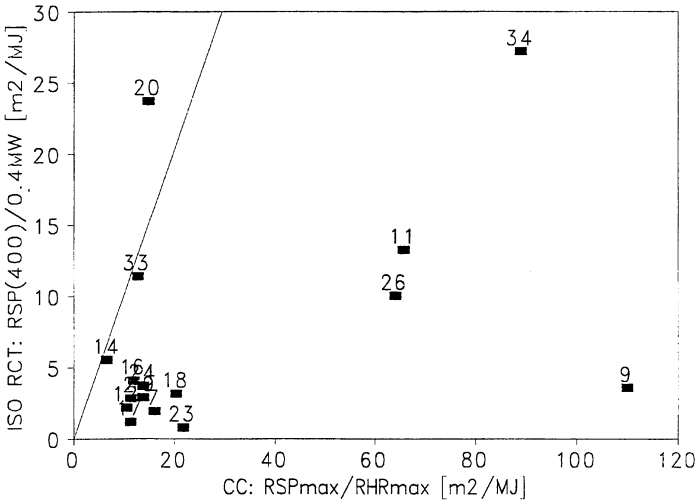

Figure 6-3 Correlation plot between the bench scale maximum smoke to flame ratio and the full scale instant smoke to flame ratio at 400 kW.

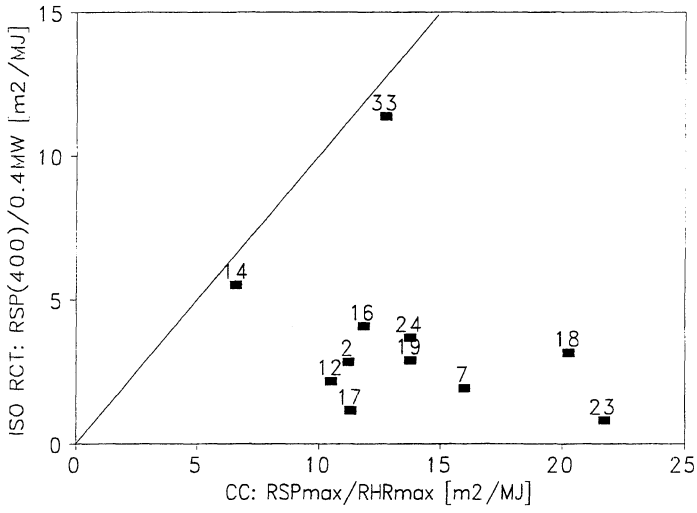

Figure 6-4 Enlargement of Figure 6-3.

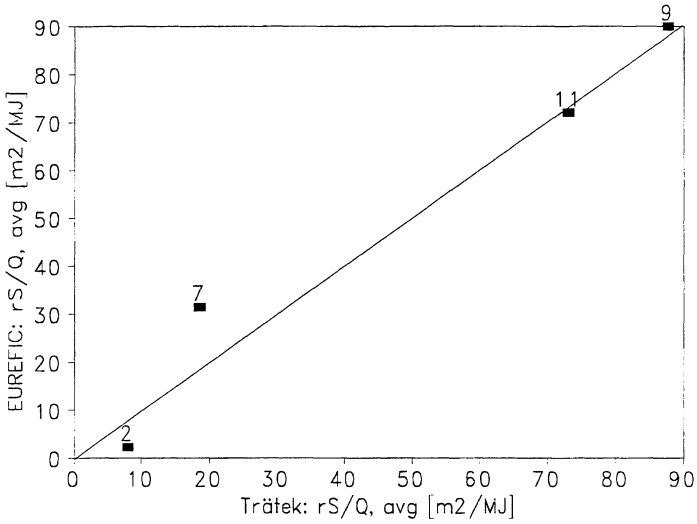

Figure 6-5 The comparison of the bench scale average smoke to flame ratio obtained by Trätek and within the EUREFIC programme.

6.3.2 The simple Correlation Analysis

Correlation analyses were conducted on the 46 bench scale fire parameters; 18 extensive test fire parameters (including two dummies) and 15 intensive deducted fire parameters (13 of the deducted fire parameters have both a maximum value and an average value). The analyses consisted of considerations of the correlation plots. The analysis revealed that the bench scale CO data has the best possibilities to predict the full scale smoke data. TMCO had the highest correlation coefficient, and it was about 0.90. A regression analysis on TMCO gave the prediction model

$$RSP(400)_{pred} = 0.952 + 0.0685 \cdot TMCO$$

Eq. 6.2

The correlation plot between the predicted values according to Eq. 6.2 and the experimental full scale smoke production at 400 kW is shown in Figure 6-6. The figure shows that the model is not especially good; it discriminates only the data. The model fails also on prediction of smoke production for nos. 20 and 25. Also the residual plots indicated a bad model. Thus predictions are not good with simple regression models.

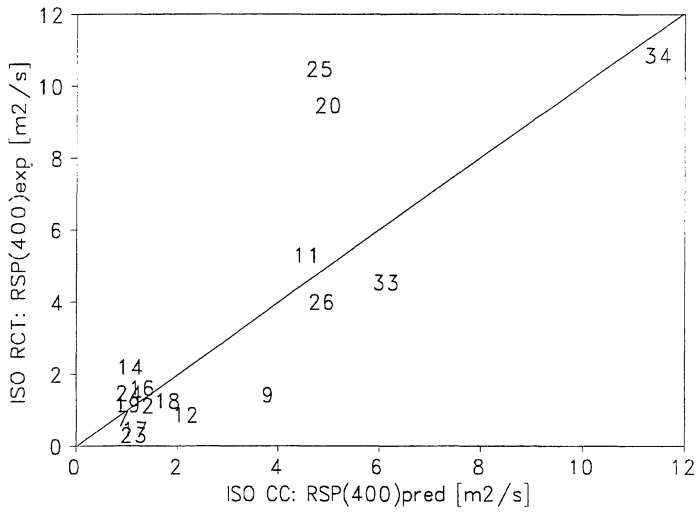

Figure 6-6 The correlation plot between the predicted values according to Eq. 6.2 (X-axis) and the experimental full scale smoke production at 400 kW (Y-axis).

6.3.3 Multiple Regression Models

The model building study was conducted in accordance with the six step procedure described in the Research Design section (Section 6.2). The results of the initial stepwise regression analysis on the 46 regressors is given below [10]. 15 of the 17 products in product group 1 were included (i.e. nos. 9 and 25 were left out).

```
Stepwise regression of RSP(400) on 50 (i.e. 46) predictors, with N = 15
 N(cases with missing obs.) = 2 N(all cases) = 17

    STEP         1         2         3         4         5
CONSTANT    0.9516    0.1895   -0.1054    1.7500    1.1800

TMCO        0.0685    0.0680    0.0590    0.0611    0.0593
T-RATIO       7.34     10.85      8.48     12.89     14.29

tw,CO                0.00292   0.00290   0.00187   0.00218
T-RATIO                 4.10      4.62      3.71      4.78

(plst?)                           1.23      2.12      2.35
T-RATIO                           2.12      4.62      5.76

muKPCSav                                    -5.7      -6.9
T-RATIO                                   -3.75     -4.85

RHRmax                                                0.0031
T-RATIO                                                 2.14

S             1.50      1.01     0.888     0.600     0.516
R-SQ         80.56     91.89     94.25     97.61     98.41
```

As the printout shows a prediction model which includes three predictors obtain a multiple correlation coefficient of 94.3% and a standard deviation about the regression line of 0.89 m^2/s (i.e. the predictors TMCO, $t_{w,CO}$ and [plst?]).

In general, regressors which are correlated should be avoided in a model. This is because the prediction value of adding a new term (i.e. another regressor) into a regression equation is limited by the correlation between the new term and the

---

[10] This is the printout from the analysis conducted with MINITAB Release 9.2. Any manipulations on the printout are done with *italic* letters.

In the printout «S» is the standard deviation about the regression line (S has the same units as the response variable) and R-SQ is the coefficient of determination.

On the printout N is the number of observations. Since product group 1 consisted of 17 products N=17. The printout says 50 regressors (and not 46). This is because four parameters which were proportional to other ones were included.

regressors already included. Thus if there is doubt about which one of two regressors that should be added to an equation, the collinearity structure can be studied.

A replacement of the bench scale regressors was considered. TMCO could be replaced by $\mu_{CO,avg}$, $f_{CO,avg}$ or $\phi_{CO,avg}$. t_{wCO} could be replaced by t_{width}, $t_{w,CO2}$, $t_{w,S}$, t_{ign} or $t_{max\text{-}ign}$.

The «best» [11] model included $f_{CO,avg}$, $t_{w,S}$ and the dummy variable [plst?]. The model based on them obtained a standard deviation about the regression line and a coefficient of determination of 0.88 m^2/s and 94.3% respectively.

If $t_{w,S}$ were excluded, then $t_{max\text{-}ign}$ was chosen. A model which included $\phi_{CO,avg}$, $t_{max\text{-}ign}$ and [plst?] obtained the standard deviation about the regression line and the coefficient of determination were 0.96 m^2/s and 93.3% respectively

Three regressors were chosen to be included in the model; $f_{CO,avg}$, $t_{w,S}$ and the dummy variable [plst?]. The model is called the FITS2 model, and the printout of the regression analysis is given below.

```
The regression equation is (FITS2)
RSP(400) = - 1.93 + 117 fCOavg + 0.0161 tw,S + 1.50 (plst?)

Predictor       Coef        Stdev    t-ratio        p
Constant     -1.9298       0.5049      -3.82    0.003
fCOavg        116.99        13.01       8.99    0.000
tw,S        0.016110     0.002417       6.67    0.000
(plst?)       1.4964       0.5673       2.64    0.023

s = 0.8808      R-sq = 94.3%     R-sq(adj) = 92.8%

Analysis of Variance

SOURCE       DF          SS          MS          F        p
Regression    3     142.284      47.428      61.14    0.000
Error        11       8.533       0.776
Total        14     150.818

SOURCE       DF      SEQ SS
fCOavg        1      98.881
tw,S          1      38.005
(plst?)       1       5.398

Unusual Observations
no.     fCOavg    RSP(400)        Fit  Stdev.Fit   Residual     St.Resid
 20     0.0158       9.479      7.871      0.695      1.608        2.97R
```

[11] In terms of statistical measures.

The correlation plot between the predicted values according to the FITS2 model and the full scale data is given in the upper left panel of Figure 6-7. The plot indicates that there is a non-linear relationship. This is also indicated of the residualplot for the predicted values ; cf. upper right panel of Figure 6-7. In the residual plots in Figure 6-7 it is no. 20 that has the largest (standardized) residual (cf. the «Unusual Observations» in the Minitab printout). Figure 6-8 shows the same plot as the upper left panel of Figure 6-7, but with identification of the dots. The plots show that the model has several weaknesses. It does not take the non-linearity into account, and the melamine products are badly predicted.

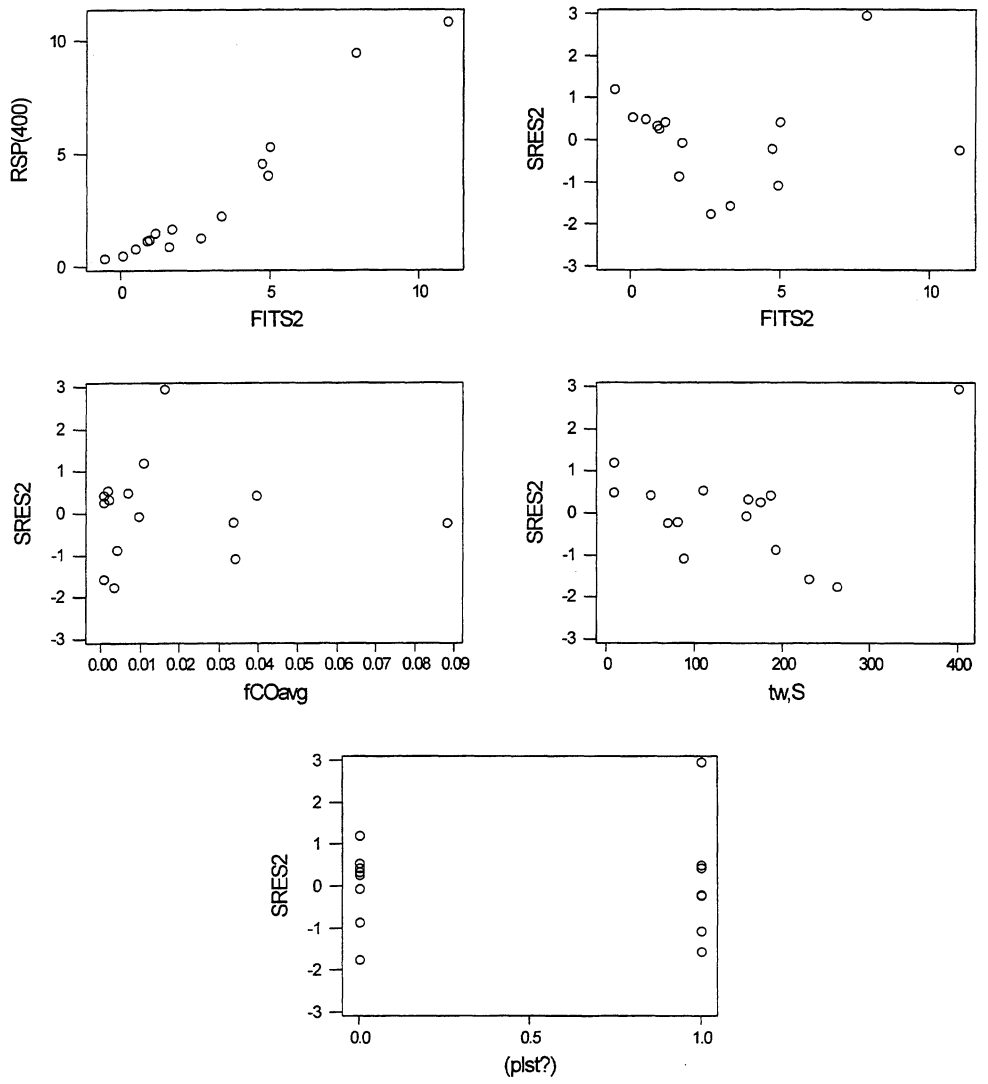

Figure 6-7 *Upper left panel: the correlation plot between the predicted values (FITS2) and the experimental full scale data, The rest of the panels: the residual plots.*

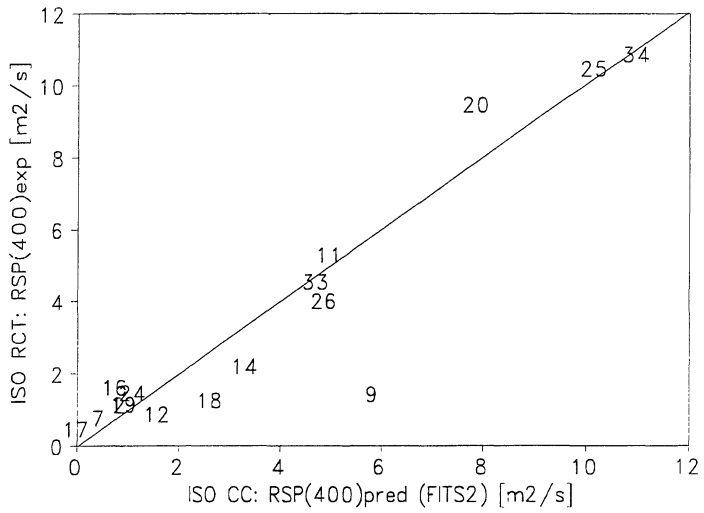

Figure 6-8 *The correlation plot between the values predicted from the FITS2 model and the experimental full scale values. (Note: No. 9 disregarded)*

6.3.4 The Logistic Model Approach

The data have to be transformed to obtain linearity. An appropriate transformation was found to be the logistic model. This model is of the form

$$y = \frac{e^{\beta_0 + \beta_i z_i}}{1 + e^{\beta_0 + \beta_i z_i}}$$

Eq. 6.3

where y is the response and z_i is the predictor (several predictors can be included).

In this model the response variable has to be in the range between 0 and 1, thus the full scale experimental data have to be transformed. This means that a maximum value on RSP(400) has to be chosen. No. 34 (rigid polyurethane) had the highest smoke production at 400 kW; approximately 10.9 m^2/s. An upper limit of RSP(400) on 11.4 m^2/s was found to be applicable.

To obtain linearity in the logistic model the response has to be transformed into

$$y' = \ln \frac{y}{1 - y}$$

Eq. 6.4

Then linear regression analysis can be conducted. Thus the transformation of the full scale data are done according to

$$RSP(04)_T = \ln\left(\frac{RSP(400)/11.4}{1-RSP(400)/11.4}\right)$$

Eq. 6.5

The model building study was conducted according to the six-step procedure. Many models were found, and some of them had approximately the same prediction possibilities. Thus a selection had to be done.

In terms of statistical measures one of the best models included $f_{CO,avg}$, $t_{w,S}$ and the dummy variable [plst?]. The model is called the FITS3 model, and the printout of the regression analysis on it given below.

```
The regression equation is (FITS3)
RSP(04)T = - 4.09 + 64.5 fCOavg + 0.00906 tw,S + 0.814 (plst?)

Predictor        Coef       Stdev    t-ratio        p
Constant      -4.0883      0.1939     -21.09    0.000
fCOavg         64.469       4.995      12.91    0.000
tw,S       0.0090605   0.0009280       9.76    0.000
(plst?)        0.8139      0.2178       3.74    0.003

s = 0.3382      R-sq = 97.2%     R-sq(adj) = 96.4%

Analysis of Variance
SOURCE       DF          SS          MS          F        p
Regression    3      43.205      14.402     125.93    0.000
Error        11       1.258       0.114
Total        14      44.463

SOURCE       DF      SEQ SS
fCOavg        1      29.619
tw,S          1      11.989
(plst?)       1       1.597
```

The correlation plot between the FITS3 model and the transformed full scale data is given in the upper left panel in Figure 6-9. The rest of the panels are the residual plots.

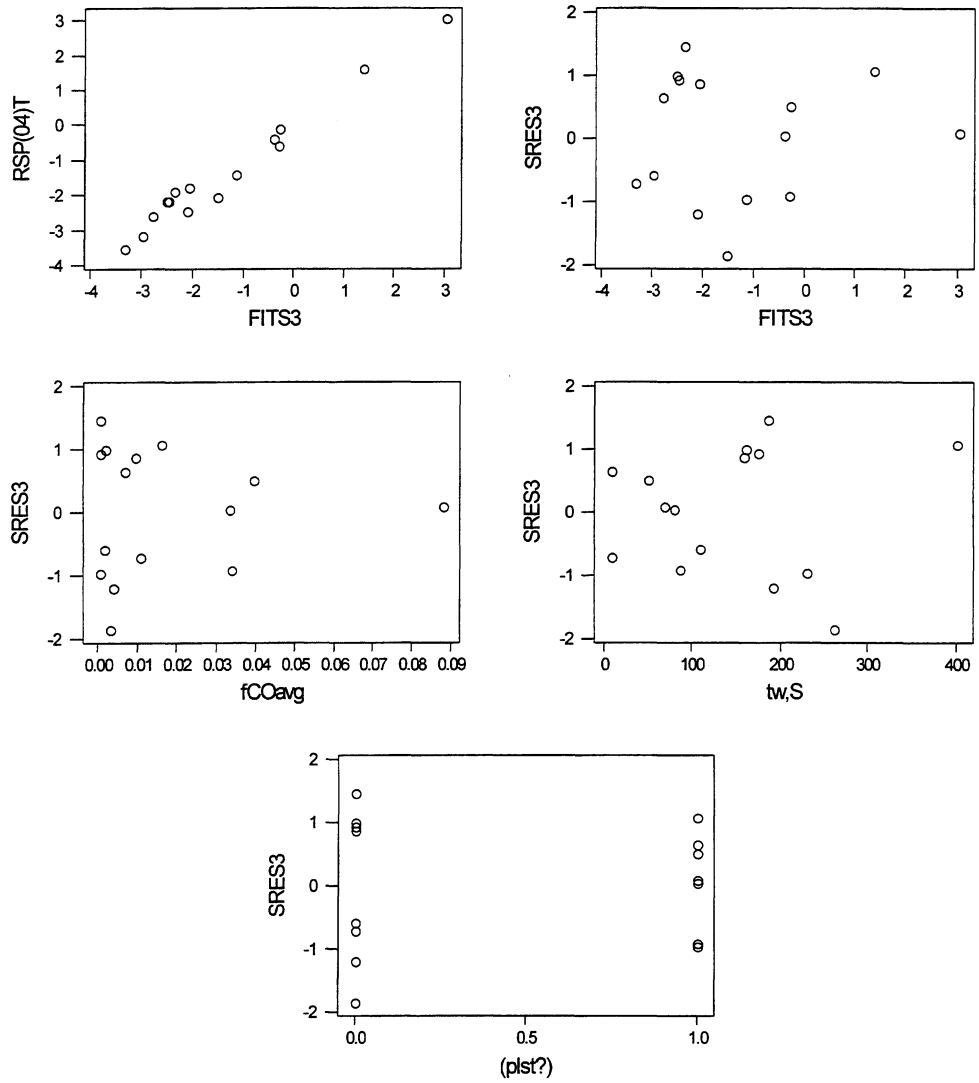

Figure 6-9 *Upper left panel: the correlation plot between the predicted values and the experimental transposed full scale values. The rest of the panels: residual plots.*

Prediction according to the FITS3 model is shown in Figure 6-10. Close to the origin the FITS3 model underpredicts the smoke production of the particle boards (since both nos. 16 and 24 are on the upper side of the «equal values» line). No. 18 is also badly predicted, but this might have been caused by bad bench scale data (TMCO has large variation). Except for the above mentioned cases the prediction is good, and the ranking, in the main, is preserved.

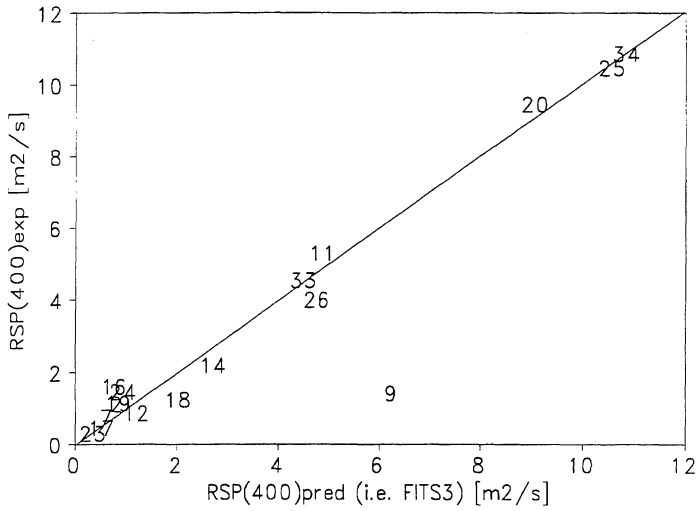

Figure 6-10 The correlation plot between the values predicted from the FITS3 model and the experimental full scale data.

Another relevant model included the bench scale $\phi_{CO,avg}$, $t_{max\text{-}ign}$ and the dummy variable [plst?]. The model is called the FITS4 model and the printout from the regression analysis is given below.

```
The regression equation is (FITS4)
RSP(04)T = - 3.80 + 57.2 phiCOavg + 0.00341 tmax-ign + 1.66 (plst?)
Predictor        Coef       Stdev    t-ratio        p
Constant      -3.7986      0.2095     -18.13    0.000
phiCOavg       57.226       5.870       9.75    0.000
tmax-ign   0.0034128   0.0004146       8.23    0.000
(plst?)        1.6599      0.2554       6.50    0.000

s = 0.4025      R-sq = 96.0%     R-sq(adj) = 94.9%

Analysis of Variance

SOURCE        DF          SS          MS          F        p
Regression     3      42.681      14.227      87.83    0.000
Error         11       1.782       0.162
Total         14      44.463

SOURCE        DF      SEQ SS
phiCOavg       1      27.928
tmax-ign       1       7.912
(plst?)        1       6.841

Unusual Observations
no.    phiCOavg    RSP(04)T        Fit   Stdev.Fit    Residual    St.Resid
 34      0.0827       3.038      2.853       0.361       0.185        1.04 X
X denotes an obs. whose X value gives it large influence.
```

The upper left panel of Figure 6-11 shows the correlation plot between the predicted values (FITS4) and the transposed experimental data. The rest of the panels are the residual plots. These have a fairly random distribution.

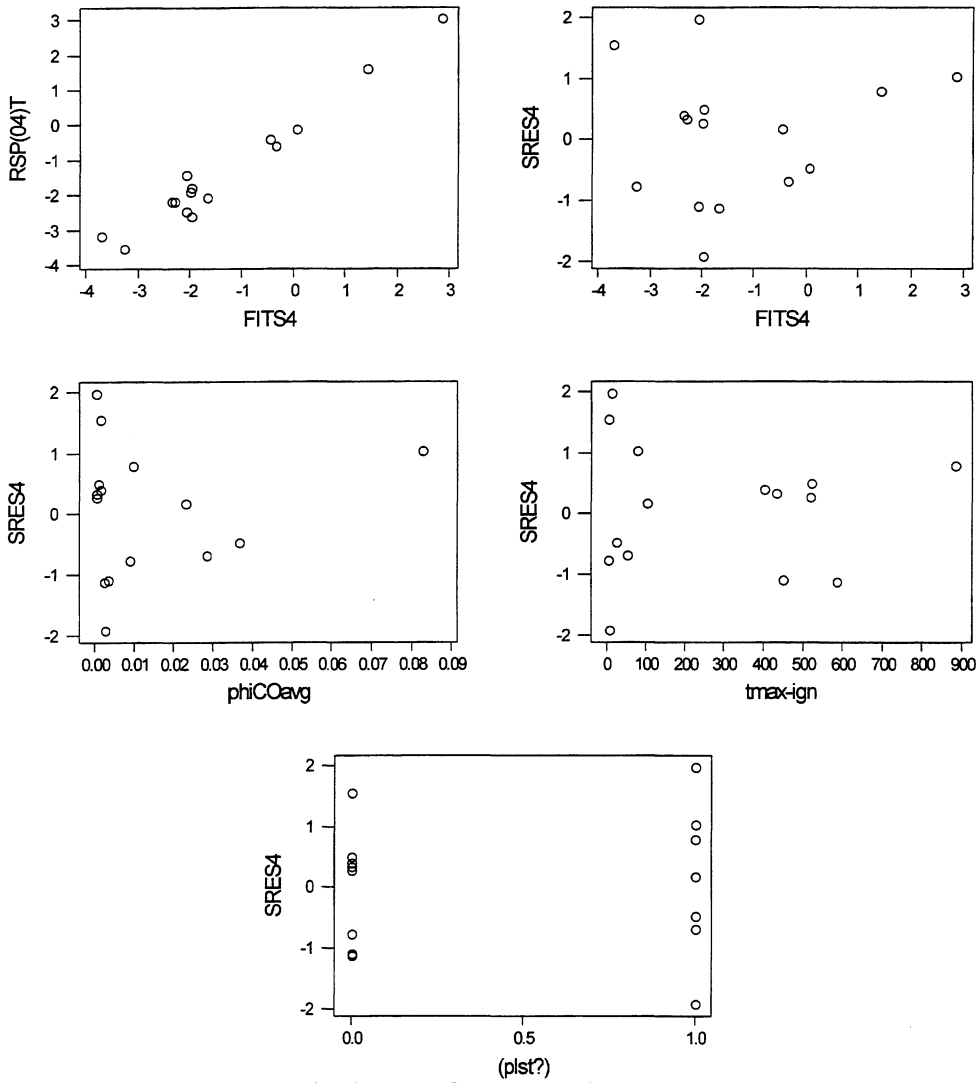

Figure 6-11 Upper left panel: the correlation plot between the predicted values and the experimental transposed full scale values. The rest of the panels: residual plots

The prediction by the FITS4 model is shown in Figure 6-12. No. 14 is badly predicted. Except from this, the prediction is good and the ranking is mainly preserved.

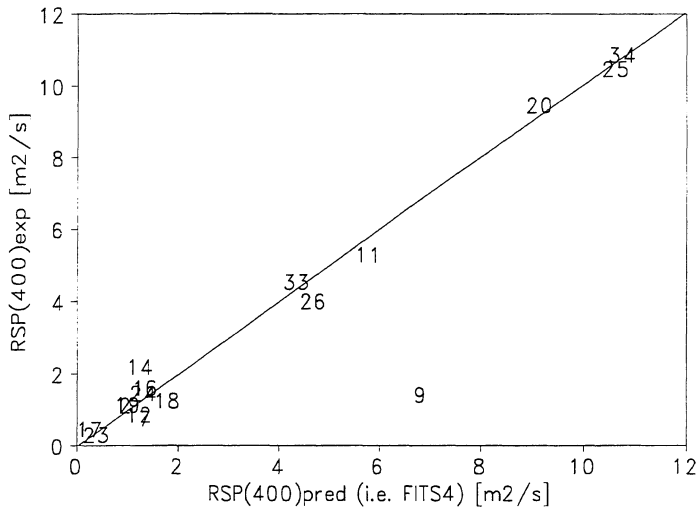

Figure 6-12 The correlation plot between the values predicted from the FITS4 model and the experimental full scale values.

6.3.5 The Approaches on a Reduced Data Set

The model building approaches are very much influenced by product nos. 20 and 34 (these two are so called high leverage points). If their experimental data are wrong, then they might have governed the model building study in a wrong way.

Leaving out no. 34 (and no. 7)
A way to verify the relationships determined in the FITS3 and FITS4 models is to leave out no. 34 (since this is the maximum value [51]). The verification supported the two models that were determined.

If nos. 7 and 34 were left out it was also possible to build a model which included the bench scale smoke data instead of the bench scale CO data. A model which included $\phi_{S,avg}$, $t_{max\text{-}ign}$ and the dummy variable [plst?] was found. The model is called the FITS5 model and the regression analysis is given below.

```
The regression equation is (FITS5)
RSP(04)T = - 3.55 + 2.76 phiSavg + 0.00287 tmax-ign + 2.44 (plst?)

Predictor        Coef        Stdev    t-ratio        p
Constant      -3.5463       0.1641     -21.61    0.000
phiSavg         2.757        1.288       2.14    0.061
tmax-ign   0.0028720    0.0003121       9.20    0.000
(plst?)        2.4361       0.1897      12.84    0.000
```

```
s = 0.2848      R-sq = 96.8%     R-sq(adj) = 95.8%

Analysis of Variance

SOURCE        DF          SS          MS         F        p
Regression     3     22.2178      7.4059     91.29    0.000
Error          9      0.7301      0.0811
Total         12     22.9479

SOURCE        DF       SEQ SS
phiSavg        1       3.1708
tmax-ign       1       5.6678
(plst?)        1      13.3792
```

The correlation plot between the predicted values according to the FITS5 model and the experimental transposed data is given in the upper left panel of Figure 6-13. The rest of the panels are the residual plots, and they seem to be fairly good.

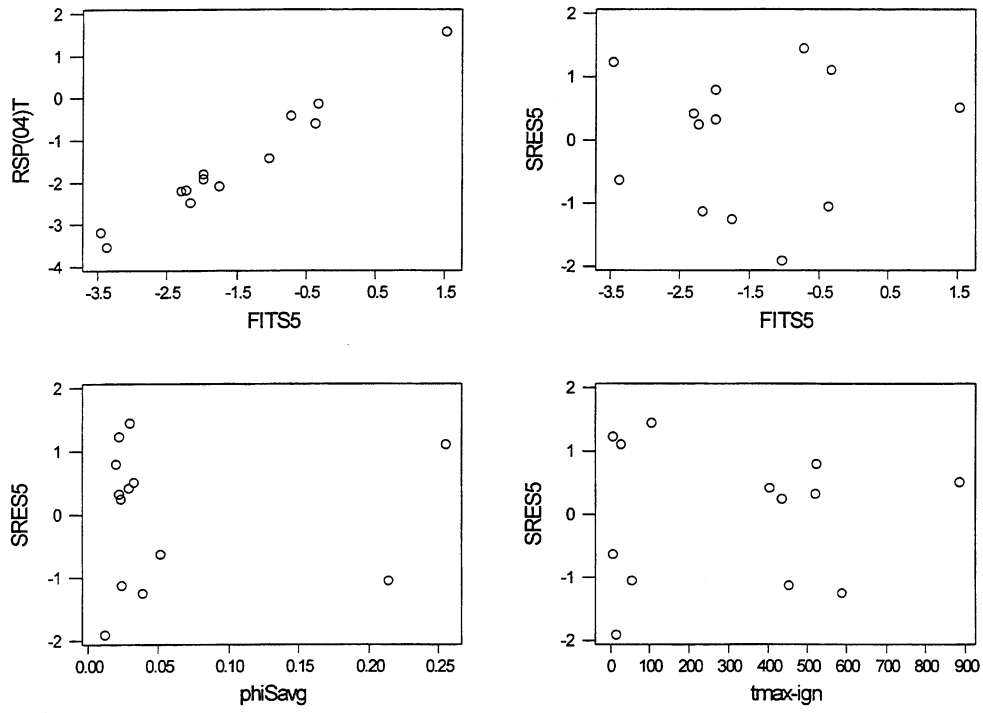

(cont.)

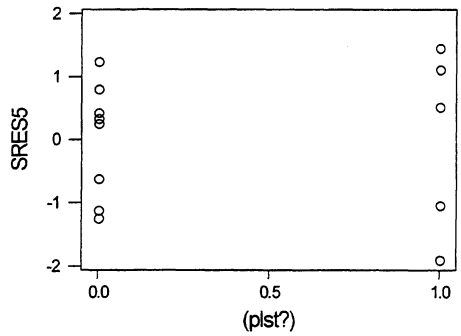

Figure 6-13 Upper left panel: the correlation plot between the predicted values and the experimental transposed full scale data. The rest of the panels: residual plots.

Prediction according to the FITS5 model is shown in Figure 6-14. The model fails on prediction of no. 7 and the PU-foams (i.e. nos. 25 and 34).

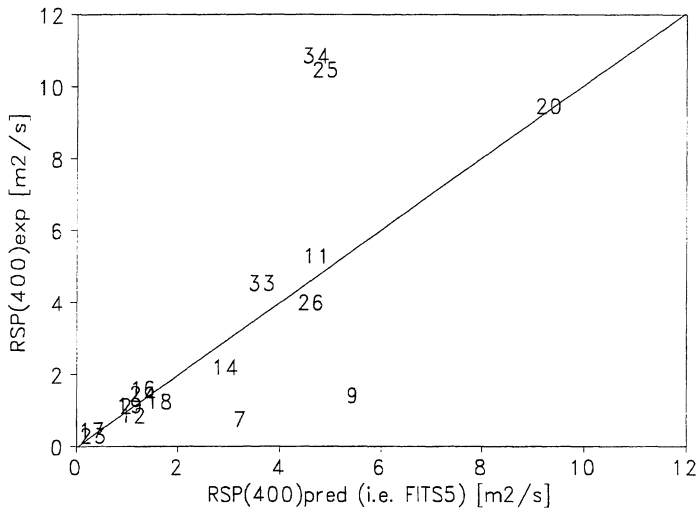

Figure 6-14 The correlation plot between the values predicted from the FITS5 model and the experimental full scale values.

Leaving out no. 20

Also no. 20 Melamine faced particle board influences the determination of the smoke prediction models. Thus an approach where this product was left out was done. The best found model is presented in Eq. 6.6 (the model is called the FITS6 model)

$$RSP(400)_{prediction} = -0.6087 + 117.1 \cdot f_{CO,avg} + 0.00408 \cdot t_{width} + 0.72 \cdot [plst?]$$

Eq. 6.6

The correlation plot between the predicted values and the experimental transposed values is given in the upper left panel of Figure 6-15. (The rest of the panels are the residual plots.) The choice of the best suitable prediction model is done in Section 6.7.

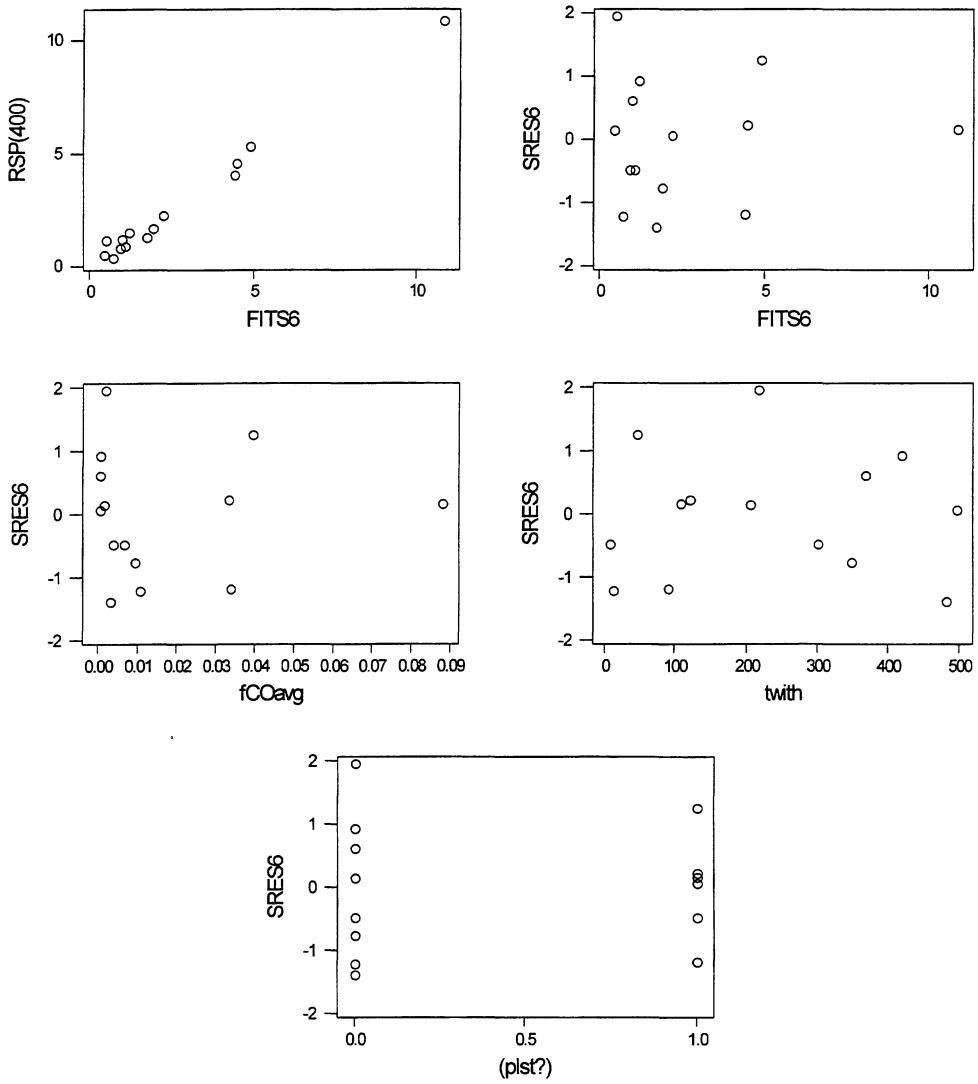

Figure 6-15 Upper left panel: the correlation plot between the predicted values and the experimental full scale data. The rest of the panels: residual plots.

6.4 Prediction of Smoke Production in Flashover Fires

There are two common choices of flashover criterion in the ISO Room Corner Test; when the rate of heat release exceeds 1000 kW and when flames emerge out of the opening.

6.4.1 The Rate of Heat Release of 1000 kW as the Flashover Criterion

Figure 6-16 shows the correlation plot between the bench scale average smoke to flame ratio and the full scale smoke to flame ratio at 1 MW. Figure 6-17 shows the correlation plot between the bench scale maximum smoke to flame ratio and the full scale smoke to flame ratio at 1 MW. The plots indicate that there is hardly any correlation. The plots also show that the full scale smoke test data seem random: The two particle boards (nos. 16 and 24) have large differences (this was not the case at 400 kW; cf. e.g. Figure 6-4). Also the two polystyrene foams (nos. 11 and 26) have large differences. The distinction between the wood and plastic based products also has disappeared. The full scale data seem to vary randomly and independent of the type of chemical composition of the building products.

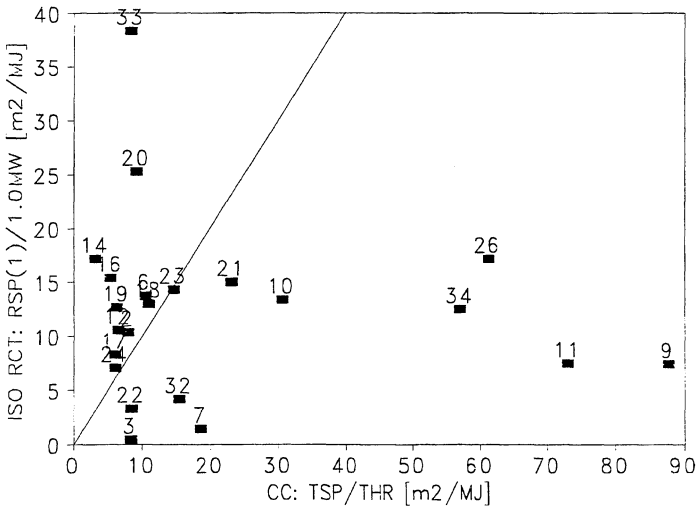

Figure 6-16 The correlation plot between the bench scale average smoke to flame ratio and the full scale smoke to flame ratio at 1000 kW (i.e. flashover).

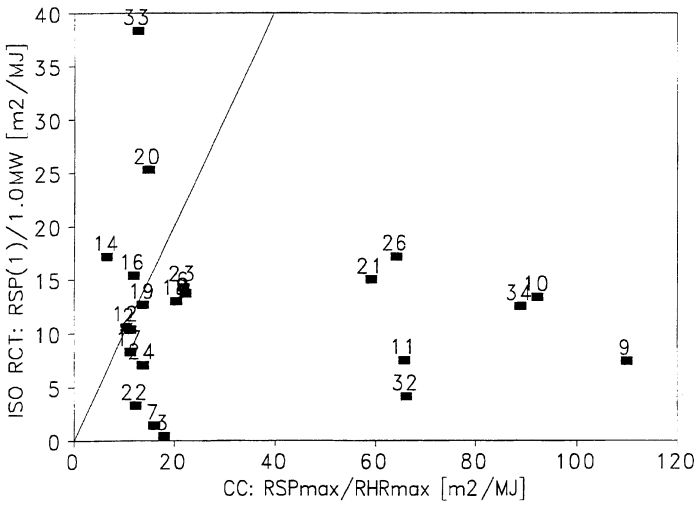

Figure 6-17 The correlation plot between the bench scale maximum smoke to flame ratio and the full scale smoke to flame ratio at 1000 kW (i.e. flashover).

Neither the simple correlation analysis nor the multiple regression approaches revealed any interesting results. Thus prediction does not seem to be possible within the framework of these approaches.

6.4.2 Flames Emerge Out of the Opening as the Flashover Criterion

Approaches were also attempted to predict full scale instant smoke to flame ratio when flames emerge out of the opening (i.e. $r_{S/Q,feo}$).

Figure 6-18 shows the correlation plot between the bench scale average smoke to flame ratio and the full scale instant smoke to flame ratio when flames emerge out of the opening. (Due to limited accessibility to the data not all products are included in the figure.) The plot shows that the full scale values are more in accordance with each other:

- The particle boards (nos. 16 and 24) have approximately the same values).
- The wood based materials have approximately the same values (nos. 2, 18 and 19). No. 17 was an outlier for unknown reasons.
- The polyurethane foams (nos. 26 and 34) have approximately the same values.

But the smoke production seems random and independent of the product; the products that are considered to be smoky in bench scale (i.e. the plastics) do not give

more smoke in flashover fires than the products considered as less smoky on bench scale (i.e. the wood based products).

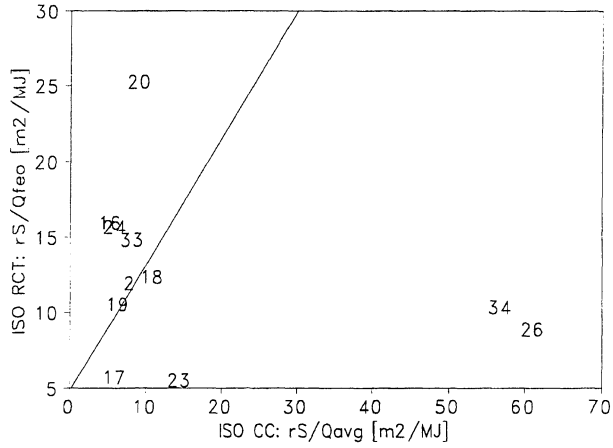

Figure 6-18 The correlation plot between the bench scale average smoke to flame ratio and the full scale instant smoke to flame ratio when flames emerge out of the opening.

6.5 The Prediction of Smoke Production in Small Non-Flashover Fires

6.5.1 Preliminary Considerations

The fires in the ISO Room Corner Test which did not go to flashover within 10 minutes are called *small non-flashover fires*. The notation «small» is related to the burner heat release rate of 100 kW during the 10 first minutes of the test.

The building products which did not cause flashover within 10 minutes are grouped in product group 2, and 17 of the 34 products considered are grouped here.

Two full scale smoke parameters are used as response variables: the full scale smoke production accumulated over the 10 first minutes of the test and the full scale smoke to flame ratio averaged over the 10 first minutes of the test. They are denoted TSP(10) and the latter $r_{S/Q}(10)$ respectively. The latter is determined by

$$r_{S/Q}(10) = \frac{TSP(10)}{THR(10)}$$

Eq. 6.7

where THR(10) is the full scale total heat release for the 10 first minutes.

Figure 6-19 is the correlation plot between the bench scale total smoke production and the full scale total smoke production (for the 10 first minutes). Except from the two outliers (nos. 8 and 15) there is a little correlation and a regression analysis estimated the model

$$TSP(10) = 17 + 2.0 \cdot TSP_{CC}$$

Eq. 6.8

where TSP_{CC} is the total smoke production (per m^2 specimen) in the Cone Calorimeter. The coefficient of 2.0 of TSP_{CC} can be interpreted as the burning area in full scale is approximately 2 m^2. Such interpretation presumes three premises

1. There has been a minor flame spread.
2. The ignited area has approximately the same degree of pyrolysation as in bench scale.
3. The effect of scale on the smoke production is minor.

If these three premises are satisfied, then the full scale total smoke production after 10 minutes can easily be predicted by bench scale smoke data. On the other hand if some flame spread occurs and/or the ignited area is not fully pyrolysed in depth, then there are better possibilities to find correlations by use of the full scale smoke to flame ratio because this parameter is roughly independent of pyrolysed mass (for well ventilated flaming fires).

Figure 6-20 shows the correlation plot between the bench scale average smoke to flame ratio and the full scale smoke to flame ratio averaged over the 10 first minutes (i.e. $r_{S/Q}(10)$). (The line in the figure is the «equal value» line.) The outlier tendencies of nos. 8 and 15 disappeared, but instead no. 5 became an outlier (the bench scale value of no. 5 is about 140 m^2/MJ and probably wrong).

In Figure 6-21 the maximum bench scale $r_{S/Q}$ is plotted versus the full scale data. Some correlation might exist, but at least nos. 6 and 31 are outliers.

The full scale $r_{S/Q}(10)$ values in Figure 6-20 and Figure 6-21 are calculated according to *gross* values, i.e.

$$r_{S/Q}(10) = \frac{TSPgross(10)}{THR_{gross}(10)} = \frac{TSP_{net}(10) + TSP_{burner}(10)}{THR_{net}(10) + THR_{burner}(10)} = \frac{TSP_{net}(10) + 55\,m^2}{THR_{net}(10) + 55\,MJ}$$

Eq. 6.9

Figure 6-22 is the same correlation plot as Figure 6-20, but with the full scale average smoke to flame ratio corrected for the burner. Now there is a tendency for the data to plot around the «equal values» line. Four of the 17 products in product group 2 are not plotted; nos. 5, 21, 30 and 31, because they all obtained negative values after the correction. This can happen for products which have little heat release or if the burner heat release rate was lower than 100 kW.

Figure 6-23 is the same correlation plot as Figure 6-21, but with the full scale average smoke to flame ratio corrected for the burner. The interesting thing is that in Figure 6-23 nos. 6 and 8 are better predicted than in Figure 6-22. This indicates that bench scale values might become easier to correlate with full scale if they are averaged over just the flaming period of burning.

The correction of the full scale smoke to flame ratio for the burner output is critical, and non-linearity is induced if it is not done because a very smoky product can obtain the same full scale $r_{S/Q}(10)$ value as a moderate smoky product if the former has little heat release. The reason for this is that the diluting effect of the burner increases with decreasing heat release from the burning product.

Thus the net full scale average smoke to flame ratio is the best response. The disadvantage with net calculations are that the data have to be obtained very accurately, and that is especial critically for products with small heat releases.

Data evaluation

Outliers were often nos. 29, 30, 31 and 32 (i.e. the IMO products). The bench scale tests of the IMO products were by a mistake done with the grid [12], and there were some doubts about their values. Thus they were left out of the model building study.

In Figure 6-24 the bench scale values of the EUREFIC products are compared to the tests data obtained within the EUREFIC programme. Unfortunately there are quite large deviations for four of the products; nos. 4, 5, 6 and 10. (no. 5 is not included in the figure due to the high value from the test done at Trätek. The value obtained within the EUREFIC programme for no. 5 was about 28 m^2/MJ.)

[12] The grid is normally used in Cone Calorimeter testing when the specimen is mounted vertically and there is a risk for that the specimen might leave the frame.

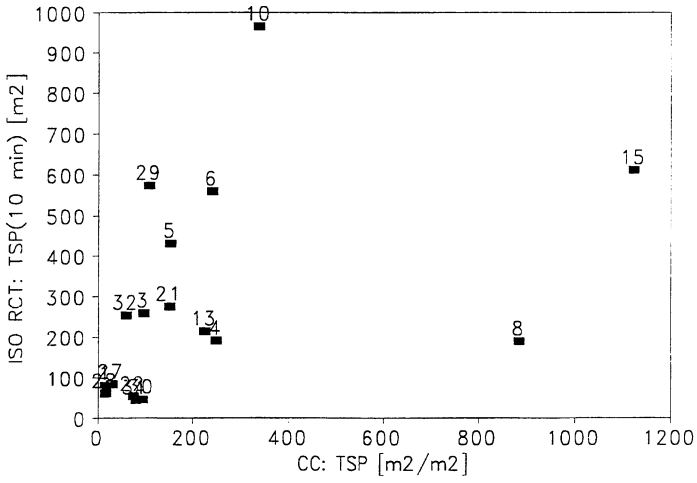

Figure 6-19 *Correlation plot between the bench scale total smoke production and the full scale smoke production accumulated over the first 10 minutes. (Some products close to the origin are difficult to identify in the plot. That is nos. 1, 22, 27, 28, 30 and 31.)*

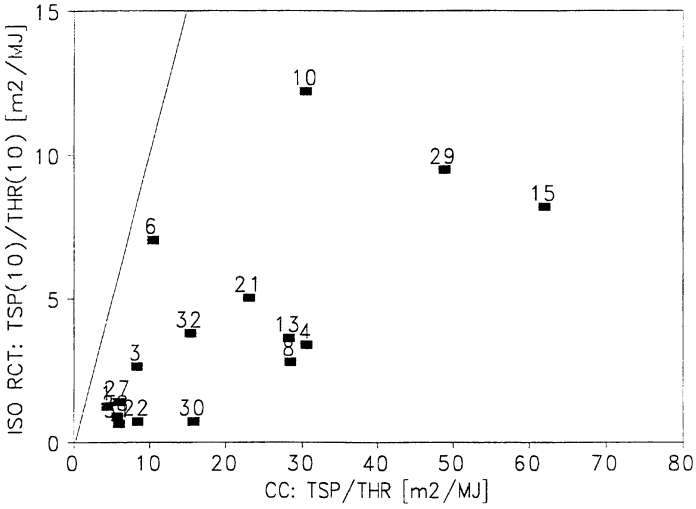

Figure 6-20 *Correlation plot between the bench scale average smoke to flame ratio and the full scale smoke to flame ratio averaged over the first 10 minutes.*

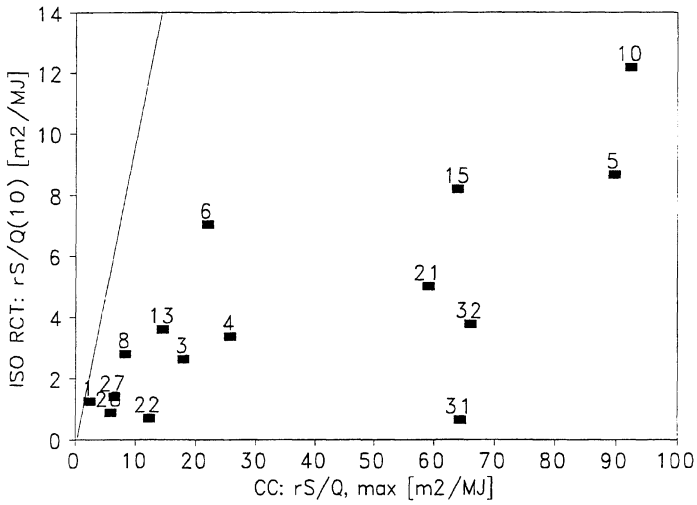

Figure 6-21 *Correlation plot of bench scalemaximum smoke to flame ratio versus full scale smoke to flame ratio averaged over the first 10 minutes.*

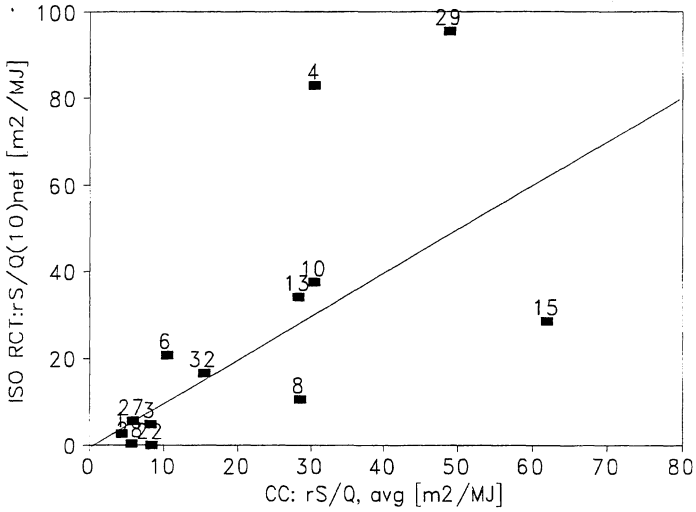

Figure 6-22 *The same correlation plot as Figure 6-20 but with full scale data corrected for the heat and smoke output from the fire source.*

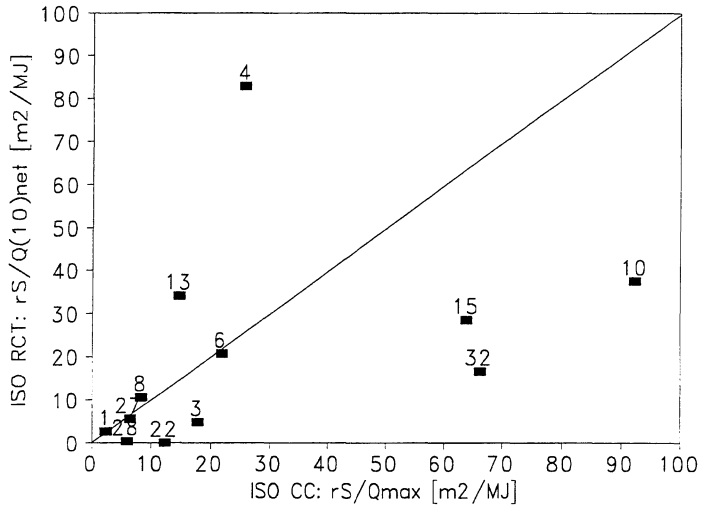

Figure 6-23 *The same correlation plot as Figure 6-21 but with full scale data corrected for the heat and smoke output from the fire source.*

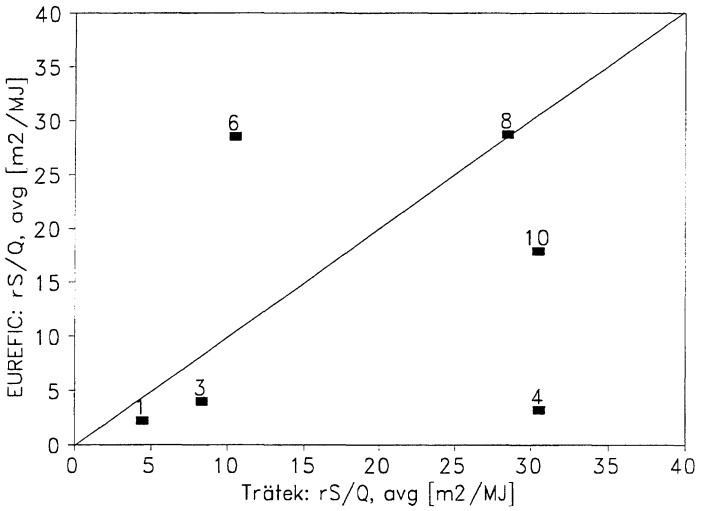

Figure 6-24 *Comparison of Cone Calorimeter data from several organizations.*

6.5.2 Summary of the Model Building Study

Prediction of TSP(10)

Attempts have been made to develop models to predict the full scale smoke production for the first 10 minutes. Models were only possible if nos. 8 and 15 were

left out. Then a prediction model which included $\phi_{S,max}$ and t_{width} seemed to make quite good predictions. However there is no good argumentation to leave out nos. 8 and 15. Thus no models are presented.

Prediction of the $r_{S/Q}(10)$
No good models to predict the *gross* smoke to flame ratio averaged over 10 minutes were found. The same was also the case for the *net* smoke to flame ratio.

Prediction of the full scale instant net smoke to flame ratio at maximum heat release rate was also attempted. Prediction could be done with a model which included $\phi_{S,max}$ and t_{width}. However the model was only based on 5 products (nos. 1, 3, 6, 8 and 10), thus the data set is too small to generalize.

6.6 The Prediction of Smoke Production in Large Non-Flashover Fires

6.6.1 Preliminary Considerations

The fires in the ISO Room Corner Test which did not go to flashover at all are called *large* non-flashover fires. The notation «large» is related to that the data being averaged over a period where the burner heat release rate was (partly) 300 kW. The study was done for the 11 products in product group 2B (i.e. the products which did not cause flashover).

At a heat release rate of 300 kW, the burner has a background value for smoke production of about 0.23 m^2/s. Thus during 20 minutes the burner itself produces about 190-200 m^2 smoke, and this gives an average smoke to flame ratio of about 0.8-1 m^2/MJ.

Figure 6-25 shows the correlation plot between the bench scale total smoke production and the full scale total smoke production after 20 minutes. A line is drawn in the figure. The line represents bench scale smoke production from a burning area of 5 m^2, plus an addition of 200 m^2.

Figure 6-26 is the correlation plot between the bench scale average smoke to flame ratio and the full scale smoke to flame ratio averaged over 20 minutes. The full scale values are not corrected for the burner output of heat and smoke. That is done in Figure 6-27. The correction resulted in that some of the full scale values then became negative, thus only 7 products are included. No correlation seems to exist, but this can be a result of the difficulties to do the correction of the burner properly.

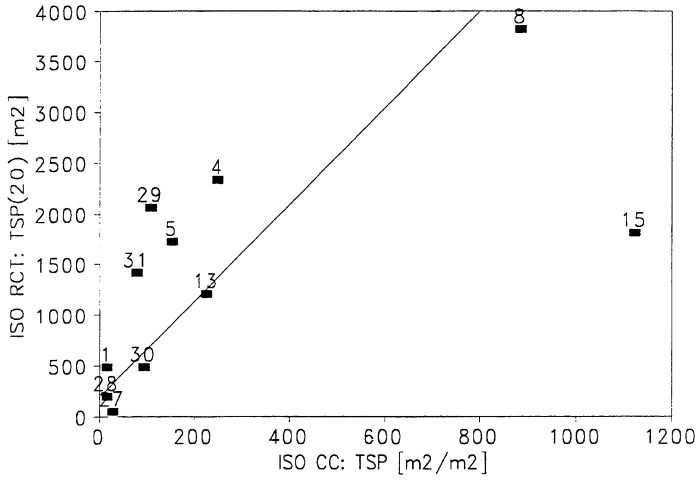

Figure 6-25 The correlation plot between the bench scale total smoke production and the full scale smoke production accumulated over 20 minutes

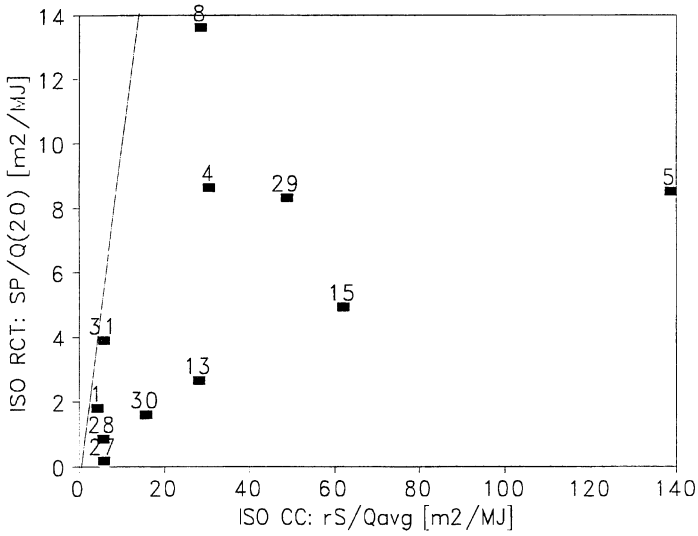

Figure 6-26 The correlation plot between the bench scale average smoke to flame ratio and the full scale average smoke to flame ratio.

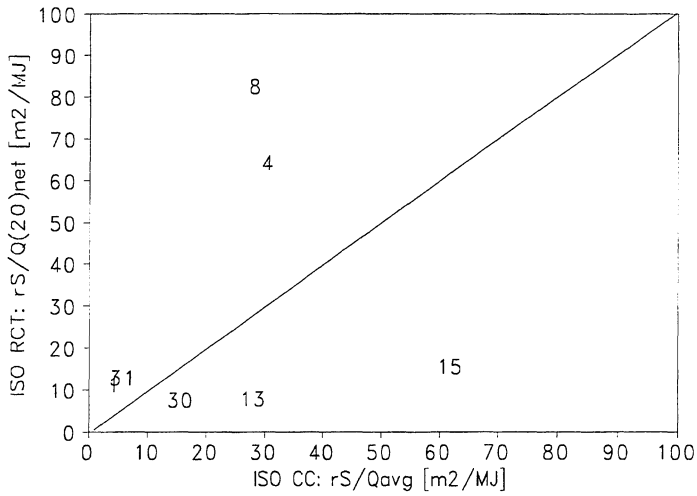

Figure 6-27 The same comparison as in Figure 6-25, but the full scale data are corrected for the heat release and smoke production to the burner.

6.6.2 Summary of the Model Building Study

The correlation analysis showed that the bench scale smoke and CO data had approximately the same correlation to full scale smoke test data. The same was the case for the bench scale t-parameters. Table 6-3 illustrates this. The table summarizes the correlation analysis between the full scale total smoke production after 20 minutes and the test fire parameters (i.e. TSP(20)). The full scale TSP(20) and $r_{S/Q}(20)$ were correlated for the data considered, thus approximately the same results were found for $r_{S/Q}(20)$.

Table 6-3 The simple correlation analysis on the extensive test fire parameters.

Z_i	t_{ign}	RML_{max}	RHR_{max}	RSP_{max}	$RMCO_{max}$	$RMCO2_{max}$	t_{width}	$t_{w,CO2}$	(..O_s?)
r	0.570	-0.435	-0.322	0.147	0.095	-0.397	0.769	0.648	-0.066
Z_i	t_{m-i}	TML	THR	TSP	TMCO	$TMCO_2$	$t_{w,S}$	$t_{w,CO}$	(plst?)
r	0.633	0.572	0.707	0.647	0.617	0.389	0.734	-0.022	0.066

Prediction of TSP(20).
The best model found for prediction of TSP(20) included $\phi_{CO,max}$ and $t_{max\text{-}ign}$. The model was

$$TSP(20) = -361 + 81224 \cdot \phi_{CO,max} - 17.2 \cdot t_{max-ign}$$

Eq. 6.10

The model obtains a standard deviation about the regression line and a coefficient of determination of 114 m^2 and 99% respectively. The model is based on 7 of the 11 products in product group 2 (i.e. nos. 28, 29, 30 and 31 were left out). The correlation plot between the predicted values and the full scale smoke production is given in Figure 6-28.

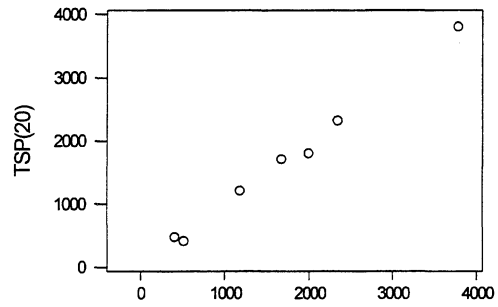

Figure 6-28 The correlation plot for the model according to Eq. 6.10 (the X-axis is TSP(20) predicted according to Eq. 6.10).

6.7 Discussion

6.7.1 Prediction of Pre-Flashover Smoke Production

The study of smoke prediction models to predict smoke production in pre-flashover fires revealed that the bench scale CO data was preferred to the smoke data (e.g. compare Figure 6-1 and Figure 6-6). Intensive CO data (i.e. ϕ_{CO} and f_{CO}) were also found to be preferred to extensive CO data (i.e. RMCO and TMCO).

The preference of CO data might be seen in view of the work of Köylü and Faeth [63]. They found a simple relationship between small scale smoke and CO production for sooty liquids:

$$f_{CO} = 0.159 \cdot f_S$$

Eq. 6.11

Figure 6-29 shows the comparison between the results of Köylü and Faeth [63] (i.e. Eq. 6.11, which is represented by the line in the figure) and the bench scale test results for the 17 products in product group 1 (to secure flaming combustion the

scale CO data being preferred to the smoke data (compare the FITS4 and the FITS5 model, i.e. Figure 6-12 and Figure 6-14). Further no. 7 spoiled the correlation of the FITS5 model, and in Figure 6-29 no. 7 is also an outlier. However it has been pointed out earlier that no. 7 has questionable bench scale smoke data. The Cone Calorimeter data are in accordance with the general observations on bench scale smoke production referred to in Section 2.2. However some deviations were found between the smoke and CO data from the Cone Calorimeter and the data from the bench scale apparatus of FMRC [13] [11] (especially as this was the case for comparison of the test data of polyethylene and polyurethane). These findings indicate that further studies should be done on the ISO Cone Calorimeter to evaluate the differences between Cone Calorimeter data and similar data from other bench scale apparatuses. Such knowledge has a general importance and forms a necessary basis for the test, and the application of it. The results presented in Chapter 4 form a starting point for such research.

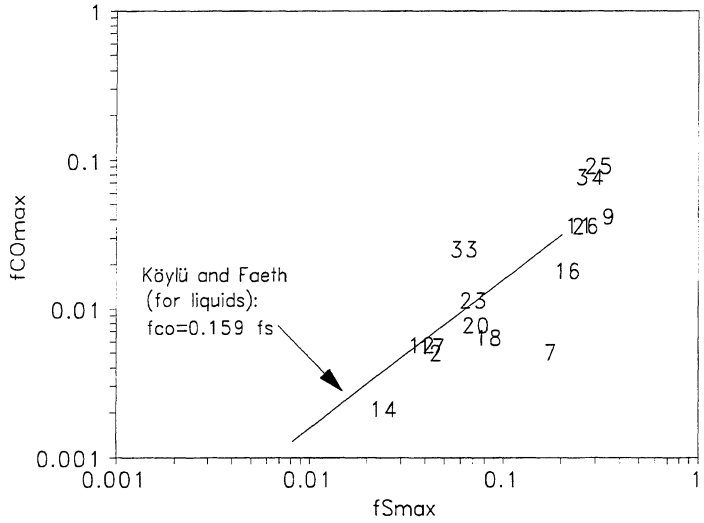

Figure 6-29 The comparison between the small scale test results of Köylü and Faeth [5] and the results obtained in the ISO Cone Calorimeter for the 17 products in product group 1.

Four actual prediction models, FITS2, FITS3 FITS4 and FITS5, are presented. The FITS2 model which uses the three regressors; $f_{CO,avg}$, t_w,S and the dummy variable [plst?] is presented to identify the non-linear relationship between bench scale and full scale test data (cf. Figure 6-7 and Figure 6-8).

Two models based on a logistic relationship are presented; The FITS 3 and the FITS4 model. Prediction done by the FITS3 model is shown in Figure 6-10. The

13 Factory Mutual Research Corporation, Norwood, MA, USA.

[plst?] is presented to identify the non-linear relationship between bench scale and full scale test data (cf. Figure 6-7 and Figure 6-8).

Two models based on a logistic relationship are presented; The FITS 3 and the FITS4 model. Prediction done by the FITS3 model is shown in Figure 6-10. The prediction is good, except that the results for the particle boards are overpredicted. This is not the case for the FITS4 model (cf. Figure 6-12). However this model predicts no. 14 badly.

When nos. 7 and 34 were left out of the model building study, good prediction was possible with a model that included $\phi_{S,avg}$, $t_{max\text{-}ign}$ and the dummy [plst?] (cf. Figure 6-14). Unfortunately the model fails on the PU-foams. It is interesting that when the products identified to have outlier tendencies in Figure 6-29 are left out (i.e. nos. 7, 25 and 34), then the bench scale smoke data is preferred to the bench scale CO data. However the meaning of this is not understood and needs further research.

When no. 20 was left out of the data set, prediction was possible without a logistic model. This is because one of the reasons for using a logistic model was actually no. 20. However the model seems to fail close to the origin (cf. Figure 6-15).

The choice of the logistic model can be discussed. The full scale smoke production for products with low smoke generation is governed by the smoke production of the burner. Thus there is a lower attainable level for the smoke production, therefore the initial shape of the curve to the model is possible. On the other hand, the logistic model presumes that there is a maximum smoke production. This might be theoretically possible. Then it has to be assumed that the combustion is influenced by the concentration of partly burnt species (e.g. as smoke and CO), and that high enough concentrations of such species might result in further combustion. In other words, there is a higher reachable upper level for the concentration of partly burnt species. However this is a complex and extensive topic of which it seems to be difficult to find relevant references ([64], [65], [66] and [67] were among others studied).

Altogether the bench scale f_{CO}, ϕ_{CO}, t_{width} and $t_{max\text{-}ign}$ and the dummy variable [plst?] were identified as the most interesting regressors. In the model presented it is the average values of the CO data which are used. Nearly the same results were often obtained with the maximum values. But these were difficult to estimate in bench scale, and often had large variation. Thus they were avoided. Indications were found that bench scale data that were averaged over the flaming period of the test might be easier to correlate.

$t_{w,S}$ was also identified as a good regressor, but there is a risk that this is caused by the correlation between $t_{w,S}$ and t_{width}. Thus it was omitted.

The choice between the CO- and t-parameters is difficult to make, because the differences are small, and the choices are influenced by the uncertainty of the data (i.e. variation and outliers). Most of the other bench scale parameters developed in Chapter 4 were inferior to the above-mentioned parameters.

The FITS4 model was chosen in favour of the other three models. FITS5 is not general, because it does not predict all plastic products (i.e. the PU-foams). The FITS3 model seems to predict and conserve the ranking better than FITS4, thus this model could also have been chosen. But if $t_{w,S}$ is replaced by t_{width}, then the FITS4 model becomes better. However $t_{max\text{-}ign}$ and t_{width} are correlated, thus the choice is not critical.

Approximately half of the variation explained by the prediction model (i.e. «SS Regression» which is defined in Section 5.3) is done with the bench scale CO data. The rest is explained by $t_{max\text{-}ign}$ and [plst?] (cf. the analysis of variance in the printout of the regression analysis to the FITS4 model). $t_{max\text{-}ign}$ correlates the other t-parameters, beside they also correlate other parameters, thus the interpretation of its meaning in the model can be extensive. t_{width} is related to the «burn time» of a «fuel element» during the growth of the fire in full scale, and this might be of importance. However, interpretations of this kind are only speculations.

The dummy variable [plst?] is easier to accept on a scientific basis, because it is recognized that plastics yield more smoke than other types of building products.

Thus the model to assess smoke production of building products is

$$RSP(400)_{prediction} = 11.4 \cdot \left(\frac{e^{-3.80+57.2\cdot\phi_{CO,avg}+0.00341\cdot t_{max-ign}+1.66\cdot[plst?]}}{1+e^{-3.80+57.2\cdot\phi_{CO,avg}+0.00341\cdot t_{max-ign}+1.66\cdot[plst?]}}\right)$$

Eq. 6.12

The panels in Figure 6-11 show the range of the bench scale parameters (i.e. the predictors) that the prediction model is based on. It is recommended that $\phi_{CO,avg}$ is averaged over the flaming period.

The influence of the irradiance level has not been studied. Neither has a further optimization of Eq. 6.12 been conducted. There is an upper limit of how accurate Eq. 6.12 can or needs to be. The variation in the full scale data governs the upper reachable level of prediction accuracy (cf. Section 5.6). Due to the distribution of the full scale data, it is hard to evaluate whether this is the case for Eq. 6.12. For the

same reason further optimization is hard to do. The accuracy of the relation between optical density and visibility is also an upper limit of how accurate Eq. 6.12 needs to be. As outlined in Section 2.4 this relation is not accurate.

If zero value is used for the predictors, then RSP(400) becomes 0.25 m^2/s. The background value for the burner is 0.23 m^2/s at a heat release of 300 kW. These two values are in sufficient correspondence with each other. Thus the model satisfies the zero criterion.

The model is governed by no. 34 (this is a so-called high leverage point). The bench scale values of no. 34 were compared to the bench scale values of nos. 25 and 67. They were in sufficient accordance with each other. Thus the high leverage point is verified both in bench scale and full scale.

Note that the models presented here cannot be directly used in optimalization of the smoke generation properties of building products. Because then the collinearity structure between the regressors has to be taken into consideration. The model is made for evaluation purposes.

6.7.2 Prediction of Flashover Smoke Production

The most interesting criterion for flashover fires was «flames emerge out of the opening» (cf. Figure 6-18). This criterion increases the homogeneity in the data set, i.e. the combustion conditions are more identical with such a criterion.

Since both the smoke and CO production in fires result from incomplete combustion, the literature on CO formation in post-flashover fires was studied. Among other things, the research done by National Institute of Standards and Technology (NIST), USA on the global equivalence ratio concept was considered [68] [69] [70]. However, no results were found that could be used in relation to the findings within this thesis to predict smoke data from full scale flashover (and post-flashover) enclosure fires.

The reaction kinetics for smoke produced during post-flashover burning are different from the CO formation. It seems that the smoke (i.e. soot) reacts faster and more effectively than CO (cf. the ISC'94 publication for further comments). No good models to predict full scale flashover smoke data by use of the Cone Calorimeter were found. Probably such relationships do not exist. Such conclusions have been given for the abilities of bench scale data to predict full scale post-flashover CO data.

6.7.3 Prediction of Non-flashover Smoke production

As pointed out the choice of the full scale smoke parameter response influences the work on building models. Of the parameters considered, the best choice is generally the net average smoke to flame ratio, because this parameter is roughly independent of the pyrolysed mass for well ventilated flames.

However, the smoke to flame ratio does not avoid the problems with the effect of scale and combustion conditions on the smoke production. This can be exemplified by plotting the full scale smoke to flame ratio as function of the rate of heat release. In Figure 6-30 and Figure 6-31 this is done for the full scale tests of *textile wallcovering on gypsum paper plasterboard* (no. 3) and *PVC on gypsum paper plaster board* (no. 10). In both figures the instant and average smoke to flame ratios are drawn as functions of the rate of heat release. They are denoted RSP/RHR and TSP/THR respectively (the former has a heavy solid line). The data are gross values, i.e. no corrections are done for the burner.

Both figures show that the smoke to flame ratio increases with the fire (e.g. the instant smoke to flame ratio for no. 3 is approximately 5 m^2/MJ at $RHR_{max} \approx 570$ kW). The figures show that the smoke production depends on heat release and whether the fire is increasing or decreasing (arrows pointing to the right denote fire growth, while arrows pointing to the left denote fire decay). In the work on the prediction of pre-flashover data, the attempt was made to avoid such effects by selecting smoke data at a specified rate of heat release level. Thus the prediction approached on the non-flashover are *far more rough*. Thus when average values are used, then it is assumed that such data are sufficiently homogeneous. The correlations obtained showed that this was a too rough approach. Thus the lack of correlation between the bench scale and full scale data might have been caused by a such a rough approach. Though the non-flashover data might be possible to predict by bench scale test data, far more advanced approaches have to be adopted. Such approaches must probably take at least the temperature conditions into consideration. It is suggested that the needs for the prediction of such data is validated before such work are eventually started.

Some models were identified, but they all have some drawbacks (e.g. exclusion of products, which limits the generality). Thus none of the models found were assessed to be applicable on a general basis. A way to assess the smoke production for these products can be to use the smoke prediction model found for the pre-flashover fires.

Figure 6-32 shows the *comparison* of the prediction of smoke production at 400 kW done by the FITS3 and FITS4 model. The comparison is done for the products in

product groups 2 and 3. Predictions according to both models are presented to evaluate which of them is best [14]:

- The prediction of the PVC wallcoverings (i.e. nos. 10, 21 and 71) range from 8-12 m^2/s according to the FITS3 model, and 6-12 m^2/s according to the FITS4 model. PVC is a thermoplastic material which does not melt and flow, so that the ranking between the PE and PS foams and the thermosettings (i.e. the PU foams) is possible. In a full scale test in the ISO Room Corner Test of a pipe insulation of PVC, the smoke production was about 10.5 m^2/s [60]. Thus the range of the predictions is supported by these results too.
- The textiles (nos. 3 and 22) have values of about 1 m^2/s. These predictions are good.
- The polystyrenes (nos. 15 and 69) have results of about the same values as the polystyrenes in product group 1. Thus they are predicted well.
- The prediction for the only melamine faced product (i.e. no. 4) is in accordance with the results obtained for no. 20.
- The two thermosettings (nos. 63 and 67) were predicted with quite probable values. Polyisocyanurate foam was also tested in [60] and the value obtained there seems to be at least as large as the predicted value (accurate data were not possible to obtain from the report).
- The gypsum paper plasterboards (nos. 1, 27 and 28) have too high values. This is especially the case for no. 1.
- Both prediction models fail on the fire retarding wood based products (i.e. nos. 6, 8 and 13).

The FITS3 and FITS4 model seem to give roughly the same values.

Both models fail on the fire retarding wood based products and the gypsum paper plaster boards. This is mainly caused by the way the bench scale data are obtained. If the accumulated data (i.e. TMCO and THR) were only obtained over the flaming period, then the predictions of these products would have been better. This can be verified by using the value for the maximum CO data in Eq. 6.12 [15]. Some of the values seem still to be somewhat too high, however this might be caused by the difficulties in estimating maximum bench scale values for these products (their variations were large, cf. Table 5-2 and the related figures). Thus they are probably best predicted by use of the bench scale CO data averaged over the flaming period of the combustion.

---

14 The IMO products are not commented on due to questionable bench scale data.

15 The FITS4 model could also be developed by use of the $\phi_{CO,max}$, instead of the $\phi_{CO,avg}$. Then the coefficients in the model were only slightly changed, and the standard deviation about the regression line and the coefficient of determination became practically unchanged.

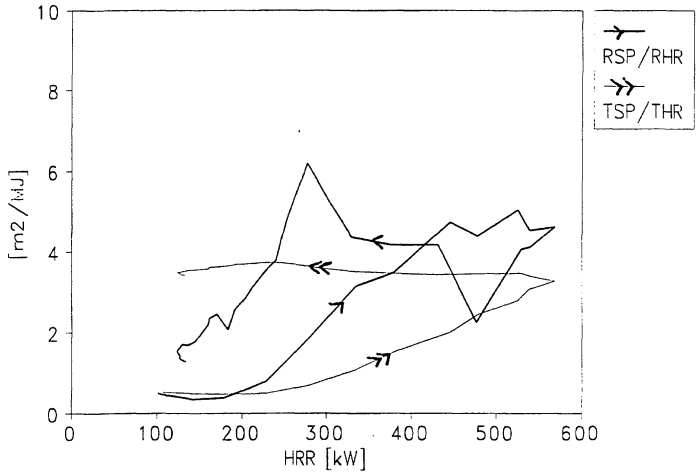

Figure 6-30 The instant and average smoke to flame ratio as a function of the rate of heat release for no. 3 Textile wallcovering on gypsum paper plaster board.

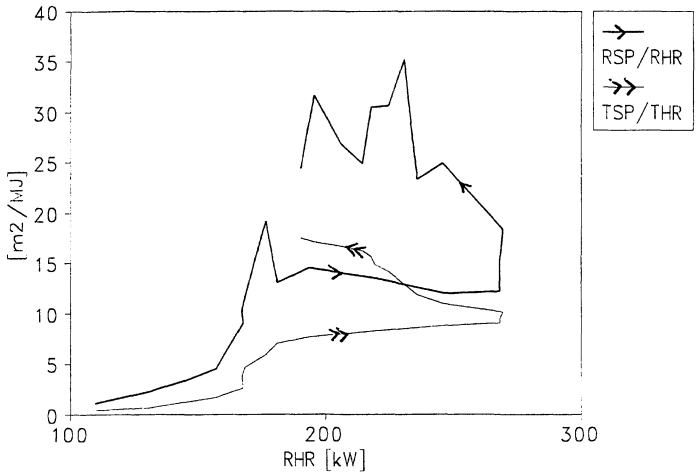

Figure 6-31 The instant and average smoke to flame ratio as a function of the rate of heat release for no. 10 PVC wallcovering on gypsum paper plaster board.

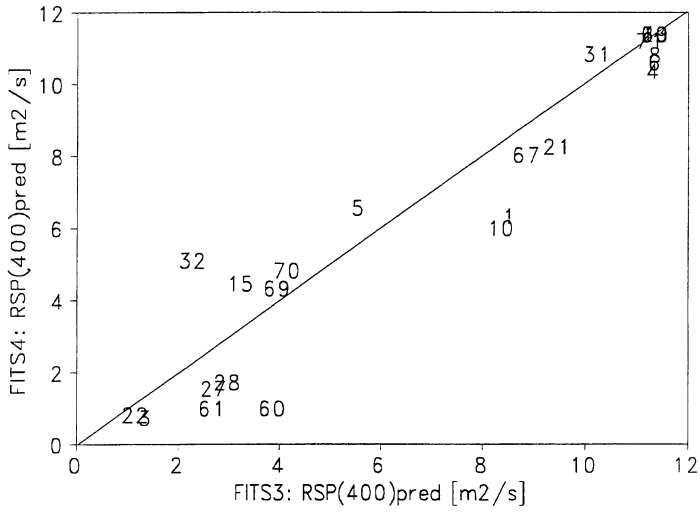

Figure 6-32 Comparison of the predicted smoke production at 400 kW according to the Prediction models FITS3 and FITS4. The comparison is done for the products in product groups 2 and 3.

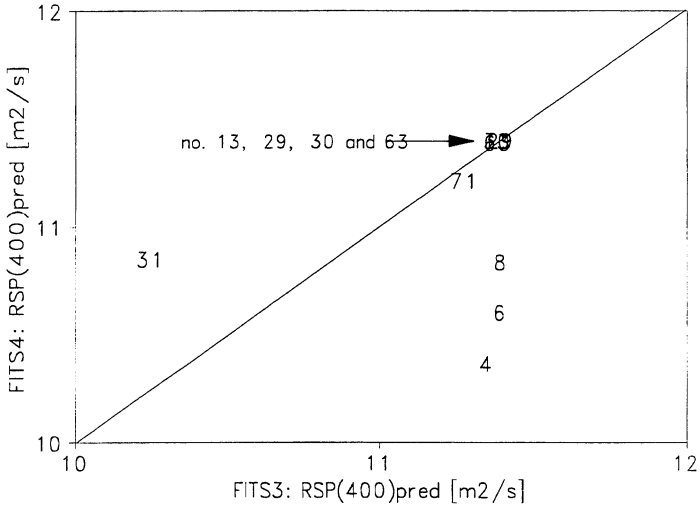

Figure 6-33 Enlargement of Figure 6-32.

7 ASSESSMENT OF ISO FIRE TEST METHODS

7.1 Introduction

If the smoke production from burning building products is governed by the fire conditions rather than the type of building product, then the representation of the fires by the ISO Room Corner Test is only valid in those cases where the fire conditions are more or less identical to the conditions in the ISO Room Corner Test. If this is the case, then smoke classification according to a system based on the ISO Room Corner Test cannot be considered to be general. This chapter is about to verify the use of the ISO Room Corner Test as a core in a smoke classification system. This has been denoted to verify the generality of full scale smoke test data and the consistency of the ISO Room Corner Test. The way this is done is explained in Section 7.2.

A general assessment of the ISO fire test methods considered is also given. Note that the results found in Chapter 8 extend these assessments.

7.2 Research Design

The verification of the generality of real scale smoke test data and the consistency of the ISO Room Corner Test is done by comparing smoke test data from the ISO Room Corner Test to smoke test data from other enclosure tests. The other enclosure tests are

- The Full Scale CSTB Room Fire Test
- The Enlarged Scale Room Corner Test
- The Medium Scale Room Corner Test

The verification is limited by the range of enclosure fires that si considered by the tests considered. The medium scale test can be considered to be a lower extreme case of enclosure sizes, while the enlarged scale test is an upper limit. The verification is also limited to fires where the fuel load consists of building products and a fire source (i.e. a propane burner or a wood crib). Only flaming fires are considered, and as before they are divided into three types

- pre-flashover fires
- non-flashover fires
- flashover and post-flashover fires

The verification of the *generality* of smoke data is done by data from the ISO Room Corner Test as the starting point. Such data are evaluated against data from the above-mentioned tests. If the comparisons of the data show that they are in sufficient accordance with each other, then the generality of real scale smoke data is validated. Implicitly, the *consistency* of the ISO Room Corner Test is also validated, since data from the test formed the starting point for the comparisons.

Pre-flashover fires are represented by data from the ISO Room Corner Test where flashover occurred within 10 minutes (i.e. product group 1). The data used are the smoke production rates at 400 kW heat release rate. The flashover and post-flashover test data also originate from product group 1. Non-flashover fires are related to the tests in the ISO Room Corner Test where smoke test data without influence of flashover burning conditions can be obtained. This is the case for product group 2 (i.e. the products which caused a possible flashover after 10 minutes).

Generally, the full scale smoke test data from the pre-flashover and non-flashover fires are not influenced by flashover burning conditions. However non-flashover data from the ISO Room Corner Test might originate from burning conditions where the heat release rate exceeded 400-500 kW. Such burning conditions can be especially due to low combustion temperatures in combination with the fire gradually turning from a fuel controlled fire and into a ventilation controlled fire. In addition high rates of heat release might include the combustion of ceiling specimens. Such burning conditions are complex and are not yet fully understood. In connection with the work reported in the ISC'94 publication it was recognized that there might be poor material dependence concerning the smoke data produced during such conditions.

The verification has to be done with intensive fire parameters. In contrast to extensive fire parameters these are roughly independent of the area of burning or the degree of pyrolysation of the area burning (for well ventilated flaming fires). The smoke to flame ratio is used in the comparisons

$$r_{S/Q} = \frac{SEA}{\Delta h_{c,eff}}$$

Eq. 7.1

Both instant and average values of $r_{S/Q}$ are used. This is identified by the addition of subscript «i» and «a» respectively.

7.3 The ISO Room Corner Test

7.3.1 Pre-Flashover Verification

Unfortunately neither the data from the Medium Scale Room Corner Test nor the full scale CSTB Room Fire Test are accessible in a way that permits accurate data selection in the growth stage of the fires (i.e. during pre-flashover burning). Thus the starting point verification was only possible to do against the Enlarged Scale Room Corner Test.

Two products caused flashover in both full scale and enlarged scale: No. 2 Plywood and no. 7 Combustible faced mineral wool. Unfortunately, flashover did not occur during the first 10 minutes in enlarged scale. This in combination with the large room volume of the enlarged test showed that intensive enlarged scale data were not suitable for the comparison. Instead the *average* smoke to flame ratio for the first 10 minutes period in the Enlarged Scale Room Corner Test can be used. The data were calculated according to

$$r_{S/Q,avg} = \frac{TSP_{ES}(0-10min)}{THR_{ES,g}(0-10min)}$$

Eq. 7.2

where subscript ES and g denote enlarged scale and gross values (i.e. burner not subtracted) respectively. These data were compared to intensive ISO Room Corner Test smoke to flame ratio data selected at 400 kW. The comparison is shown in Figure 7-1. The number on the dots identify the product number and the line indicates equal values. None of the values were corrected for the burner output. This was not necessary because both the full scale and enlarged scale data had been equally influenced by the burner (since the burner output was 100 kW during the first 10 minutes for both tests). The figure shows a reasonable relationship between the data.

No. 7 went to flashover in the third period in enlarged scale (i.e. between 20 and 30 minutes). Thus for this product the average smoke to flame ratio could also be calculated for the first 20 minutes according to

$$\frac{TSP_{ES}(0-20min)}{THR_{ES,g}(0-20min)}$$

Eq. 7.3

The comparison is included in Figure 7-1 as the unidentified dot. For this value the one to one correlation is lost. This is not explained by the change in the burner output, because that should eventually decrease the value in enlarged scale (instead of increasing it) [16]. Instead it might be caused by a change in the enlarged scale burning conditions, and the phenomena are not fully understood. Visual observations stated that the ceiling was ignited during the second period, and that also might be some of the reason.

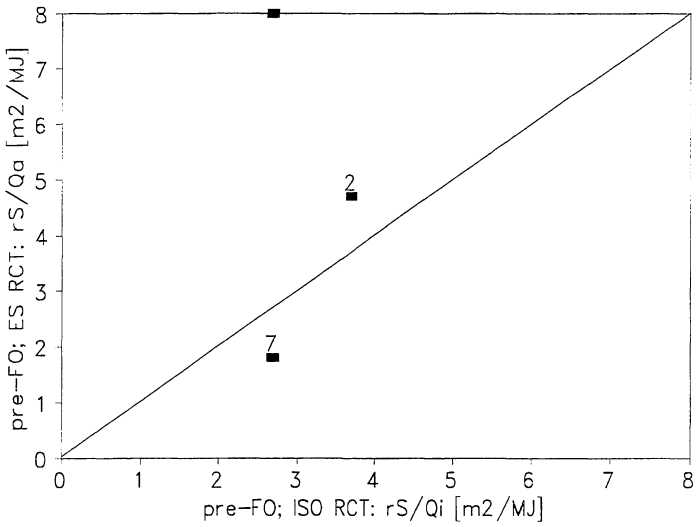

Figure 7-1 *Comparison of the instant smoke to flame ratio selected at RHR=400 kW in the ISO Room Corner Test (X-axis) versus the average smoke to flame ratio in the Enlarged Scale Room Corner Test.*

7.3.2 Non-flashover Verification

Non-flashover smoke data from the ISO Room Corner Test are compared with smoke data from Enlarged Scale and Medium Scale.

The ISO Room Corner Test can also be compared internally for the products which did not cause flashover (i.e. product group 2B). For these 11 products the smoke to flame ratio can be averaged over the first 10 minutes, and the whole test time (i.e. 20 minutes). The comparison is shown in Figure 7-2. No corrections are done for the burner output. Thus if the influence of the combustion conditions were equal, then there should be a tendency to location of the dots below the «equal values» line. The figure indicates some correlation, but four outlier exist: nos. 4, 8, 15 and 31. The

16 Due to the thin out effect of the burner on intensive smoke data.

three outliers located over the «equal values»-line might be caused by the change in combustion conditions.

Verification versus the Enlarged Scale Room Corner Test
Three products did not cause flashover during the first 10 minutes in neither the ISO Room Corner Test nor the Enlarged Scale Room Corner Test

- No. 3 Textile wallcovering on gypsum paper plaster board
- No. 6 FR particle board, type B1
- No. 10 PVC-wall carped on gypsum paper plaster board

In full scale and enlarged scale the average smoke to flame ratio were calculated according to Eq. 7.2. During the first 10 minute period both tests had a burner output of 100 kW, thus the correction of the burner was avoided. The comparison is shown in Figure 7-3. As the figure shows the ranking is preserved and the values are somewhat lower in enlarged scale. This could be expected since the combustion can be better in the Enlarged Scale Room Corner Test , due to larger room height.

Since the three products considered did not cause flashover at all, comparison can also be done versus the enlarged scale data averaged over 20 and 30 minutes. Such comparisons are shown in Figure 7-4 and Figure 7-5 respectively. Corrections were not made due to the burner output. As in Figure 7-1 this caused a tendency to increase enlarged scale smoke production. The tendency seems to increase with the growth of the fires.

Comparison Versus the Medium Scale Room Corner Test
Four of the products tested in full scale and medium scale did not cause flashover within 10 minutes in any of the tests. For these products the average smoke to heat ratios are found for the first 10 minutes. The comparison is shown in Figure 7-6. No corrections are made for the burner output. As the figure shows, correlation exists between the data.

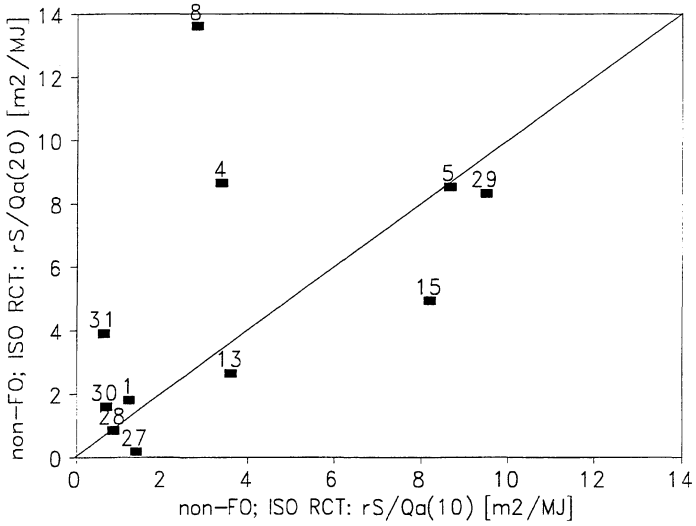

Figure 7-2 *Comparison of the average smoke to flame ratio in the ISO Room Corner Test for the products which did not at all cause flashover. The X-axis is the values averaged over the first 10 minute period, and the Y-axis is the values averaged over the whole test time (i.e. 20 minutes).*

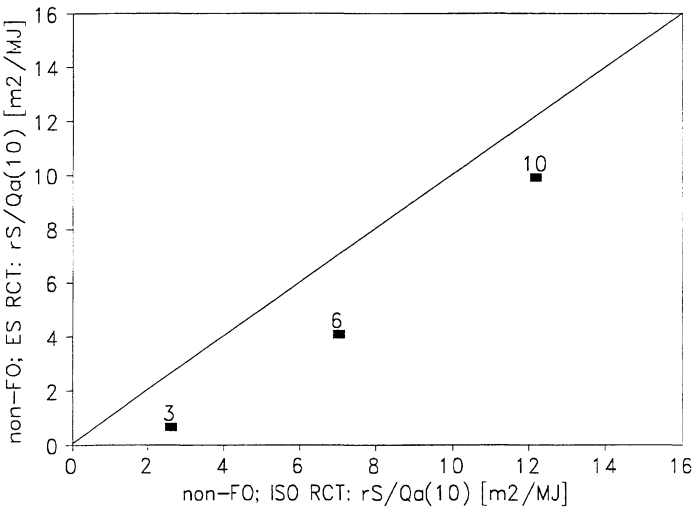

Figure 7-3 *Comparison of non-flashover average smoke to flame ratio ($r_{S/Q,avg}$) between the ISO Room Corner Test and the Enlarged Scale Room Corner Test.*

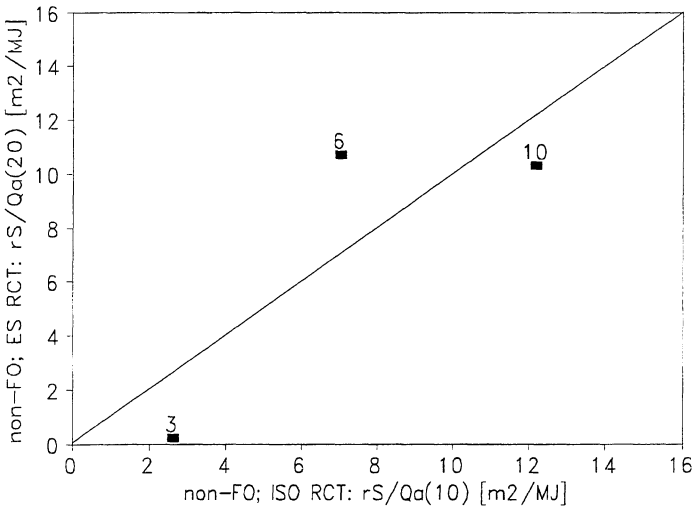

Figure 7-4 *Comparison of non-flashover average smoke to flame ratio ($r_{S/Q,avg}$) between the ISO Room Corner Test and the Enlarged Scale Room Corner Test. The Enlarged Scale data are averaged over the first 20 minutes of the test.*

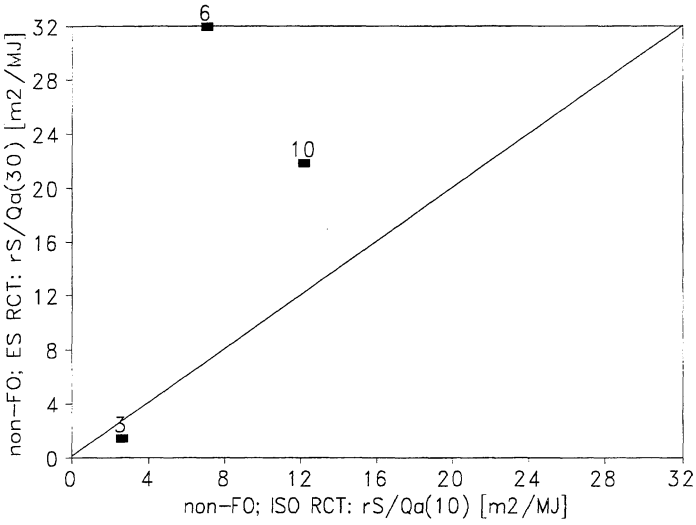

Figure 7-5 *Comparison of non-flashover average smoke to flame ratio ($r_{S/Q,avg}$) between the ISO Room Corner Test and the Enlarged Scale Room Corner Test. The Enlarged Scale data are averaged over the first 30 minutes of the test.*

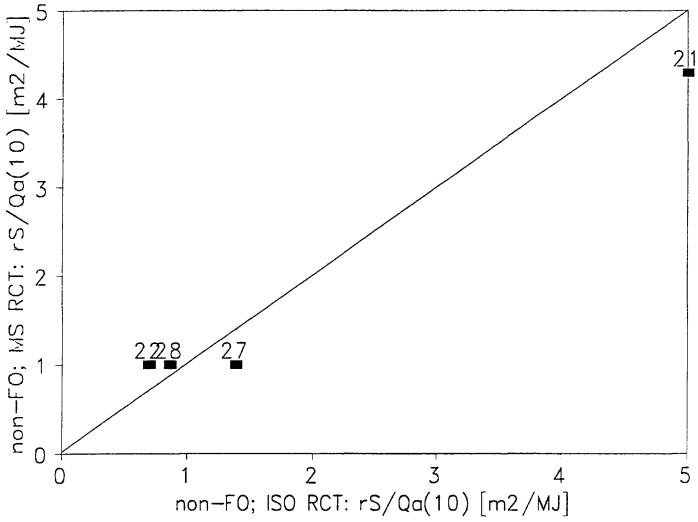

Figure 7-6 Comparison of the average smoke to flame ratio for the first 10 minutes in the ISO Room Corner Test and the Medium Scale Room Corner Test.

7.3.3 Flashover and Post-Flashover Verification

The flashover and post-flashover fires in the ISO Room Corner Test can be verified versus all three enclosure tests considered.

Verification Versus the Enlarged Scale Room Corner Test
Figure 7-7 shows the comparison between the ISO Room Corner Test and the Enlarged Scale Room Corner Test for flashover smoke data obtained when flames emerge out of the opening. Included in the plot are just the two products which caused flashover in both tests.

The full scale test data were produced during a burner output of 100 kW while for the enlarged scale data were selected at a burner output of 300 kW and 900 kW for nos. 2 and 7 respectively. This is corrected for by adjusting the considered data for the burner heat release. However such corrections induce uncertainty in the enlarged scale data because for these data the fraction of the burner heat release rate to the gross heat release rate was larger. In the enlarged scale tests, 10-20% of the fire gases escaped the duct measurements (due to leakage). This poses no problems for gross intensive parameters, but only when the attempt is made to correct for burner output.

The comparison indicates that there is more smoke generation in enlarged scale, but that the ranking of the products is preserved. The identified tendency to increased smoke generation also occured in the comparisons in Figure 7-1, Figure 7-4 and Figure 7-5. As stated before these phenomena are not full understood, but can have been partly caused by the ventilation factor being approximately 40% lower in enlarged scale than in full scale.

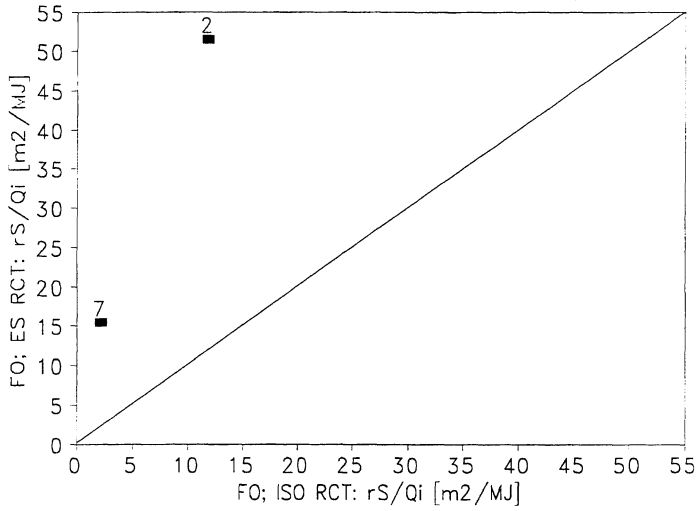

Figure 7-7 The flashover instant smoke to flame ratio compared between the ISO Room Corner Test and the Enlarged Scale Room Corner Test.

Verification versus the Medium Scale Room Corner Test

The Scandinavian products were also tested in the Medium Scale Room Corner Test. Nine of these caused flashover within 10 minutes in both the ISO Room Corner Test and the Medium Scale Room Corner Test. Besides, two products (nos. 21 and 22) caused flashover after 10 minutes in both tests.

The smoke to flame ratio was calculated at flashover conditions for both tests and corrections were made for the burner (by subtracting the burner heat release rate). The flashover criterion used was when flames emerge out of the opening.

The comparison is shown in Figure 7-8. No. 20 is not in the plot, because this product had a medium scale value far out of the range of the figure. In medium scale nos. 20 and 26 had the flashover in the second period (i.e. after 10 minutes). In the figure, no. 23 is an outlier. No. 23 was also tested without combustibles in the ceiling, and this value corresponds better to the full scale value (this comparison is the unidentified dot just below no. 17). However no. 22 is also an outlier, and both nos. 22 and 23 are textile wallcovering. Also nos. 16 and 19 were outliers, but

excepting these products the figure indicates that there is some correlation between the methods.

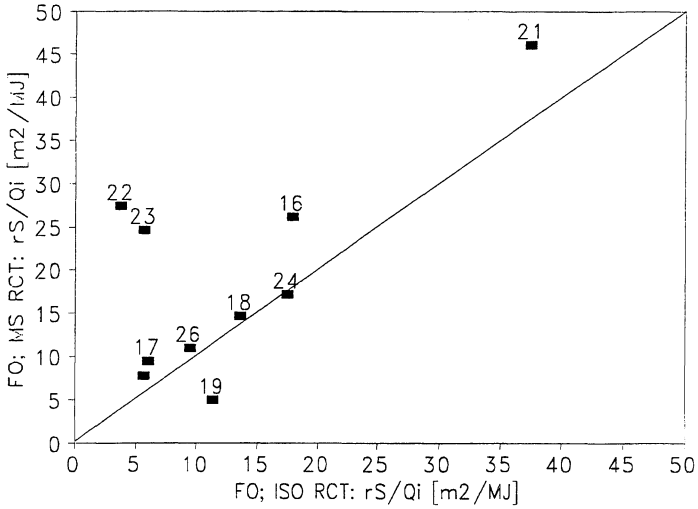

Figure 7-8 *Comparison of the flashover instant smoke to flame ratio ($r_{S/Q,inst}$) between the ISO Room Corner Test and Medium Scale Room Corner Test.*

Verification versus the Full Scale CSTB Room Fire Test

The ISO Room Corner Test and the CSTB Room Fire Test do not always address the same products, but in the cases where the same type of building products are tested, comparisons can be done. Four comparisons are done according to the type of building products, and they are shown in Figure 7-9, Figure 7-10, Figure 7-11 and Figure 7-12.

Figure 7-9 shows the comparison between the instant smoke to flame ratio for the plywoods. The test used from the ISO Room Corner Test conserns no. 2 Plywood. For this product the instant smoke to flame ratio is plotted as a function of the heat release rate (as done for the smoke generation factor in Figure 1 in the ISC'94 publication). The smoke data from the CSTB Room Fire Test are from tests done on no. 60 Plywood. The values used are the instant smoke to flame ratio at maximum heat release rate (the numbers refer to the test identification of CSTB (cf. Section 3.9)).

Figure 7-10 shows a similar comparison for the particle boards, Figure 7-11 shows the comparison for the polystyrene (PS) foams and Figure 7-12 shows the comparison for the polyurethane foams [17].

[17] Note that the full scale test of no. 9 is questioned.

These comparisons are not as simple as the previous one, because the design of the French test differs from the other tests considered. The French test has another duct system design (cf. Chapter 3) which means that a distinct two zone environment might be built up during a test. The interface between the zones is lowered as the fire grows, and for high rates of heat release the interface can be close to the floor of the room. Such fires then become highly underventilated. This is probably the reason for the smoke to flame ratio increasing with the rate of heat release. During the CSTB tests it was also observed that the small entrainment of ambient air which occurred incinerated the smoke [18]. The opposite trend is the case for the tests in the ISO Room Corner Test. Ambient air is here entrained in the parts of the fire plume outside the opening, and obviously the temperature conditions are high enough to further incinerate the partly combusted species (as smoke and CO). Thus these two tests have fire scenarios which differ. Yet the smoke data are in some accordance with each other.

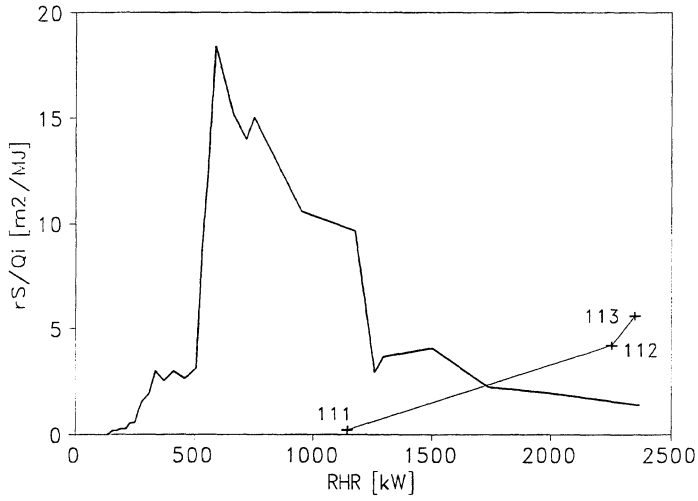

Figure 7-9 *The comparison of the post-flashover instant smoke to flame ratio ($r_{S/Q,i}$) for plywood and wood tested in the ISO Room Corner Test and the CSTB Room Fire Test.*

18 Visual observations done by Bernard Hognon, CSTB.

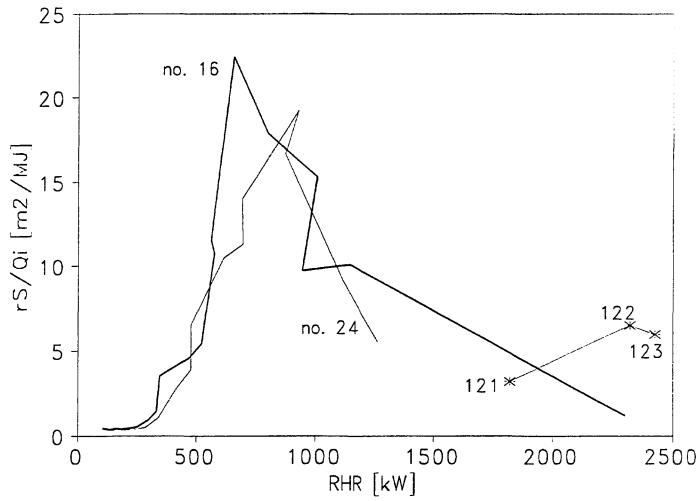

Figure 7-10 The comparison of the post-flashover instant smoke to flame ratio ($r_{S/Q,i}$) for particle board tested in the ISO Room Corner Test and the CSTB Room Fire Test.

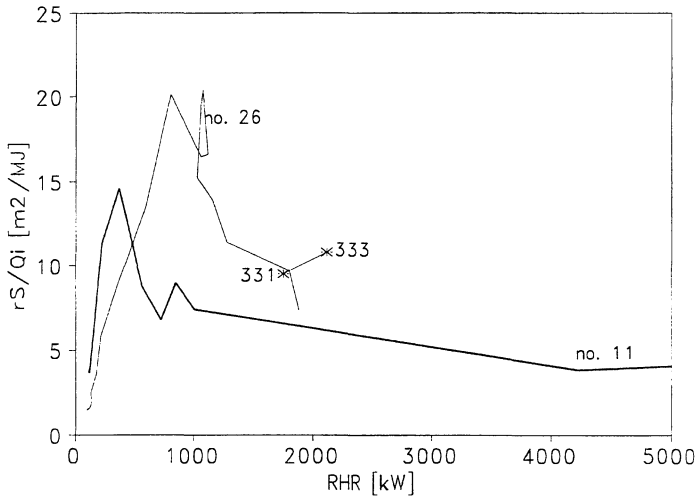

Figure 7-11 The comparison of the post-flashover instant smoke to flame ratio ($r_{S/Q,i}$) for polystyrene foam tested in the ISO Room Corner Test and the CSTB Room Fire Test.

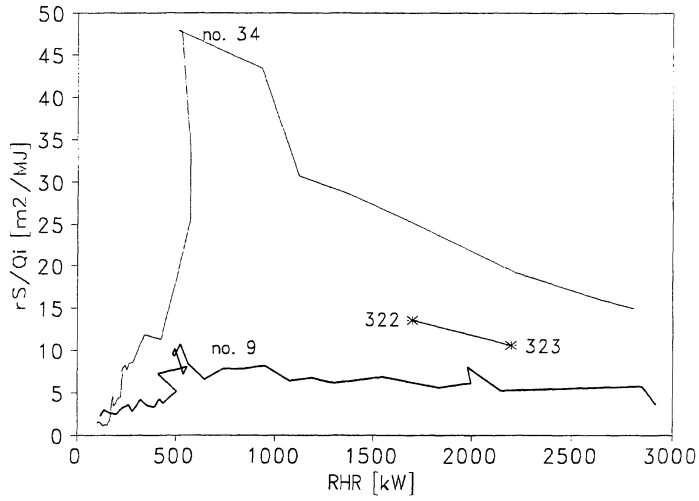

Figure 7-12 *The comparison of the post-flashover instant smoke to flame ratio ($r_{S/Q,i}$) for polyurethane foams tested in the ISO Room Corner Test and the CSTB Room Fire Test.*

7.3.4 General Assessment of the Test

The ISO Room Corner Test seems to be consistent for well ventilated fire scenarios where the combustion conditions are not characterized as what happens when the fire grows beyond 400-500 kW.

A problem identified with the test was corrections for the time delays and the response times of the analysers.

7.4 The ISO Cone Calorimeter

In the ISO Cone Calorimeter the combustion is well ventilated. The test seems to have interesting features for assessment of smoke production from building products in growing flaming fires.

However further research has to be done on the test (cf. Chapter 9).

7.5 The ISO/TR Dual Chamber Box

Results from this test method are presented in the INTERFLAM'93 and the NORDTEST publication.

Due to the limited amount of data from the test, these were left out from further studies because they could not be used in further advanced research on the prediction of full scale smoke test data.

A drawback of the test is that the closed box principle induces more variables into the burning conditions that are hard to understand.

As the ISO/TR Dual Chamber Test is not meant to simulate flaming conditions, the correlation approaches in the NORDTEST publication were questioned [19].

(The background for the proceeding comments are presented in Chapter 9:) The standard does not describe such kind of limitations in the use of the method. Research should also be done to give an accurate definition of what this test is designed to regulate, and why.

7.6 Discussion

7.6.1 Pre-Flashover and Non-Flashover Verification

The only pre-flashover comparison of smoke data is shown in Figure 7-1. Only two products were involved, so the generality of the results is limited. The comparison shows that the data are roughly in accordance. The same is also found for the comparison of non-flashover data shown in Figure 7-2. In Figure 7-2 the only difference between the scenarios is the scale (i.e. the size of the rooms), and the simple reasons for differences between the data are pointed out. Figure 7-6 shows the comparison between the non-flashover full scale and medium scale data. A correlation between the data is also found here. Thus for simple comparisons where the differences between the fire scenarios are only those of scale, the smoke data seem to be general.

However the generality of these types of smoke test data is influenced by the combustion conditions. This is illustrated by Figure 7-4 and Figure 7-5. The enlarged

[19] This was done by Mr. Carradori (ISO document ISO/TC92/SC1/WG4 N 254, dated October 1993).

scale data in these figures originate from more complex combustion conditions. Thus the relationships disappear. The same also happens in the comparison shown in Figure 7-2. These phenomena are not fully understood.

7.6.2 Flashover and Post-flashover Verification

The comparison between flashover full scale and enlarged scale data (i.e. Figure 7-7) showed larger smoke generation in enlarged scale, and one of the reasons for this might be the lower ventilation in enlarged scale, both due to the opening size and configuration. But at least the ranking was preserved. The full scale data were also compared to medium scale data (i.e. Figure 7-8). Outliers exist, but there seems to be correlation. Neither these comparisons seriously questioned the generality of the smoke data.

The correlation shown in Figure 7-8 is interesting due to use of reduced scale enclosure tests. The same results were found in the ISC'94 publication for both smoke and CO data (cf. Figure 7 and 8 there). This indicates that reduced scale enclosure tests might have interesting features to replace full scale enclosure tests.

Also the comparisons of flashover data from the ISO Room Corner Test and the CSTB Room Fire Test indicated that they were roughly in accordance with each other. Some differences in the design of the tests were probably the reasons for the discrepancies.

8 ASSESSMENT OF SMOKE HAZARD

8.1 Introduction

Building products are tested in room fire tests to evaluate their contribution to fire growth. The occurrence of flashover has been recognized as a benchmark of hazard [71]. A review on American fire statistics from the period of 1986-90 [72] shows that 43% of the fire deaths were located in the room of fire origin, and the heat hazard was in these cases identified to be the predominant reason of death. The rest of the fire deaths were located outside the room of fire origin, and lethality was predominantly caused of inhalation of toxic fire effluents. Such findings have led to the recognition that the toxicity of the fire effluents should be considered as the limited hazard [20] in post-flashover fires, while heat is the limited hazard in flaming pre-flashover fires [73].

In most room fire tests there is also additional equipment for the measurement of the smoke production. Yet the influence on the development and design of the tests with regard to evaluating the increase in hazard caused by the optical smoke production is probably not documented. Thus the increase in hazard caused by loss of visibility in real fires has to be identified and evaluated in relation to full scale tests. It can be evaluated whether a room fire test such as the ISO Room Corner Test is also applicable to assess the *smoke production properties* of building products. The topic is studied by use of test data from the ISO Room Corner Test and the French CSTB Room Fire Test.

8.2 Research Design

The hazards occurring in building fires depend (among other things) on the type of fires. According to the work of the British Standards Institution (BSI), building fires can be grouped into six types [74] [75]:

I. Self-sustained smoldering decomposition.
II. Non-flaming oxidative decomposition.

[20] The expression limited hazard [72] is related to which type of hazard that reaches the tenability limit first.

III.Non-flaming pyrolytic decomposition.
IV.Developing fires (pre-flashover fires)
V.Fully developed fires, high ventilation (post-flashover, fuel-controlled fires).
VI.Fully developed fires, low ventilation (post-flashover, ventilation-controlled fires).

Type IV - VI are flaming fires. Such fires are often discussed in term of five stages [76] (cf. Figure 8-1):

1. Ignition
2. Growth (the pre-flashover period of the room fire; type IV)
3. Flashover
4. Fully developed fire (the post-flashover period of the room fire; types V and VI)
5. Decay

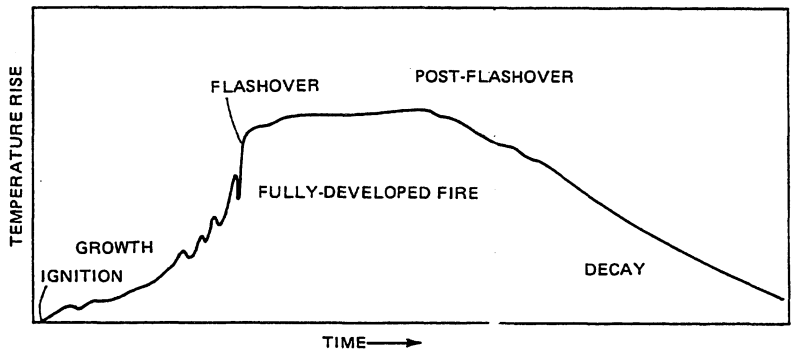

Figure 8-1 The stages of a room fire (from [76]).

In addition there are the flaming fires which do not go to flashover (i.e. non-flashover fires), for example room fires where the heat release is not sufficient to cause flashover.

The fire hazard can be divided into four types [77] [21]:

a) Loss of visibility resulting from the optical density of smoke (i.e. *smoke hazard*)
b) Painful exposure of the eyes, nose, throat and lungs caused of irritant fire effluents (i.e. *irritant hazard*).
c) Narcosis from the inhalation of toxic gases (i.e. *toxic hazard*).
d) Heat pain to exposed skin and the upper respiratory track followed by burns (i.e. *heat hazard*).

21 The hazard notations in the parentheses are used throughout the text.

The irritant hazard is caused by irritant species as inorganic acid gases (e.g. hydrogen chloride) and organic compounds (e.g. low molecular weight aldehydes as formaldehyde and acrolein) [77]. In high enough concentrations these are severe enough to prevent escape. In general, it is predicted that smoke from a mixed fuel source is strongly irritant if the extinction coefficient k exceeds 1.2 m^{-1} [78]. However the generation of irritant fire effluents depends of the type of fire, e.g. flaming fires are considered to give less than smoldering fires [78].

The types of hazard interact on each other. Thus when the smoke hazard is assessed, also the other three hazards have to be taken into consideration.

Before flashover, hazardous conditions are within the room of fire origin and its vicinity. After flashover the fire effluents might spread rapidly through large areas (volumes) of a building. Then hazardous conditions may occur far away from the origin of the fire. Fire disasters originate predominantly from post flashover fires [72].

The hazard related to loss of visibility is the decrease in the speed of escape which may prolong the exposure conditions. This can happen both in pre- and post-flashover fires, thus the smoke hazard has to be assessed for both pre- and post-flashover fire conditions.

Data from the ISO Room Corner Test are used to assess the smoke hazard in pre-flashover fires, while data from the CSTB Room Fire Test are used to assess the smoke hazard in post-flashover fires.

The approach starts with an outline of a way to quantify the heat and the toxic hazard (Section 8.3). Then smoke hazard is identified (Sections 8.4 and 8.5) and evaluated (Section 8.6).

8.3 Quantification of Heat and Toxic Hazard

8.3.1 Heat Hazard

The heat hazards are incapacitation by heat stroke (i.e. convective heat transfer), body surface burns (i.e. heat conduction and radiation). They are referred to as the convective and radiant heat hazard respectively.
The time to incapacitation caused by convective heat transfer can be estimated by [78]

$$t_{i,conv} = e^{(5.185 - 0.0273 T_g)} \qquad \text{(unit: min)}$$

Eq. 8.1

where T_g (units; [°C]) is the temperature of the fire effluents. The tenability limit is approximately 150°C [79]

Figure 8-2 shows the time to severe skin pain versus irradiance level [78]. Radiant heat skin pain and burns occur rapidly at intensities above 2.5 kW/m^2, and the tenability limit to radiant heat is about 25 kW/m^2.

The received radiance q" ([W/m^2]) is a function of the configuration factor (ϕ), the emmisivity (ε) and the temperature T_g ([K]) of the fire effluents [80]

$$q'' = \phi \cdot \varepsilon \cdot \sigma \cdot T_g^4$$

Eq. 8.2

where σ is the Stefan Boltzmann constant.

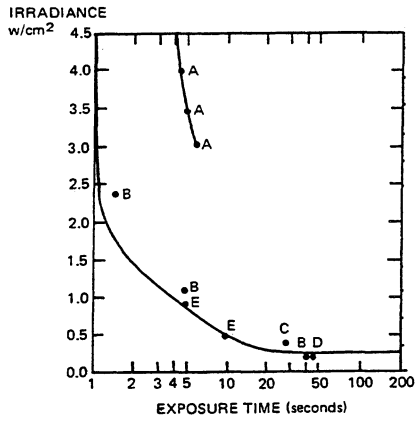

Figure 8-2 Time to severe skin pain from radiant heat (from [78]).

8.3.2 Toxic Hazard

A common method for toxicity assessment of fire effluents is the Fractional Effective Dose (FED) method. The method estimates whether an evacuee is incapacitated after an exposure of duration t_i of a toxic atmosphere. The model relies on a few gases (N) being responsible for the incapacitation, and that the toxic effect of the gases is additive. A FED dose equal to 1 means that the evacuee is incapacitated.

If the necessary escape *duration* $t_{i,min}$ through the fire atmosphere is known, then the maximum rate of the received fractional dose can be estimated from

$$FEDR_{N,max} \leq \frac{1\ fiu}{t_{i,min}} \qquad \text{(units: fiu / min)}$$

Eq. 8.3

Units for $FEDR_N$ are *fraction of an incapacitating unit per minute*; *fiu/min*. For a given fire atmosphere $FEDR_N$ is [77]

$$FEDR_N = VCO_2 \cdot \sum_{i=1}^{N} FEDR_i + FEDR_{O2} \vee FEDR_{CO2}$$

Eq. 8.4

where $FEDR_i$ is the received *fraction rate* of the toxic gas i, VCO_2 is a multiplication factor due to the fact that CO_2 stimulates the breathing rate and $FEDR_{O2}$ is incapacitation due to decrease of the oxygen concentration. $FEDR_{CO2}$ is the fraction rate due to high concentration of CO_2. Eq. 8.4 is determined by equations given in [78]. The maximum escape duration is found by integration of Eq. 8.4.

8.3.3 The Volume and Temperature of the Fire Effluents

Two notations of the volume of the fire effluents are used: *fire plume* and *fire atmosphere*. They are used in relation to pre- and post-flashover smoke assessment respectively. Fire plume is used when the volume is hot and has relatively strong buoyancy forces and the dilution of fire effluents into the ambient air is minor. This is normally the case when the volume of the fire effluents is a well stratified, heated upper layer. This volume is referred to as m_e. Fire atmosphere is used when the buoyancy forces are less and the temperature of the fire effluents is closer to the ambient temperature (T_a). Then the distinction between the volume of the fire effluents and the ambient air more or less disappears and the dilution of the fire effluents into ambient air increases. m_{mix} is the volume of the ambient air which the fire effluents have diluted into. Thus the mass of the volume occupied by the fire effluents is

$$m_{fe} \approx m_e + m_{mix}$$

Eq. 8.5

The mass of the pyrolysed fuel is minor and not included. Generally it is parts of m_e that take part in the combustion and forms the buoyancy plume. Then the air entrainment due to small buoyancy forces is initially minor. However, as the

temperature differences decrease, the fire effluents are increasingly diluted and mixed with ambient air. Then m_{mix} becomes the dominant part of m_{fe}.

The temperature of the fire effluents T_g is governed by m_{fe}, the heat release (HR) and the heat losses. The heat losses are radiate heat losses from the hot dense plume (q_{rad}) and convective heat losses to the adjacent boundaries (q_{conv}). Thus the bulk temperature can be estimated by

$$HR = m_{fe} \cdot c_p \cdot (T_g - T_a) + q_{rad} + q_{conv}$$

Eq. 8.6

where c_p is the specific heat of the fire effluents (≈1.0 kJ/kg·K). If the fraction of energy *conserved* in the volume of the fire effluents (i.e. the plume) is denoted χ, then the bulk temperature T_g is

$$T_g = T_a + \Delta T = T_a + \frac{\chi \cdot HR}{m_{fe} \cdot c_p}$$

Eq. 8.7

The adiabatic gas (flame) temperature $T_{g,ad}$ is found by setting $\chi = 1$. $T_{g,ad}$ is the upper limit of the fire gas temperature. The volume which the fire effluents are dispersed into is denoted V_{fe}. The volume at temperature T_g can be estimated by

$$V_{fe,g} = m_{vfe} \cdot \frac{R_u \cdot T_g}{M_{W,air} \cdot p} = V_{e,a} + 0.0028\chi HR + V_{mix,a} \qquad (\text{units: } m^3)$$

Eq. 8.8

where $V_{e,a}$ and $V_{mix,a}$ are the volume of the entrained and mixed air at ambient temperature, R_u is the universal gas constant, $M_{W,air}$ is the molar mass of air and p_{atm} is the ambient pressure.

8.4 Identification of the Pre-Flashover Smoke Hazard

8.4.1 Introduction

The identification of the hazard related to loss of visibility is done by use of test data from three products tested in the ISO Room Corner Test

- no. 2 Ordinary birch plywood
- no. 7 Combustible faced mineral wool

- no. 11 FR polystyrene foam

These three products are chosen because they represent a range of building products. The identification of smoke hazard (i.e. loss of visibility) is based on quantification of the heat and toxic hazard. The assessment starts with the identification. To do this the plume volume and temperature conditions first have to be estimated (Section 8.5.2). Then the hazardous situation can be identified and evaluated.

8.4.2 Estimation of Plume Size and Temperature

Estimation of plume volume

In the full scale experiments with the Scandinavian products the mass flow rates out of the opening were crudely estimated. It was found that at flashover conditions (defined as flames emerge out of the opening) the mass flow rates varied between 0.7 kg/s and 0.9 kg/s. In measurements done at SINTEF [81] [22], the mass flow rates increased from 0.7-0.9 kg/s to 1.0-1.1 kg/s as the heat release rate increased from about 300 kW to a peak between 1000 kW and 1500 kW. N. A. Dembsey et al. estimated the mass flow rate to increase slightly from 0.74 kg/s to 0.98 kg/s (± 20%) as the rate of heat release increases from 330 kW to 980 kW [82] [23]. The referred results vary, thus there are some doubts about how m_{fe} (i.e. m_e) should be modelled. m_e was chosen to vary linearly between 0.8 kg/s and 0.9 kg/s for the rate of heat release of 300 and 1000 kW respectively. Above 1000 kW 0.9 kg/s was used.

Estimation of gas temperature

The bulk gas temperature T_g of the plume has to be estimated to quantify the convective heat hazard. This can be done by use of the gas temperature measurements in the room. However, two other ways are also evaluated

1. By use of the adiabatic temperature according to χ=1 and Eq. 8.7.
2. By use of the measured temperature in the duct (i.e. T_d).

---

22 The gas burner was either in the middle of the room or in an inner corner and the fuel load were both (combustible) furnishing and wall linings.

23 They used a propane burner located 0.61 m over the floor and either in the middle of the room or in the inner corner. The room boundaries were lined with ceramic fire boards (thus χ should be expected to be relatively high), and the mass flow rate was estimated by measurements of the temperature in the room and in the doorway.

The second way has to be done with an estimate of the heat losses outside the doorway and in the duct system. Using temperature measurements done in the doorway, the heat conservation factor χ_1 within the room can be estimated by

$$\chi_{1,FEO} = \frac{RHR_{conv,FEO}}{RHR_{FEO}}$$

Eq. 8.9

where $RHR_{conv,FEO}$ is the heat release convected out of the door when flames emerge out of the opening. Then the corresponding mass flow rate and temperature in the duct were found ($m_{d,FEO}$ and $t_{d,FEO}$ respectively), and the heat conservation factor in the duct system ($\chi_{d,FEO}$) was estimated by

$$\chi_{d,FEO} = \frac{1}{\chi_{1,FEO} \cdot RHR_{FEO}} \cdot m_{d,FEO} \cdot c_p \cdot (T_{d,FEO} - T_a)$$

Eq. 8.10

$\chi_{d,FEO}$ was crudely estimated to be about 0.9. The method gave in some cases poor values because when flames emerge out of the opening, some parts of the combustion also occur outside the door. Thus in some cases $\chi_{1,FEO}$ became greater than 1, resulting in an underestimation of $\chi_{d,FEO}$.

The radiant heat hazard is quantified by the heat flux measurements done in the middle of the floor and ceiling. The heat conditions are identified in terms of the fire size (i.e. as the rate of heat release of the fire).

The identification of the heat conditions of the tests runs of plywood, combustible faced mineral wool and polystyrene foam are done by Figure 8-3, Figure 8-4 and Figure 8-5 respectively. In the figures the irradiance conditions are expressed by the heat flux meters in the floor and the ceiling, and the convective heat exposure is illustrated by three estimates of the plume gas temperature (T_g):

- The adiabatic plume temperature estimated by χ=1 and Eq. 8.7.
- The gas temperature measurements 2.1 m and 1.3 m above the floor (G1 and G5 respectively) in the room [24].
- The plume temperature estimated by use of the temperature measurements in the duct and a constant value of χ_d of 0.9.

[24] The gas temperature measurements are done in the corner right to the doorway (30 cm from the walls). G2 is mounted 1.7 metres above the floor.

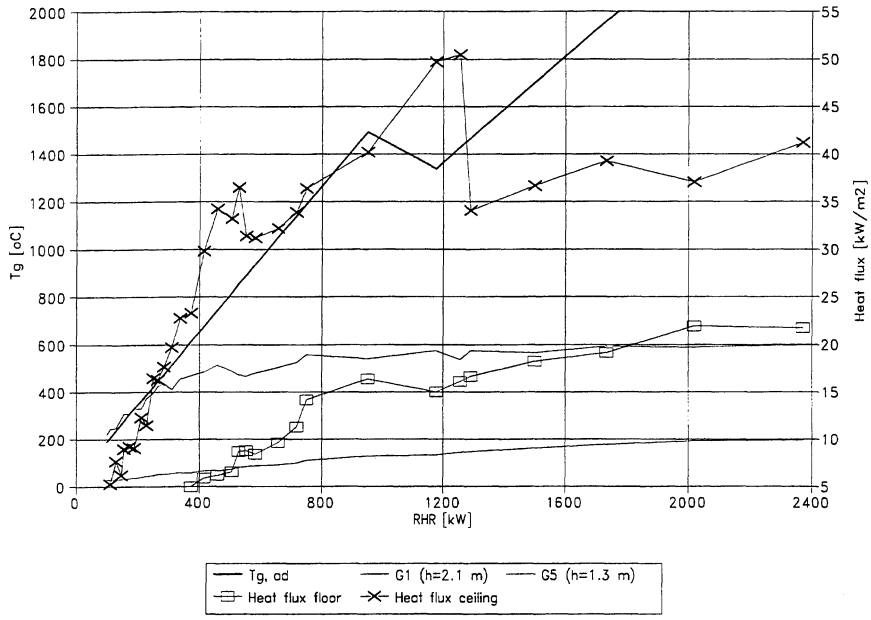

Figure 8-3 Temperature and heat fluxes as a function of heat release rate of the test of ordinary plywood (no. 2) in the ISO Room Corner Test.

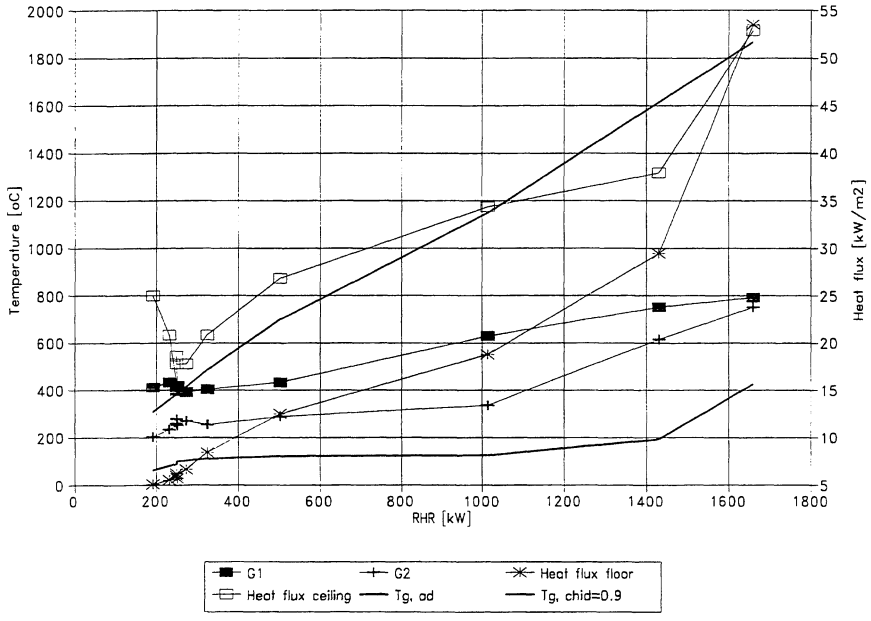

Figure 8-4 Temperature and heat fluxes as a function of heat release rate of the test of combustible faced mineral wool (no. 7) in the ISO Room Corner Test.

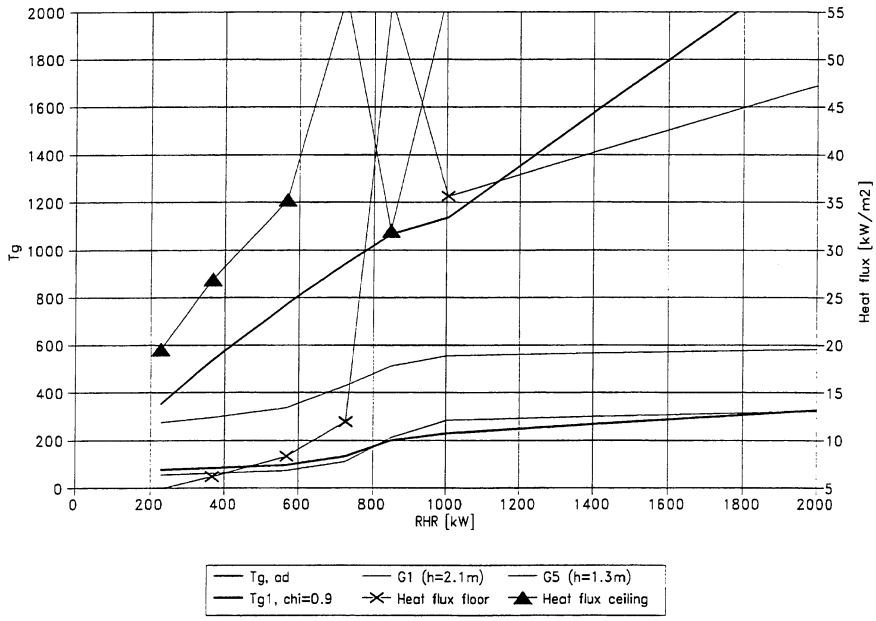

Figure 8-5 Temperature and heat fluxes as a function of heat release rate of the test of FR polystyrene foam (no.11) in the ISO Room Corner Test.

None of the two alternative ways to estimate the gas temperature seem to be good; either the temperatures are overpredicted or underpredicted. Thus the measured gas temperatures within the room are used to identify the convective heat hazard in the proceeding section. At 400 kW the gas temperature was 300-400 °C at 2.1 metres above the floor, while about 100 °C at 1.3 metres above the floor.

Since the heat flux meter in the ceiling is surrounded by flames and hot gases, the measured flux levels are high; about 25 kW/m^2 when the fires are of the size 400 kW. The corresponding measured heat flux to the floor is about 5-10 kW/m^2.

8.4.3 Smoke Hazard Identification

The identification of smoke hazard is done by consideration of the toxicity and heat hazard. The convective heat exposure is quantified by

$$FEDR_{heat} = \frac{1}{t_{i,conv}} \qquad \text{(units: [fiu / min])}$$

Eq. 8.11

The toxic hazard is based on Eq. 8.4. It is assumed that the only toxic fire effluents present are CO and CO_2, and that the plume size is estimated by the outline given in Section 8.4.2.

The optical density of the plume is estimated by

$$k_{bulk} = \frac{SP}{V_{fe,g}} \qquad (\text{units: } m^{-1})$$

Eq. 8.12

where $V_{fe,g}$ is according to Eq. 8.8. The estimation of $V_{fe,g}$ is based on Section 8.4.2.

The identification of smoke hazard is done by consideration of Figure 8-6, Figure 8-7 and Figure 8-8. The first Y-axes show the FED rates of toxic hazard (noted «FEDRn») and convective heat hazard (noted «FEDRheat»). The second Y-axes give the bulk smoke extinction coefficient (noted «k»). The radiant heat hazard is identified by use of the Figure 8-3, Figure 8-4 and Figure 8-5.

The hazardous conditions depend on whether there is exposure *outside* or *within* the plume. Outside the plume the hazards are radiant heat exposure and loss of orientation due to impaired vision (i.e. if the escape routes are covered by smoke). Inside the plume the hazards are the convective heat hazard, the toxic hazard and the irritant hazard.

Figure 8-6 is a consideration of the hazard for a wood based product. The figure shows that the toxic hazard is minor to the convective heat hazard . Besides they are not both critical; at a fire size of 400 kW the convective heat hazard is about 1 fiu/min, which means incapacitation after about one minute. At 400 kW, the irradiance level to the floor flux meter is about 5-10 kW/m^2. It should also be taken into account that the configuration factor (cf. Eq. 8.2) for an occupant is higher than for the floor heat flux meter. Thus severe skin pain occurs probably within seconds (cf. Figure 8-2). At 400 kW the visibility through the plume is about 1-2 metres for non-irritant smoke (cf. Section 2.4). Thus outside the plume the limited hazard is identified as the radiant heat hazard. Within the plume the tenability limit for the irritant hazard is approximately reached (i.e. $k=1.2\ m^{-1}$). Thus within the plume the irritant hazard is the limited hazard.

The hazard consideration of the test of the polystyrene foam is done with Figure 8-8. Figure 8-5 shows that at 400 kW the heat flux level exposed to an occupant is at least 5-10 kW/m^2, thus severe skin pain occurs within seconds. In this fire the loss of visibility is significantly larger: At 400 kW the visibility through the plume is less

than about a half metre for non-irritant smoke. Within the plume the tenability of smoke hazard is far over exceeded, thus escape through the plume is very risky.
Figure 8-7 shows the hazard consideration for the combustible faced mineral wool. As for the other two examples it is the radiant level which poses a hazard to an occupant outside the plume. The visibility is about 2 metres.

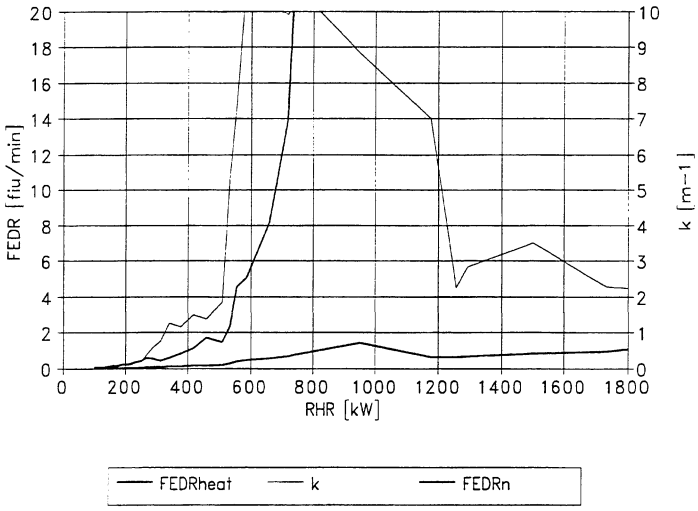

Figure 8-6 *The convective heat hazard ($FEDR_{heat}$), the toxic hazard ($FEDR_N$) and the smoke density (k_{bulk}) as function of the heat release rate of the test of ordinary plywood (no. 2) in the ISO Room Corner Test..*

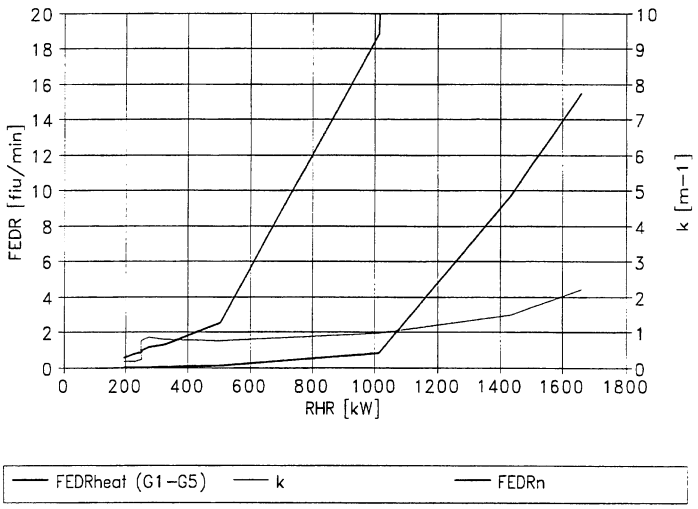

Figure 8-7 *The convective heat hazard ($FEDR_{heat}$), the toxic hazard ($FEDR_N$) and the smoke density (k_{bulk}) as function of the heat release rate of the test of combustible faced mineral wool (no. 7). in the ISO Room Corner Test.*

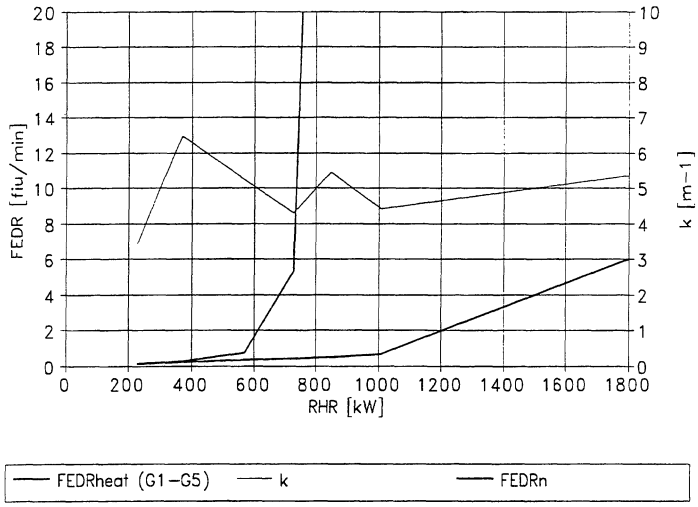

Figure 8-8 *The convective heat hazard ($FEDR_{heat}$), the toxic hazard ($FEDR_N$) and the smoke density (k_{bulk}) as function of the heat release rate of the test of FR polystyrene foam (no. 11).in the ISO Room Corner Test.*

8.5 Identification of the Post-Flashover Smoke Hazard

8.5.1 Introduction

In post-flashover fires the occupants are exposed to hazardous conditions during escape through smoke filled building areas. The remonstrance of escape through a smoke filled area increases with the loss of visibility [83]. However, this is influenced by many factors such as the knowledge of the escape routes and the presence of active and passive fire protection systems (e.g. the emergency marking system).

If the fire atmosphere is so toxic that safe conditions cannot be reached even if the speed of escape is not decreased by impaired vision, then escape should not be tried. In such cases the loss of visibility is no hazard. However if safe conditions could be reached *without* the decrease in speed of escape, then smoke is the limited hazard. The next section outlines how smoke hazard should be evaluated together with the other hazards.

8.5.2 A Method for Evaluation of Post-Flashover Smoke Hazard

The method outlined here to evaluate post-flashover smoke hazard assumes that the distance S of the escape routes which has to be covered is known. The *evacuation speed* v depends on the hazardous conditions, i.e. smoke hazard and irritiancy hazard

$$v = v(k, irritancy)$$

Eq. 8.13

In addition, v is influenced by personal characteristics of the evacuees and the influence of fire protection systems. Successful escape is conducted if Eq. 8.14 is satisfied

$$t_i \geq \frac{S}{v}$$

Eq. 8.14

Thus according to Eq. 8.3

$$v \geq FEDR \cdot S$$

Eq. 8.15

FEDR can include both heat and toxic hazards. If the production of toxic species and smoke from the post-flashover room fire are known, then smoke hazard can be assessed by three steps:

1. Determine the escape distance S.
2. Determine the volume that the fire effluents are dispersed in (i.e. the volume of the fire atmosphere).
3. Calculate FEDR and verify whether Eq. 8.14 is satisfied.

The practical use of this method depends on the efforts made on the estimation of v and FEDR. However, the method illustrates the general relationships between the hazards.

8.5.3 Smoke Hazard Identification

The post-flashover smoke hazard is identified by use of post-flashover data from the French CSTB Room Fire Test. It is assumed that the temperature conditions do not cause heat hazard, thus smoke hazard is considered only in relation to the irritant hazard and the toxic hazard.

The identification of smoke hazard is not done in accordance with the method outlined in Section 8.5.2, because here it is not a specific situation that is to be evaluated. The wanted information is *when* loss of visibility is considered to be a hazard.

All hazards depend on the volume the fire effluents are dispersed into. If the volume is large enough, there is no limited hazard. However for some dispersions of the fire effluents, one of them becomes the limited hazard. A way to illustrate and quantify this is to decide a vision distance through the fire atmosphere, and then find out the other hazards.

The tenability limit due to the irritancy of the fire effluents is reached for a smoke extinction coefficient of 1.2 m^{-1}. Based on test data from the CSTB tests, V_{fe} is then determined by Eq. 8.12 to give k equal to 1.2 m^{-1}. Then the production rates of CO and CO_2 are used to determine time to incapacitation in such a fire atmosphere (this is done according to Eq. 8.3). Such calculations are done for all the fires in the CSTB Room Fire Test, and the results are presented in Table 8-1.

$t_{i,k=1.2}$ ranges from approximately 8 to 50 minutes. This means that even while the visibility is less than 2 metres, the atmosphere is not validated as specially toxic. However escape will fail due do the irritant hazard. Thus the loss of visibility does not represent an important hazard.

Table 8-1 Time to incapacitation as a function of the smoke extinction coefficient.

No:	Product	Full scale test number	$t_{i,k=1.2}$ [min]
60	Plywood	112	8
		113	6
61	Particle board	122	12
67	Polyurethane foam	322	49
69	Polystyrene foam	331	50
		333	32
70	Plastic wallcovering on gpp	211	22
		212	19

gpp gypsum paper plaster board

Loss of visibility might be identified as a critical hazard if the fire atmosphere size is increased. However such identifications require a better quantification of the irritant hazard. Such identifications are probably best done by a starting point in the method described in Section 8.5.2.

8.6 Discussion

8.6.1 Pre-Flashover Smoke Hazard Evaluation

During the ignition stage of the fire there is normally enough time for successful escape (if the occupant is aware of the situation). But if escape is not conducted before the fire goes into the growth stage, then the risk of being overcome by the fire increases.

How the occupant eventually is overcome by the fire depends on the conditions. Generally the radiant heat hazard was identified as the main hazard in the growth stage of the fires. During such conditions escape has to be conducted immediately. Even though escape through a dense plume is associated with a severe risk. If the visibility is very bad, then the risk can be interpreted as exceedingly high, resulting in the occupant becoming *psychically* incapacitated. Thus escape might not even be attempted. If the occupant has a knowledge about the exit routes, then escape attempts through the plume (fire effluents) might be tried. However then there is a risk of being overcome by the *irritant* hazard, and the risk increases with loss of visibility. Thus in such scenarios the risk of being overcome by the fire increases with the loss of visibility. As a consequence of this the hazard posed by the optical smoke production should be considered to be regulated.

The two examples with the wood and the plastic based product identify that the hazard related to loss of visibility increases significantly from a fire with wood based product to a fire with plastic based product. This indicates that a *benchmark* of smoke hazard in pre-flashover fires is governed by the material choice. Thus regulation which distinguishes between smoke production rates in the range of the two products mentioned above can *effectively* regulate the hazard related to loss of visibility in pre-flashover fires.

The results show that the ISO Room Corner Test is applicable to assess the hazard related to loss of visibility in growing fires.

8.6.2 Post-flashover Smoke Hazard Evaluation

The smoke hazard is only relevant to consider if successful evacuation can be done *without* the reduction in the speed of escape caused by loss of visibility. Such cases can be identified by use of the general method outlined in Section 8.5.2 as a starting point.

The analysis of post-flashover hazard was a very simple approach. The heat hazard was assumed to be neglible, however this is valid when large volumes of ambient air is mixed into the fire effluents [79].

Data from post-flashover fires conducted in the French CSTB Room Fire Test identified smoky low toxic atmospheres. Since these atmospheres had an extinction coefficient of 1.2 m^{-1}, the main hazards were identified to be the irritant hazard. If the irritant hazard is not considered, then the smoke hazard can eventually occur. However, such conditions cannot be identified with these approaches. Such approaches require a more precise quantification of the other hazards. The toxic hazard depends on the products burning, thus a general benchmark of smoke hazard in post-flashover fires is harder to identify. Besides the effects of smoke ageing has also to be considered and quantified. Alltogether this make identification of smoke hazard so complicate that it cannot be assessed further with the limited data set considered here.

The results here have not been able to identify the smoke hazard related to post-flashover fires.

If post-flashover hazard is to be regulated, then the design of the full scale tests has to be considered. In a way the ISO Room Corner Test and the French CSTB Room Fire Test represent two opposite types; the former yields post-flashover fires of type V and the latter of type VI (see Section 8.2). This has also to be taken into consideration if post-flashover smoke hazard assessment is wanted to be made.

9 DISCUSSION, CONCLUSIONS AND RECOMMENDATIONS

9.1 Overall Discussion

The assessment, in terms of identification and evaluation, of the fire hazard occurring in real fires is of vital importance for the framework of a classification system. Considerations have to be given on *how* the identified hazards should be classified. The framework is also influenced by the assumed *effects* of the overall fire safety regulation. The issue is complex, however the success of the outcome is governed by these factors. The work in this thesis is a comprehensive approach to some of the main factors underlying this issue.

To some degree, the issue has generally been considered within Nordtest [84]. However other works that treat the issue in a comprehensive way have not been found.

The loss of visibility was found to be a hazard in growing fires. The full scale test data showed that according to the smoke hazard, the data could be grouped into two groups: the wood based products and the plastic based products. At a fire of size 400 kW the wood based products had smoke production rates less than 1.6 m^2/s, while the plastic products had smoke production rates in the range of 4 m^2/s and 11 m^2/s. The hazard identification showed that the smoke hazard increased significantly from a wood based product to a plastic based one. Thus there is a limit between these two types of products where the smoke hazard markedly increases. Two *smoke classes* can be defined based on these results.

The choice of the exact limit between the classes is hard to do because there are so many unknown variables. A choice of 3 m^2/s was done. Thus if the smoke production is less, then the product is classified as *moderately smoky* and in *smoke class 1*, else as *highly smoky* and in *smoke class 2*. This could have been done in a more sophisicated manner, but then the effect of the more sophisticated regulation has to be documented. This cannot be done here.

The limit on 3 m^2/s corresponds to a visibility of less than one metre and the tenability limit of k=1.2 m^{-1} (the tenability limit of irritant hazard) being definitely

exceeded. Thus severe conditions exist when the rate of smoke production is of this size.

Within the EUREFIC classification system, the products are divided into five classes (A, B, C, D, E and UC) according to the time and occurrence of flashover. The smoke classification proposed here could be used together with this system. The EUREFIC system has another way of classification of the smoke hazard. However, the advantage of the classification method proposed here is that differentiations can be made between heat classification and smoke classification. This is important, because the smoke hazard increases with the heat hazard. For example, loss of visibility in a fast fire is more critical than in a slow fire.

The work here has only managed to develop a smoke prediction model for the pre-flashover fires, and it was proposed that this model could also be used to classify products that had a possible flashover after 10 minutes in the ISO Room Corner Test. The limit of 3 m^2/s corresponds to a gross flame to smoke ratio of 7.5 m^2/MJ. A consideration of the data and the results in Chapter 6 show that most of the products that obtain a gross smoke to flame value over 7.5 m^2/MJ in full scale, are also classified in smoke class 2 by the smoke prediction model.

The sort of smoke regulation proposed here fits well into functionally based regulation codes. The results could also be used in performance based classification systems.

The generality of smoke test data was not verified for corridor configurations. Yet it can be assumed that smoke test data also are general for such scenarios because the combustion conditions in the early stage of a corridor fire are not significantly different from the conditions in a room.

A way to regulate the hazard related to loss of visibility in post-flashover fires has not been determined. No general benchmark of post-flashover smoke hazard was found, and the results indicate that the smoke hazard depends on both the scenario and the product burning in a complex way. It should also be taken into consideration that a post-flashover fire atmosphere is governed by fire effluents from the burning of both building contents and building products. Thus if the smoke production from building products should be assessed due to smoke production in post-flashover fires, this presumes that the smoke from the building products is responsible for the obscuration hazard. There is little meaning in regulating the use of the building products, if the same is not done for the building content. Possibly, this is why the building content has been denoted «the weak or missing link» within fire safety [85]. Based on these results, the post-flashover smoke hazard should be provisionally left out of material classification.

This work has been limited to flaming fires. If building product classification also should be done in consideration of non-flaming fires, then the smoke hazard related to such scenarios has to be assessed and quantified. Based on such work «static» tests, as the ISO Dual Chamber Box, could be verified.

Finally it should be emphasized that the *fire risk* has only been considered in a very general and superficial way in this work. Neither the *effect* of regulating the smoke production of building products in relation to growing fires has been studied. Thus the study has not procured documentation on what the society gains and lose by the classification proposed here. Such documentation is necessary for the regulators to do cost-benefit analyses for the society (some interesting thoughts on the subject are given in [86]).

A way to argue the smoke classification proposed here could be based on «qualitative» arguments, i.e. relevant experiences and intuitive feelings, that the benefits far exceeds the costs. This is not a scientific way, but acceptable, because fire protection engineering still is more «art» than science [87]. Another way to argue is that some evacuation scenarios should be tried eliminated by regulation, irrespective of risk. Such a scenario might be an evacuee that could have survived if the smoke density in the lethal growing fire had been less.

The author feels that this is an item which have not been given sufficient priority. Such considerations are crucial for further directing of the fire safety research in a way that is most convenient for the society.

9.2 Overall Conclusions

According to the division of the issue into three topics, there are three main conclusions:

This work has shown that smoke production in the growth stage of pre-flashover fires of building products in the ISO Room Corner Test can be predicted by the use of data from the ISO Cone Calorimeter and a model. The model is

$$RSP(400)_{pred} = 11.4 \cdot \left(\frac{e^{-3.80+57.2\cdot\phi_{CO,avg}+0.00341\cdot t_{max-ign}+1.66\cdot[plst?]}}{1+e^{-3.80+57.2\cdot\phi_{CO,avg}+0.00341\cdot t_{max-ign}+1.66\cdot[plst?]}}\right)$$

where

$RSP(400)_{pred}$ = The predicted smoke production rate at 400 kW in the ISO Room Corner Test

$\phi_{CO,avg}$ = The average CO equivalence ratio factor

$t_{max-ign}$ = The time difference between the occurrence of maximum rate of heat release (tmax) and time to ignition.

[plst?] = A dummy variable which is 0 for wood based products and 1 for plastic based products.

(Chapter 4 explains the parameters.) The equation predicts full scale smoke production at a rate of 400 kW to sufficient accuracy to regulate the smoke hazard related to growing fires.

A benchmark of smoke hazard in growing fires was identified to be related to a change from a wood based product and to a plastic based product. This was identified with a limit of the full scale smoke production of 3 m^2/s at 400 kW. Products with lower smoke production are classified in smoke class 1, and products with higher smoke production are classified in smoke class 2.

The hazard associated with the loss of visibility is hard to assess, and it might not be possible to do this in a general way. Until this has been further quantified, the post-flashover smoke hazard should be left out of classification.

For pre-flashover and non-flashover fires, full scale smoke test data were found to be general and the ISO Room Corner Test was implicitly considered to be consistent with the fire scenarios it is meant to cover. However, smoke test data were found to be complicated when the fire increased in size.

The ISO Room Corner Test was found well applicable to assess the hazard related to loss of visibility in pre-flashover fires.

9.3 Recommendations for Further Work

Documentation to do cost-benifit analyses for the society on what will be gained and lost by the society by regulation should be procured. The outcome of such work will form a sound general guidance for future research within fire safety science and engineering.

In general the relationship between the hazard related to the loss of visibility and the other types of fire hazards should be considered more closely, to assess the optimum way to assess smoke production from building products.

Within this work the necessity for a general and improved understanding of the burning conditions in enclosures was revealed. Topics included here are

- The effect of scale on smoke generation.
- The influence of the configuration of the fire load.
- The influence on the production of fire effluents on temperature and ventilation conditions.

Further research should be done on the ISO Cone Calorimeter. Topics identified are

- Development of parameters and studies of the relationship between the parameters.
- Assessment of the variation of the data and procedures to evaluate the data
- Comparison of data obtained in the Cone Calorimeter with data obtained in other bench scale test apparatus.

Better understanding of the apparatus and a improved interpretation of the results could be obtained. This might also result in an optimalization of the design of the apparatus.

REFERENCES

[1] EUREFIC. European Reaction to Fire Classification. Proceedings of the EUREFIC Seminar. Interscience Communications, Ltd. London, UK. 1991.

[2] Summary report of the EUREFIC programme. U. Wickström, ed. Swedish National Testing and Research Institute. Borås, Sweden. 1993.

[3] Sixth International Fire Conference INTERFLAM'93. Proceedings. Interscience Communications Ltd. London. 1993.

[4] A.W. Heskestad and P.J. Hovde, Evaluation of Smoke Test Methods for Classification of Building Products. NORDTEST technical report 220. University of Trondheim, The Norwegian Institute of Technology, Department of Building and Construction Engineering, Trondheim, Norway. 1993.

[5] Fire Safety Science - Proceedings of the Fourth International Symposium. International Association of Fire Safety Science. 1994.

[6] 25th International Symposium on Combustion. Abstract of Work-in-Progress Poster Sessions Presentations. The Combustion Institute, Pittsburgh, PA, USA. 1994.

[7] W.M. Pitts, Carbon Monoxide Formation in Fires by High-Temperature Anaerobic Wood Pyrolysis. Paper presented at the 25th International Symposium on Combustion, The Combustion Institute, Pittsburg, PA, USA. 1994.

[8] D.T. Gottuk, R.J. Roby and C.L. Beyler, The Role of Temperature on Carbon Monoxide Production in Compartment Fires. Work-in-progress poster presented at the 25th International Symposium on Combustion, The Combustion Institute, Pittsburgh, PA, USA. 1994.

[9] D.S. Ewens, B. Lattimer, U. Vandsburger and R.J. Roby, Compartment Fire Exhaust Gas Transport and Oxidation. Work-in-progress poster presented at the 25th International Symposium on Combustion, The Combustion Institute, Pittsburgh, PA, USA. 1994.

[10] J.H. Troitzsch, International Plastics Flammability Handbook. 2nd edition. Hanser publishers, Munich, Germany. 1990.

[11] A. Tewardson, Generation of Heat and Chemical Compounds in Fires. The SFPE Handbook of Fire Protection Engineering. NFPA, Boston, MA, USA. 1988.

[12] B. Östman, Smoke and Soot. Heat Releases in Fires. Elsevier Science Publishers Ltd. England. 1992.

[13] D.D. Drysdale, An Introduction to Fire Dynamics. John Willey & Sons Ltd., Great Britain. 1985.

[14] G.W. Mulholland, How Well Are We Measuring Smoke? Fire & Materials, vol 6, no. 2, 1982.

[15] J.S. Newman and J. Steciak, Characterization of Particulates from Diffusion Flames. Combustion and Flame 67: 55-67 (1987).

[16] V. Babrauskas and G. Mulholland, Smoke and Soot Data Determinations in the Cone Calorimeter. Mathematical Modelling of Fires, ASTM STP 983, American Society for testing and Materials, Philadelphia, 1987.

[17] W. K. Chow and K. F. Lai, Optical Measurements of Smoke. Fire and Materials, Vol. 16 (1992).

[18] K. Maries, Measurements of Smoke in Fires - A Review. Fire and Materials, vol. 2, no. 1, 1978.

[19] J. H. Klote and J. A. Milke, Design of Smoke Management Systems. American Society of Heating, Refrigerating and Air-Conditioning Engineers, Inc. Atlanta, GE, USA. 1992.

[20] D. D. Drysdale and F. F. Abdul-Rahim, Smoke Production in Fires: Small-Scale Experiments. Fire Safety: Science and Engineering. ASTM STP 882. T. Z. Harmaty, Ed., American Society for Testing Materials. USA. 1985.

[21] G. Atkinson and D. D. Drysdale, A Note on the Measurements of Smoke Yields. Fire Safety Journal 15 (1989) 331-335.

[22] H.P. Morgan and P.J. Geake, Smoke Particle Sizes: A Preliminary Comparison between Dynamic and Cumulative Smoke Production Tests. Fire Research Station. UK. 1988.

[23] Nordtest NT fire 025. Surface Products: Room Fire Tests in Full Scale. NORDTEST Helsinki, Finland. 1986.

[24] J. Söderbom, EUREFIC - Large Scale Tests according to ISO DIS 9705. Project 4 of the EUREFIC fire research programme. Swedish National Testing and Research Institute (SP), Sweden. 1991.

[25] J. Mangs, E. Mikkola and M. Kokkala, ISO - Room Corner Test Round Robin Report. ISO-document; ISO/TC 92/SC1 N 223.

[26] J. Mangs, E. Mikkola, M. Kokkala, J. Söderbom, E. Stenhaug and I. Østrup, Room/corner test round robin. Project 2 of the EUREFIC fire research programme. Technical Research Centre of Finland. 1991.

[27] B. Sundström, Full Scale Fire Testing of Surface materials. Measurements of Heat Release and Productions of Smoke and Gas Species. Swedish National Testing and Research Institute (SP), Sweden. 1986.

[28] A.S. Hansen and P.J. Hovde, Surface Products for Ships and Offshore Constructions (in Norwegian). Assessment of Fire Test Methods and Acceptance Criteria. SINTEF NBL Norwegian Fire Research Laboratory, Norway. 1993.

[29] B. Hognon, Etude en vraie grandeur de la toxicité des effluents de combusion de produits de construction. Centre Scientifique et Technique du Bâtiment, France. 1992.

[30] B. Hognon, Etude des possibilities d'utilisation des resultats d'essais au cone calorimetre dans la reglementation sur la securite incendie des bâtiments. Resultats d'essais grandeur sur des revetements minces colles. Centre Scientifique et Technique du Bâtiments, France. 1991.

[31] ISO 9705 Fire tests - Full scale room test for surface products. International Organization for Standardization, Geneve, Switzerland. First edition. 1993.

[32] ISO 5660-1. Fire Tests - Reaction to Fire - Part 1: Rate of heat release from building products (Cone calorimeter method). International Organization for Standardization, Geneve, Switzerland. First Edition. 1993.

[33] L. Lønvik and K. Opstad, Software User's Guide for DCS. A Data Converting System. DCS version 1.20. Project 4 in the EUREFIC programme. SINTEF NBL Norwegian Fire Research Laboratory, 1991.

[34] V. Babrauskas, R.D. Peacock, M. Janssens and N.E. Batho, Standardisation of Formats and Presentation of Fire Data - the FDMS. Fire and Materials, Vol. 15, pp. 85-92 (1991).

[35] L. Tsantaridis and B. Östman, Smoke, Gas and Heat Release Data for Building Products in the Cone Calorimeter. Swedish Institute for Wood Technology Research (Trätek), Sweden. 1989.

[36] L. Tsantaridis and E. Mikkola, Cone Calorimeter Results for four Nordic materials tested earlier in full scale. Swedish Institute for Wood Technology Research (Trätek), Sweden. 1990.

[37] B. Östman, L. Tsantaridis, J. Stensås and P.J. Hovde, Smoke production in the Cone Calorimeter and the Room Fire test for Surface Products - Correlation Studies. Swedish Institute for Wood Technology Research (Trätek), Sweden. 1992.

[38] J.S. Helleren, Smoke Evolution from Building Products (in Norwegian). M.Sc. thesis at Department of Building and Construction Engineering, the University of Trondheim The Norwegian Institue of Technology, Norway. 1992.

[39] M. Kokkola, U. Göranson and J. Söderbom, EUREFIC - Large scale fire experiments in a room with combustible linings. Some results from project 3 of the EUREFIC fire research programme. Swedish National Testing and Research Institute (SP), Sweden. 1990.

[40] M. Kokkala, U. Göranson and J. Söderbom, Five large-scale room fire experiments. Project 3 of the EUREFIC programme. Technical Research Centre of Finland. 1992.

[41] B. Andersson, Model Scale Compartment Fire Tests with Wall Lining Materials. Lund University, Sweden. 1988.

[42] Toxicity of combustion products. Part 2. Guide to the relevance of small-scale tests for measuring the toxicity of combustion products of materials and composites. PD 6503: Part 2 . British Standards Institution, London, UK. 1988.

[43] M. M. Hirschler, Soot from Fires II:. Mechanisms of Soot Formation. Journal of Fire Sciences, Vol. 3-November/December 1985.

[44] K. K. Kuo, Principles of Combustion. J. Wiley & Sons, Inc., USA. 1986.

[45] S. Léonard, G. W. Mulholland, R. Puri and R. J. Santaro, Generation of CO and Smoke During Underventilated Combustion. Combustion and Flame, volume 98, no. 1/2, July 1994 (p. 20 - 34).

[46] A. Tewarson, F. H. Jiang and T. Morikawa. Ventilation-Controlled Combustion of Polymers. Combustion and Flame 95: 151-169 (1993).

[47] E. R. Dougherty, Probability and Statistics for the Engineering, Computing and Physical Sciences. Prentice-Hall International Editions. 1990.

[48] G.E.P. Box, W.G. Hunter and J.S. Hunter, Statistics for Experimenters. An Introduction to Design, Data Analysis and Model Building. John Wiley & Sons, Inc. 1978.

[49] R.A. Johnson and D.W. Wichern, Applied Multivariate Statistical Analysis. 2nd edition. Prentice-Hall International Editions. 1988.

[50] A.A. Afifi and V. Clark, Computer-Aided Multivariate Analysis. 2nd edition. Van Nostrand Reinhold Company Inc. 1990.

[51] S. Chatterjee and B. Price, Regression Analysis by Example. 2nd edition. John Wiley & Sons, Inc. 1991.

[52] S. Weisberg. Applied Linear Regression, John Wiley & Sons, Inc.1980

[53] D. Baroudi and M. Kokkala, Statistical Methods for Fire Testing. Nordtest technical report 221. 1991. Technical Research Centre of Finland, Espo, Finland

[54] J.R. Hall, Probability Concepts. The SFPE Handbook of Fire Protection Engineering. Society of Fire Protection Engineering, Boston, MA, USA.

[55] J.R. Hall, Statistics. The SFPE Handbook of Fire Protection Engineering. Society of Fire Protection Engineering, Boston, MA, USA.

[56] MINITAB. Reference Manual. Release 9 for Windows. 1993.

[57] W.A. Fuller, Measurement Error Models. John Wiley & Sons, Inc. 1987.

[58] S. Chatterjee and A.S. Haidi, Sensivity Analysis in Linear Regression. John Wiley & Sons, Inc. 1988.

[59] G. V. Hadjisophocleous and D. Yung, A Model for Calculating the Probabilities of Smoke Hazard from Fires in Multi-Storey Buildings. Journal of Fire Protection Engineering. 4 (2), 1992.

[60] I. Wetterlund and U. Göranson, New Method for Fire Testing of Pipe Insulation on Full Scale. Nordtest project 576-85. Swedish National Testing and Research Institute, Borås, Sweden. 1986.

[61] K. Opstad, Experimental modelling of pool and jet fires in an enclosure with combustible items. SINTEF NBL the Norwegian Fire Research Laboratory, Trondheim, Norway. 1989.

[62] P. Thureson, EUREFIC - Cone Calorimeter Test Results. Project 4 of the EUREFIC fire research programme. Swedish National Testing and Research Institute, Borås, Sweden. 1991.

[63] Ü.Ö. Köylü and G.M. Faeth, Carbon Monoxide and Soot Emissions from Liquid-Fueled Buoyant Turbulent Diffusion Flames. Combustion and Flame 87: 61-76 (1991).

[64] C. L. Beyler, Ignition and Burning of a Layer of Incomplete Combustion Products. Combustion, Science and Technology, 1984, Vol. 39.

[65] R. Friedman, Some Unresolved Fire Chemistry Problems. Fire Safety Science - Proceedings of the First International Symposium. International Association for Fire Safety Science. Springer-Verlag, Berlin. 1986.

[66] C. Breillat, J. M. Souil et J.P. Vantelon, Effet de la Température sur l'évolution de l'opacité des fumées. Le Laboratoire de Chimie Physique de la Combustion, Université de Poitiers, France. 1992.

[67] C. Breillat et J.P. Vantelon, Reflexions sur les conditions de formation de fumées, pour un feu de materiau donné, en function de la ventilation. Le Laboratoire de Chimie Physique de la Combustion, Université de Poitiers, France. 1990.

[68] W. M. Pitts, Executive Summary for the Workshop on Developing a Predictive Capability for CO Formation in Fires. NISTIR 89-4093, NIST, GEh, MA, USA. 1989.

[69] W. M. Pitts, Long-Range Plan for a Research Project on Carbon Monoxide Production and Prediction. NISTIR 89-4185, National Institute of Standards and Technology, Gaithersburg, MA, USA. 1989.

[70] W. M. Pitts, The Global Equivalence Ratio Concept and the Prediction of Carbon Monoxide Formation in Enclosure Fires. NIST Monograph 179, National Institute of Standards and Technology, Gaithersburg, MA, USA. 1994.

[71] B. Sundström, Classification of wall and ceiling linings. Proceedings of the EUREFIC seminar, 11 - 12 September 1991, Copenhagen, Denmark.

[72] R. G. Gann, V. Babrauskas, R.D. Peacock and J.R. Hall, Fire Conditions for Smoke Toxicity Measurements. Fire and Materials, vol. 18, 193-199 (1994).

[73] Toxic Potency Measurement for Fire Hazard Analysis. NIST Special publication 827. National Institute of Standards and Technology, Gaithersburg, MD, USA. 1991.

[74] Guide for the assessment of toxic hazard in fire in buildings and transport. Draft for Development. DD 180. British Standards Institution. London. UK. 1989.

[75] Toxicity of Combustion Products. Part 2. Guide to the relevance of small-scale tests for measuring the toxicity of combustion products of materials and composites. PD 6503: part 2: 1988. British Standards Institution, London, UK. 1988.

[76] W. D. Walton and P. H. Thomas, Estimating Temperatures in Compartment Fires. The SFPE Handbook of Fire Protection Engineering. National Fire Protection Association, Quincy, MA, USA. 1988.

[77] D. A. Purser, Interactions between Behaviour Patterns and Physiological Impairment in Escape from Fire. Interflam'93. Proceedings from the sixth International Fire conference. Interscience Communications Ltd. England. 1993.

[78] D. A. Purser, Toxicity Assessment of Combustion Products. The SFPE Handbook of Fire Protection Engineering. National Fire Protection Association, Quincy, MA, USA. 1988.

[79] F. B. Clarke, On Oxygen Depletion in Large Fires. Viewpoint. Fire Technology, February 1985.

[80] C.L. Tien, K. Y. Lee and A. J. Stretton, Radiation Heat Transfer. The SFPE Handbook of Fire Protection Engineering. National Fire Protection Association, Quincy, MA, USA. 1988.

[81] K. Opstad, Experimental modelling of pool jet fires in an enclosure with combustible items. SINTEF NBL Norwegian Fire Research Laboratory, Trondheim, Norway (confidential report). 1989.

[82] N. A. Dembsey, J. Trelles, R. B. Williamson and P. J. Pagni, Fire Near Field Entrainment Measurements. Work-in-progress poster presented at the 25th International Symposium on Combustion, 31 July - 5 August 1994, Irvine, California, USA. The Combustion Institute, Pittsburgh, PA, USA.

[83] J.L. Bryan, Human Behaviour and Fire. Fire Protection Handbook, 17th Edition. National Fire Protection Association, Quincy, MA, USA. 1991.

[84] O. Petterson and S.E. Magnusson, Fire test methods - background, philosophy, development trends and future needs. Nordtest project 34-75, Nordtest, Stockholm, Sweden. 1977.

[85] G. H. Damant, Burning Issues: The Role of Furnishing. Journal of Fire Sciences, no. 1 1991.

[86] W. P. Meade, A First Pass at Computing the Cost of Fire Safety in a Modern Society. Technical Notes. Fire Technology, november 1991.

[87] R. Friedman, Fire Protection Engineering - Science or Art?. Journal of Fire Protection Engineering, 2 (1), 1990.

ISBN 82-7119-742-8
ISSN 0802-3271